# SISSA–International School for Advanced Studies

## Doctoral Thesis

---

# Probing the spacetime fabric:

## from fundamental discreteness to quantum geometries

---

*Author:*
Marco Letizia

*Supervisor:*
Prof. Stefano Liberati

*A thesis submitted in partial fulfillment of the requirements for the degree of Doctor of Philosophy*

*in*

Astroparticle Physics

September 14, 2017

SISSA

# Declaration of Authorship

The research presented in this thesis was conducted in SISSA – International School for Advanced Studies between September 2013 and August 2017. This thesis is the result of the author's own work, except where explicit reference is made to the results of others. The content of this thesis is based on the following research papers published in refereed Journals or preprints available on arxiv.org:

- R. G. Torromé, M. Letizia and S. Liberati
  *Phenomenology of effective geometries from quantum gravity*
  In: **Phys. Rev. D**92.12, p. 124021, arXiv: 1507.03205 [gr-qc].

- M. Letizia and S. Liberati
  *Deformed relativity symmetries and the local structure of spacetime*
  In: **Phys. Rev. D**95.4, p. 046007, arXiv: 1612.03065 [gr-qc].

- A. Belenchia, M. Letizia, S. Liberati, and E. Di Casola
  *Higher-order theories of gravity: diagnosis, extraction and reformulation via non-metric extra degrees of freedom*
  In: arXiv: 1612.07749 [gr-qc]

To be published or submitted soon:

- A. Belenchia, D. M. T. Benincasa, M. Letizia and S. Liberati
  *Entanglement entropy in discrete spacetimes*
  to appear in the Classical and Quantum Gravity focus issue on the Causal Set approach to quantum gravity (early 2018).
  In: arXiv: 1710.xxxxx [gr-qc]

- E. Alesci, M. Letizia, S. Liberati and D. Pranzetti
  *Poymer scalar field in Loop Quantum Gravity (temporary)*
  In preparation.

SISSA–INTERNATIONAL SCHOOL FOR ADVANCED STUDIES

# *Abstract*

Doctor of Philosophy

**Probing the spacetime fabric:
from fundamental discreteness to quantum geometries**

by Marco LETIZIA

This thesis is devoted to the study of quantum aspects of spacetime. Specifically, it targets two frameworks: theories that predict, or have a built in, fundamental spacetime discreteness and effective models where the departure from a classical spacetime emerges at intermediate scales.

The first part of this work considers the effects of the coexistence of Lorentz invariance, spacetime discreteness and nonlocality in Causal Set Theory, from the point of view of entanglement entropy. We show that, in a causal set, the entanglement entropy follows a spacetime volume law and we investigate how to recover the area law. Furthermore, we discuss how our results are a direct consequence of the intrinsic nonlocality of the theory.

Whether Lorentz invariance is preserved in Loop Quantum Gravity is, on the other hand, still a subject of debate. We address this theme by deriving the equations of motion of a scalar field coupled to the quantum geometry. We show what is the outcome of the different way fundamental discreteness is achieved in this theory.

On the other end of the spectrum, models in which modifications to the classical description of spacetime can be considered in the continuum regime at a mesoscopic scale are examined. In particular, we analyze a certain class of models in which quantum gravitational degrees of freedom are integrated out and the effective dynamics for matter is given in terms of a momentum-dependent spacetime metric. We show that some of these cases can be embedded in a consistent geometrical framework provided by Finsler geometry.

Finally we review and compare our main results and discuss future perspectives.

# *Acknowledgements*

*You know who you are, thank you.*

# Contents

# List of Figures

# List of Tables

*To my family*

# Chapter 1

# Introduction

## 1.1 Quantum gravity phenomenology

Our current description of physical phenomena is based on two fundamental blocks: Quantum Field Theory (QFT) and General Relativity (GR). These theories have seen an extraordinary experimental success in their respective range of applicability. The former has revolutionized our understanding of matter and forces at the microscopic level. The latter is by far the most successful theory providing a classical description of gravity, and its interaction with matter, at sufficiently large scales. On the other hand, a full characterization of gravity at the quantum level is still missing.

One could actually be satisfied with this picture. Indeed, there is no unambiguous proof that gravity should be described as a quantum interaction at some energy (or length) scale. Still, there are a number of arguments suggesting that we should at least change our understanding of gravity at a microscopic level. Some of them come from the QFT side such as, for example, the presence of unpleasant ultraviolet divergences (typically removed through a renormalization procedure) and the singular behavior of correlation functions in the coincidence limit. Others coming from the gravity side, like the presence of singularities in spacetimes which are solutions of Einstein's equations (see the Penrose--Hawking singularity theorems [71, 73]). Some other arguments are more conceptual and aesthetic, like the "quest" for a unified framework for gravitational and quantum physics.

However, we do know that the typical scale at which QG effects are predicted to be relevant is given by the Planck scale $\ell_P \approx 10^{-35}$ m ($E_P \approx 10^{19}$ GeV). This expectation emerges from various arguments dealing with situations in which one cannot ignore either quantum or gravitational effects. For example, if one combines the speed of light $c$, the Newton constant $G$ and the reduced Planck constant $\hbar$ one gets the following length and mass scales

$$\ell_P = \sqrt{\frac{G\hbar}{c^3}}, \quad m_P = \sqrt{\frac{c\hbar}{G}}.$$
(1.1)

These are the natural scales emerging when relativistic, gravitational and quantum effects are non-negligible[1]. Another, more operational, possibility is to study the way localization of a particle is achieved in QFT and in GR. Starting from some very simple arguments [45], though heuristics, it is possible to obtain the well established relation $\delta x \gtrsim c\hbar/E$, where $c$ is the speed of light and $\hbar$ is the reduced Planck constant, which tells us that in order to localize a point particle of mass $m$ in its rest frame the procedure

---

[1]There are other set of scales that one can consider, e.g. the Planck energy $E_P = \sqrt{\hbar c^5/G}$ and the Planck time $t_P = \sqrt{\hbar G/c^5}$

should involve an exchange of energy between the probe (a point massless or ultra-relativistic particle) and the target greater than $1/m$. According to Special Relativity this is sufficient to create extra copies of the particle of which we want to measure the position. In order to have a meaningful procedure we get to the limit $\delta x_{\rm rest} \gtrsim \hbar/(m\,c)$. This fact seems to suggest that is not possible at all to define a sharp position in QFT.

We can however recover the infinitely sharp position measurement in the (ideal) limit $m \to \infty$ where the pair production becomes ineffective. Let us turn to analyze the problem of localization in QFT when gravitational effects are not negligible. In this case the infinite mass limit is not an option, even ideally. In the framework of GR we know that when a certain amount of energy E is confined in a region $\delta x \leq R_{\rm Schw} \propto G\,E/c^4$, where G is the Newton constant, there is a black hole formation. Therefore if we try to localize a particle with a precision better than $\delta x = R_{\rm Schw}$ one ends up with a black hole. Putting all the relationships together one gets

$$E^2 = \frac{c^5 \hbar}{G} \Rightarrow \delta x \propto \sqrt{\frac{G\hbar}{c^3}} = \ell_P. \qquad (1.2)$$

Since the Schwarzschild radius increases with the particle mass while the Compton wavelength decreases with it, one cannot do any better than the Planck length.

Due to the nature of the above arguments the phenomenology associated with QG models has been relegated to the realm of theoretical (or philosophical) speculation for a long time. As a matter of fact, research on the QG problem started almost right after the introduction of GR and the Quantum theory (1930s, see [126]), while a substantial effort in the direction of an associated phenomenology programme did not start until the second half of the 1990s. Nowadays, there are several theories, or models, approaching the QG problem, e.g. Loop Quantum Gravity (LQG) [125], String Theory (ST) [122], Causal Set Theory (CST) [49], Causal Dynamical Triangulation (CDT) [11], Group Field Theory (GFT) [115], Asymptotically safe quantum gravity [117], Hořava—Lifshitz (HL) gravity [76] just to name a few. Each of these approaches is at a different stage of development and, for the most part, they are unable to provide a direct prediction that could be testable experimentally or observationally and that could be used to disprove any of these proposals. However they gave rise to a number of effective (or toy) models, incorporating one or more features of the full theories. These models have played in the past twenty years a major role in the phenomenological investigations of QG effects [12, 77]. Some instances of typical QG effects that can be incorporated into effective models include:

- Lorentz violation and modified dispersion relations

- Spacetime discreteness

- Nonlocality

- Deformations of relativistic symmetries

- Non-standard quantization techniques

- Generalized uncertainty principles

- Higher derivative models

- Extra dimensions

Some possibilities have been extensively explored, e.g. Lorentz violating effects in matter [95], while others, such as nonlocal effects, represent largely uncharted territories.

In the rest of this chapter, we will dedicate some space to some (expected) QG features which are of phenomenological interest and we will introduce the reader to some theories incorporating these elements. It is also worth pointing out that, to different degrees, all that we are going to discuss is intimately related to the faith of Lorentz symmetry at the fundamental quantum level. For instance, spacetime discreteness (to be discussed in the next section) has dramatically different consequences in a model that preserve Lorentz invariance (LI) (and/or the relativity principle) with respect to a framework that does not.

Typically symmetries simplify our lives by restricting the possible allowed processes in a given theory. If we break a symmetry, what usually happens (depending on the way a given symmetry is broken) is that a given phenomenon that was not permitted becomes permitted, e.g. if we break Lorentz symmetry in the matter sector we have vacuum Cherenkov radiation and photon decay. Most of the time this is good news for QG phenomenology as it allows us to say something about a given theory if a certain process is not observed (even better if it is observed).

If we instead change a bit our "low-energy" theories in such a way that symmetries are untouched (or deformed), then the new effects are more subtle and the phenomenological investigation is more challenging. That is why in QG phenomenology is not enough to just "crank up" the energy in ground based experiments but one has to resort to multiple lines of experimental/observational investigations such as high energy accelerators [46], cosmological and astrophysical tests [80, 139] and, more recently, low-energy, macroscopic quantum systems [42].

Also, we should stress that the Planck scale does not need to be the only scale associated with QG effects. For instance, in HL gravity, the mass scales related to Lorentz violating effects are typically (and sometimes required to be) different and below the Planck scale. A similar situation emerges in nonlocal theories. The nonlocality scale does not need to coincide with the Planck scale. This poses an opportunity for QG phenomenology as its effects could potentially be observed at much lower energies than expected.

### 1.1.1 Space(time?) discreteness in quantum gravity

A rather straightforward step in the direction of trying to solve the problem of singularities in gravity and QFT is to assign some degree of discreteness to the background spacetime structure. This is indeed a crucial feature of many QG proposals and there are ways to argue that this would be a natural outcome when trying to merge gravity with the quantum paradigm (see, for example, the the issue of localization discussed in Sec.1.1 and [10, 67, 78] for a discussion about the existence of a minimal length in QG). On the other hand there is not a unique way of introducing a minimal scale in a quantum theory of gravity. In particular we will be interested in two cases: theories in which discreteness is a built in feature and theories in which

one starts with a continuum structure and discreteness emerges as a "side effect" of the quantization.

CST falls into the first category. In CST, spacetime is given by a discrete set of points with some partial ordering relation (a *causal set*). We can find an example of the second kind of discreteness in LQG. In general, it is not known how to connect states in the Hilbert space of LQG to continuum classical geometries, making their interpretation rather difficult. On the other hand, one finds that the spectra of geometrical operators such as length, area and volume operators, are discrete (much like the case of the angular momentum operator in Quantum Mechanics). This is an indication that Planck scale geometry in LQG is discontinuous rather than smooth, although one does not start with a discrete structure. Note that, another key difference between the discrete structure of CST and the one of LQG lies in the fact that the first one is *covariant* in nature, meaning that it is a discretization of space AND time together. Any point in a causal set represents a "spacetime event". On the other hand, in LQG, the geometrical operators whose spectra are quantized, are operators referring to purely spatial concepts. The issue of whether, in LQG, spatial discretization implies a discrete temporal evolution is still an open question.

In this kind of approaches, discreteness is considered as a fundamental feature of nature. In other theories, such as CDT, discreteness is a computational tool (a regulator) and at the end one is interested in the continuum limit.

**Aside on entanglement entropy**

Another consequence of the fact that classical backgrounds in GR are given by continuum manifolds is the singular behavior of entanglement entropy in QFT. It is known that to get a finite results one has to impose a cutoff in momenta (or, equivalently, a minimum length). By doing so, one gets an entanglement entropy (in D spacetime dimensions) which is proportional to a hypersurface of codimension two [52]. Now, if the two subregions are the exterior and the interior of a black hole, and the minimum length is taken to be the Planck length $\ell_P$, the magnitude of the resulting entanglement entropy is the same of the Bekenstein–Hawking entropy. Whether all of the Bekenstein–Hawking entropy can be interpreted as entanglement entropy of quantum fields living on the black hole spacetime is debatable, but certainly it represents a contribution to the total balance. A natural cutoff introduced by the fundamental spacetime discreteness should instead ensure the finiteness of the entanglement entropy. Moreover, it is worth noticing that the short distance regularity of correlation functions (achieved, for instance, by modifying the equations of motion with higher derivative terms), is not guaranteed to allow for a finite entanglement entropy [111].

### 1.1.2 Classical limit vs continuum limit

Now that we have argued that fundamental discreteness may be an important feature of QG, it is natural to wonder whether the continuum limit must coincide with the classical limit. We already know that, in some sense, performing both limits one should get something that looks like GR, at least approximately. Having said that, what happens if one considers the two

limits separately? Is that even a possibility? The answer to this question heavily relies on the QG proposal at hand, but one can try to draw some conclusions on general grounds. Suppose that the discretization scale is proportional to the Planck length, $\ell_{\text{discr}} \propto \sqrt{\frac{G\hbar}{c^3}}$. The classical limit would be given by the $\hbar \to 0$ limit. This limit also implies $\ell_{\text{discr}} \to 0$. Therefore, it would seem that the classical limit implies the continuum limit and that spacetime discreteness is essentially a quantum feature. This is indeed a logical possibility. On the other hand we know that already in Quantum Mechanics, the classical limit is still partially an open question as the limit $\hbar \to 0$ is not enough to have a well defined classical limit. In order to know what is the correct procedure one would have to know more about the theory (and its dynamics). Let us now consider the continuum limit first.

If such a limit is possible and it does not imply a classical limit as well, one would expect to recover something like GR plus quantum corrections (something like higher curvature models [138, 140]). Also, one can explore the possibility that although the fundamental theory is still discrete, its dynamics at "low energies" can be well approximated by a continuum description (see for example [23, 30] and [3, 8]). Strictly speaking, the latter case is not a continuum limit but, from the phenomenological point of view, it is one of the most relevant cases.

As an illustrative example, let us consider a theory in which spacetime is fundamentally described by some quantum degrees of freedom, say simplices or spin network vertices in GFT. In that context, the "continuum approximation" is a regime in which, using some collective effective variables, the behavior of a large number of fundamental constituents is considered. In the "classical approximation" one, instead, neglects the quantum nature of those degrees of freedom. In this case, the two limits are not coincident nor they commute in general (see [114] for more details). There are also other possibilities that are both classical and continuum but non-trivial at the same time. One example is the so-called *relative locality* limit in which one neglects both $\hbar$ and $G$ while keeping their ratio fixed $E_P = \sqrt{\hbar c^5/G}$. In this limit, quantum and gravitational effects are switched off, but there may be new phenomena at scales comparable with $E_P$. Notice that, in this approximation, $\ell_P \to 0$.

As a result of these arguments, it is reasonable to not assume that the classical and continuum limits are chained one to the other or commute, and one should explore all the phenomenology associated with the fact the they might be independent limits. In particular, in Chapter 5, we will show an example of continuum but non-classical limit using a toy model developed in [30] which is based on general assumptions about the underlying QG theory.

## 1.2 Causal Set Theory

CST is an approach to quantum gravity where spacetime discreteness and causal order represent the fundamental building blocks. It was introduced the late 80s [49] and it is based on results which show the fundamental nature of causal order in Lorentzian geometry.

Given a spacetime, i.e., a couple $(\mathcal{M}, g)$ composed of a differentiable manifold $\mathcal{M}$ and a metric $g$, the causal order is defined by the set of spacetime points $\mathcal{M}$ — now seen as merely a set of events, without its standard manifold-like topological character — and a partial order relation (in spatiotemporal terms, given two points $x, y \in \mathcal{M}$, $x \prec y$ means that $x$ is in the causal past of $y$). It is known that, starting from $(M, \prec)$, it is possible to recover all the mathematical structures of spacetime geometry [72, 104, 116, 132]: its topology, differential structure and its metric *up to a conformal factor*.

This missing piece of information requires to define a measure on spacetime in order to recover the volume information and fix the conformal factor. This is one of the main motivations for the assumption of discreteness which is at the basis of CST. In fact, there is a natural notion of volume in a discrete framework which is *counting elements* [132]. Therefore, in a discrete structure, one might be able to gather all the information needed to reconstruct the full geometry. As already discussed, there are also various physical reasons to assume the small-scale structure of spacetime to be discrete and they come from quantum mechanical arguments. In this setup, the natural discretization scale emerging from these arguments — the Planck scale — is such that $\ell_P \to 0$ if $\hbar \to 0$, i.e., spacetime discreteness is inherently quantum [132] (see the discussion in Section 1.1.2).

Causal Set theory combines discreteness and causal order to produce a discrete structure on which a quantum theory of spacetime can be formulated. A causal set as a locally finite partial order. More precisely, it is a pair $(\mathcal{C}, \preceq)$ given by a set $\mathcal{C}$, and a partial order relation $\preceq$ that is

- Reflexive: $\forall\, x \in \mathcal{C}$, $x \preceq x$,

- Antisymmetric: $\forall\, x, y \in \mathcal{C}$, $x \preceq y \preceq x \Rightarrow x = y$,

- Transitive: $\forall\, x, y, z \in \mathcal{C}$, $x \preceq y \preceq z \Rightarrow x \preceq z$,

- Locally finite: $\forall\, x, y \in \mathcal{C}$, $\mathrm{card}\{z \in \mathcal{C} : x \preceq z \preceq y\} < \infty$.

The first three axioms are valid for any spacetime without closed timelike curves, while the locally finiteness axiom implies discreteness.

The basic hypothesis of the causal set programme is that, at small scales spacetime is discrete and the continuum description is recovered only as a macroscopic approximation. Thus, in CST, spacetime discreteness is fundamental and the continuum is an emergent concept.

### 1.2.1 Kinematics

Specifying a dynamics is not an easy task in CST. On the other hand a large number of results has been produced in the past years which are based on its kinematical properties. How do we generate causal sets without specifying a dynamics? For phenomenological purposes we will be interested

in causal sets which are well approximated by a given spacetime (for example Minkowski spacetime or de Sitter). For this reason, one needs to chose a procedure that respect the *Volume-Number* correspondence, i.e., the possibility of recovering volume information by counting elements, which is at the basis of the CST programme. It is important to note that, a naïve regular discretization is never compatible with this correspondence, as it can be shown by boosting a regular lattice [141]. In order to implement the volume-number correspondence a discretization given by some kind of random lattice is needed.

A causal set $\mathcal{C}$ can be generated from a Lorentzian spacetime $(\mathcal{M}, g)$ via the *sprinkling* process. This consists of a random Poisson process of selecting points in $\mathcal{M}$, with density $\rho$, so to respect the volume-number correspondence on average, i.e., the expected number of points in a spacetime region of volume $V$ is $\langle N \rangle_V = \rho V$. The sampled points are then endowed with the casual order of $(\mathcal{M}, g)$ restricted to the points, see Figure 1.1. A causal set $\mathcal{C}$ is said to be well-approximated by a spacetime $(\mathcal{M}, g)$ — $\mathcal{M} \approx \mathcal{C}$ — if it can arise with *high probability* by sprinkling into $\mathcal{M}$.
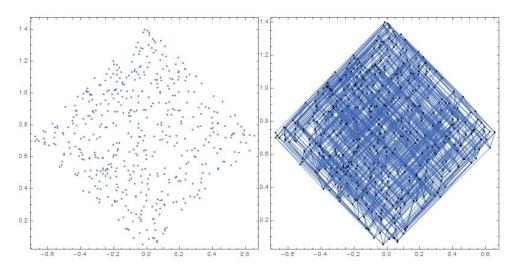


FIGURE 1.1: Sprinkling of 500 points in a $2D$ diamond of Minkowski spacetime. Blue line in the right panel represent *links*, i.e., the irreducible relations not implied by the others via transitivity.

The sprinkling process is not a process that dynamically generates causal sets, i.e., at this point we have not introduced any law for the dynamics. It is a kinematical tool. Nonetheless, this process allows one to describe, for instance, the dynamics of fields propagating on causal sets which are well-approximated by spacetimes of interest. In particular, for the rest of this work we will be mainly concerned with causal sets that are well-approximated by $D$-dimensional Minkowski spacetimes.

### 1.2.2 Discreteness, Lorentz invariance and nonlocality

A distinctive feature of CST is the preservation of LI at a fundamental level. But what does LI mean in a discrete framework? LI is refereed to the continuum approximation to the discrete structure rather than to the causal set itself. Whenever a continuum is a good approximation, discreteness must not, in and of itself, serve to distinguish a local Lorentz frame at any point

[61, 74]. The fate of LI has been study extensively, and in rigorous mathematical terms, in [48]. The conclusion is a theorem demonstrating that, not only the sprinkling process is LI, but every single realization does not define a preferred frame. The proof of the first part is based on the fact that causal information is Lorentz invariant and so is the Poisson distribution since probabilities depend only on the covariantly defined spacetime volume. The proof of the second part works by showing that there does not exist, in Minkowski spacetime, a measurable equivariant map, i.e. that commutes with Lorentz transformations, which can associate a preferred direction to sprinklings, and it is based on the non-compact nature of the Lorentz group. In spacetime other than Minkowski, the existence of local LI can be claimed on similar grounds. Also, LI has been shown to be preserved in models of QFT in causal set theory, in the continuum limit. Having said that, it is worth noticing that, even if one is not interested in CST, the sprinkling process provides a way to study QFT in a LI discrete background.

The outcome of preserving LI in a discrete framework is *nonlocality*. As an illustrative example, let us consider a causal set which is well approximated by Minkowski spacetime. Given a point $x$, we want to consider all its nearest neighbors. They will be approximately given by those points located along the hyperboloid lying one Planck unit of proper time away from the point $x$ (see Figure 1.2). There is an infinite number of those points! Another way to look at this feature is to consider two points $(x, y)$ which are causally related by an irreducible relation (a *link*). In a reference frame they might appear to be very close to one another. By performing a boost transformation they can actually be at an arbitrary coordinate distance, still remaining nearest neighbors. This is a radical nonlocal effect that is inherent to the causal set. This nonlocality also appears quite
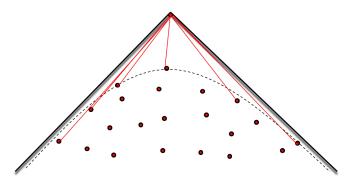


FIGURE 1.2: Considering the causal past of a given point, its nearest neighbours, i.e., the points connected with it by links, lie roughly on the hyperboloid at one Planck unit of proper time away from that point.

clearly when considering the definition of a nonlocal wave operator on the causal set. Once an average over several sprinklings of Minowski spacetime is performed, the continuum representation of this operator is given by a nonlocal d'Alembert operator $\Box_{nl}$, whose deviation from the standard d'Alembertian is parametrized by a characteristic nonlocality scale $\ell_{nl}$. For $\ell_{nl} \to 0$ one has $\Box_{nl} \to \Box$. Typically the condition $\ell_{nl} \ll \ell_P$ is required to tame the fluctuations when the averaging procedure is performed, making this scale an importance source of phenomenological investigation. We

will see in Chapter 2 how the fundamental discreteness and the nonlocality affect the behavior of the entanglement entropy of a quantum field in CST.

### 1.2.3 Dynamics

Although we will not be interested in this aspect, it is worth briefly reviewing what are the current lines of investigation in the direction of having a dynamics in CST.

Since causal sets do not admit a natural space and time splitting, it is clear that a Hamiltonian framework is not viable for describing causal set dynamics. On the other hand, a path-integral formulation should be in principle more promising. The (discrete) partition function is of the following form

$$\mathcal{Z} = \sum_{\mathcal{C}} e^{iS_{\text{BDG}}}, \tag{1.3}$$

where $S_{\text{BDG}}$ is known as the Benincasa–Dowker–Glaser action and it represents an action for causal sets which correspond to the Einstein–Hilbert action in the continuum (see [43, 44, 50, 60, 69]). Another possibility is given by the so-called Rideout–Sorkin classical sequential growth models. In this approach, starting from the empty set, a causal set is grown element by element in a Markovian way [123].

## 1.3 Loop Quantum Gravity

Loop Quantum Gravity is a theory formulated to quantize gravity at the non-perturbative level in a fully background independent fashion. The development of the theory has been pursued in mainly two directions: the canonical and the covariant approach. The first one is based on the Arnowitt–Deser–Misner (ADM) decomposition and a pair of nonstandard canonical variables defined on a fixed time hypersurface [146]. The latter is a path integral approach (the *spin foam* programme [118]).

Research in LQG is, for the most part, carried out using standard QFT techniques with minimal additional structure. In particular, in the canonical formalism, the starting point is the Hamiltonian of GR written in Ashtekar variables and the quantization techniques are inspired by methods used in lattice gauge theories.

The most relevant results obtained in the context of LQG include: the discreteness of the spectra of geometrical operators (such as the area operator) [25, 26, 127, 131]; the computation of black hole entropy [19, 20, 124]; the avoidance of the cosmological initial singularity in LQC (see [2, 3, 21, 28, 32] for reviews on the subject).

In this thesis we are interested in gaining some insights on the fate of Lorentz symmetry in LQG. We do this in a very pragmatic way, i.e. by studying the behavior of scalar fields in a quantum background described by LQG. In particular, we will quantize the scalar field using a quantization procedure, inspired by techniques used in the gravitational sector, known as *polymer quantization*, which has been shown to be background independent [27, 59, 86, 87], in the spirit of the LQG programme. We will also impose some conditions on the background geometry, inspired by the properties of homogeneity and isotropy of Minkowski spacetime, and we will derive an effective equation of motion.

In what follows we will introduce the reader to some basic elements of canonical LQG, the computation of the spectrum of the area operator and a simplified version of the theory based on symmetry reduction at the quantum level [5, 7], that will be used in Chapter 3 as a framework for our computations.

### 1.3.1 Basics of canonical Loop Quantum Gravity

The canonical approach to LQG is based on the ADM formalism and on an appropriate choice of phase space variables. In what follows we will briefly review its construction without dwelling on technicalities. We will also not discuss dynamics and we will limit ourselves to the introduction of the kinematical Hilbert space which is enough to discuss spectra of geometrical operators. We refer the reader to [24, 125, 146] for more details.

**ADM formalism and Ashtekar variables**

First of all, we foliate the four dimensional manifold $M$ into spacelike hypersurface $\Sigma_t$. This means that we are considering globally hyperbolic spacetimes. The induced splitting of the metric tensor reads as

$$g_{\mu\nu} = \begin{pmatrix} -N^2 + N_a N^a & N_a \\ N_a & q_{ab} \end{pmatrix}. \tag{1.4}$$

The physically relevant information to determine the classical solutions is contained into the pairs of conjugate variables given by the spatial three-metric $q_{ab}$ and the extrinsic curvature $K_{ab} = \frac{1}{2}\mathcal{L}_n h_{ab}$, where Latin indices from the beginning of the alphabet denote spatial indices, $n$ is the unit normal to $\Sigma_t$, and $\mathcal{L}$ is the Lie derivative.

From $K_{ab}$, we can construct

$$P^{ab} = \frac{\sqrt{q}}{2}\left(K^{ab} - q^{ab}K\right), \tag{1.5}$$

which contains the same information of $K_{ab}$. The non-vanishing Poisson brackets are

$$\{q_{ab}(x), P^{cd}(y)\} = 2\kappa\delta^c_{(a}\delta^d_{b)}\delta^{(3)}(x-y), \tag{1.6}$$

where $\kappa = 8\pi G/c^3$.

The Hamiltonian in the ADM formalism is given as

$$H = \mathcal{H}[N] + \mathcal{H}_a[N^a], \tag{1.7}$$

with

$$\mathcal{H}[N] = \int_{\Sigma_t} d^3x\, N\left[\frac{\kappa}{\sqrt{q}}\left(P^{ab}P_{ab} - \frac{1}{2}P^2\right) - \frac{\sqrt{q}}{2\kappa}\overset{(3)}{R}\right], \tag{1.8}$$

$$\mathcal{H}_a[N^a] = -2\int_{\Sigma_t} d^3x\, N^a\nabla_b P^b_a. \tag{1.9}$$

$\mathcal{H}$ and $\mathcal{H}_a$ are known as the Hamiltonian constraint and spatial diffeomorphism constraint. Consistency of the dynamics forces both of them to vanish, we write

$$\mathcal{H} \approx 0, \quad \mathcal{H}_a \approx 0, \tag{1.10}$$

where $\approx$ means *weak equality*, i.e. an equality that can be used only after Poisson brackets have been computed. This means that the Hamiltonian $H$ is weakly zero, however Poisson brackets involving it are generically non-zero.

$\mathcal{H}$ and $\mathcal{H}_a$ should be regarded as generators of gauge symmetries. In particular, only those phase space functions whose Poisson brackets are vanishing with both $\mathcal{H}$ and $\mathcal{H}_a$ are physically relevant, being independent of the choice of coordinates.

$\mathcal{H}_a[N^a]$ generates infinitesimal spatial diffeomorphisms along the vector field $\vec{N}$ while $\mathcal{H}$ encodes the dynamics of the theory. If the Einstein equations are satisfied, then $H$ generates diffeomorphisms orthogonal to $\Sigma_t$. The lapse function and shift vector appear in the as Lagrange multipliers in the Hamiltonian. They correspond to a choice of gauge and determine the relative positions of neighbouring Cauchy surfaces.

We now introduce an additional local $SU(2)$ gauge symmetry by choosing our phase space to be described by the new variables $E^a_i$ and $K^i_a$, which are related to the ADM variables by the following relations

$$q\, q^{ab} = E^{ai}E^b_i, \quad \sqrt{q}\, K_a^{\ b} = K_{ai}E^{bi}, \tag{1.11}$$

where $i = 1, 2, 3$ are internal indeces. We can look at $E^a_i$ as a densitised tetrad $\sqrt{q}e^a_i$, with $q^{ab} = e^a_i e^{bi}$, and write the extrinsic curvature as $K_{ab} = $

$K_a^i e_{ib}$, using the co-tetrad $e_b^i$. Internal indices $i, j$ are trivially raised and lowered by the Kronecker $\delta_{ij}$. The non-vanishing Poisson brackets are now written as

$$\{K_a^i(x), E_j^b(x)\} = \kappa \delta^{(3)}(x, y) \delta_a^b \delta_j^i. \tag{1.12}$$

Since we now have new degrees of freedom, we need to introduce an additional constraint known as the Gauss law

$$G_{ij}[\Lambda^{ij}] = \int_{\Sigma_t} d^3 x \Lambda^{ij} K_{a[i} E_{j]}^a \approx 0, \tag{1.13}$$

and it generates internal $SU(2)$ transformations under which observables have to be invariant.

Given this new symmetry, it is natural to introduce the spin connection $\Gamma_a^i$, defined as

$$\nabla_a e_b^i = \partial_a e_b^i - \Gamma_{ab}^c e_c^i + \epsilon^{ijk} \Gamma_a^j e_b^k = 0. \tag{1.14}$$

We can then define new variables as

$$A_a^i = \Gamma_a^i + \beta K_a^i, \quad \tilde{E}_i^a = \beta^{-1} E_i^a, \tag{1.15}$$

where $\beta$ is known as the Barbero–Immirzi parameter and it represents an ambiguity in the construction of the connection variables. It can be shown that $A_a^i$ indeed transforms as a connection. We can then compute the new Poisson brackets. They are given by

$$\{A_a^i(x), \tilde{E}_j^b(x)\} = \kappa \delta^{(3)}(x, y) \delta_a^b \delta_j^i. \tag{1.16}$$

The ADM constraints become (up to a term proportional to $G_{ij}$)

$$\mathcal{H}[N] = \int_{\Sigma_t} d^3 x N \left( \beta^2 \frac{\tilde{E}^{ai} \tilde{E}^{bj}}{2\sqrt{q}} \epsilon^{ijk} F_{ab}^k - \frac{1 + \beta^2}{\sqrt{q}} K_{[a}^i K_{b]}^j \tilde{E}^{ai} \tilde{E}^{bj} \right),$$
$$\mathcal{H}_a[N^a] = \int_{\Sigma_t} d^3 x \tilde{E}^{ai} \mathcal{L}_{\vec{N}} A_{ai}, \tag{1.17}$$

where $F_{ab}^i = 2\partial_{[a} A_{b]}^i + \epsilon^{ijk} A_a^j A_b^k$ is the curvature of the connection.

**Holonomies and fluxes**

In order to construct gauge invariant quantities we choose, as subset of phase space function to quantize, holonomies, i.e. parallel transports of our connection along curves, and fluxes, i.e. smearings of the conjugate variable $E_i^a$ over surfaces.

Holonomies $h_c^j(A)$ along a curve $c : [0, 1] \to \Sigma_t$ in a certain representation $j$ of $SU(2)$ can be defined as the solution to the following equation

$$\frac{d}{dt} h_c^j(A, t) = h_c^j(A, t) A(c(t)), \tag{1.18}$$

evaluated at $t = 1$, where $A(c(t)) = A_a^i(c(t)) \dot{c}^a(t) \tau_i^{(j)}$ and $\tau_i^{(i)}$ are the three generators of $SU(2)$ in the representation $j$. The solution can be written as

$$h_c(A) = \mathcal{P} \exp \left( \int_c A \right), \tag{1.19}$$

where $\mathcal{P}$ denotes a path-ordered integral.

Fluxes are constructed by integrating $E_i^a$ (we omit the tilde from now on), contracted with a smearing function $n^i$, over a surface $S$ as

$$E_n(S) := \int_S E_i^a n^i dS_a = \int_S E_i^a n^i \epsilon_{abc} dx^b \wedge dx^c. \tag{1.20}$$

To construct the quantum theory we need the Poisson brackets. For the sake of simplicity, we choose our surface $S$ such that it intersects the curve $c$ once in the point $c(s)$ and from below w.r.t. the orientation of $S$. In this case, we obtain

$$\{h_c^j(A), E_n(S)\} = \kappa h_{c_1}^j(A) \left( \tau_i^{(j)} n^i \right) h_{c_2}^j(A), \tag{1.21}$$

where $c_1 = c|_{t \in [0,s]}$ and $c_2 = c|_{t \in [s,1]}$.

**Kinematics**

The quantum kinematics can be constructed by promoting the above introduced variables to quantum operators obeying appropriate commutation relations.

The essential feature of LQG is to promote to operators the holonomies $h_c^j$ rather than the connections $A_a^i$ themselves. The Poisson algebra of holonomies and fluxes is well defined and the resulting Hilbert space is unique. More precisely, requiring the three-diffeomorphism invariance (there must be a unitary action of such diffeomorphism group on the representation by moving edges and surfaces in space), there is a unique representation of the holonomy-flux algebra that defines the kinematic Hilbert space $\mathcal{H}_{kin}$. This result is known as the LOST theorem [93]. The kinematical Hilbert space is also known as the *spin networks* Hilbert space.

A spin network state can be expressed as

$$|s\rangle = |\Gamma, j_c, i_n\rangle, \tag{1.22}$$

and it contains three pieces of information: the graph $\Gamma \subset \Sigma_t$, which is given by a finite number of edges $c$ and nodes $n$; a collection of spin quantum numbers $j_c$, one for each edge; the intertwiners $i_n$ at the nodes $n$.

The wave functional on the spin network is given by

$$\Psi_{\Gamma,\psi} = \psi \left( h_{c_1}^{j_{c_1}}(A), ..., h_{c_n}^{j_{c_n}}(A) \right), \tag{1.23}$$

where the wave function $\psi$ is $SU(2)$ invariant and satisfies the Gauss constraint. Specifically, this is realized by considering functions that joint the collection of holonomies (in the arbitrary spin representation) into an $SU(2)$ invariant complex number by contracting all the gauge indices with the intertwiners, the latter being invariant tensors localized at each node. The states (1.22) are called *cylindrical functions*. The space of these functions is called Cyl.

We now promote our choice of classical phase space variables to quantum operators. Their action on the state (1.22) is given by

$$\hat{h}_c^j \Psi_{\Gamma,\psi}(A) = h_c^j \Psi_{\Gamma,\psi}(A), \tag{1.24}$$

$$\hat{E}_n(S) \Psi_{\Gamma,\psi}(A) = i\{E_n(S), \Psi_{\Gamma,\psi}(A)\}, \tag{1.25}$$

where the last expression is realized by considering (1.21).

A key result in LQG is the construction of the kinematic scalar product between two cylindrical functions. Indeed, the discreteness of area and volume operators spectra, mainly based on the compactness of the $SU(2)$ group, can be obtained from it. The kinematic scalar product is defined as

$$\langle \Psi_\Gamma | \Psi_{\Gamma'} \rangle = \begin{cases} 0 & \text{if } \Gamma \neq \Gamma', \\ \int \prod_{c \in \Gamma} dh_c^j \psi_\Gamma^\dagger(h_{c_1}^{j_1}, ...) \psi_{\Gamma'}(h_{c_1}^{j_1}, ...) & \text{if } \Gamma = \Gamma', \end{cases} \tag{1.26}$$

where the integrals $\int dh_c^j$ are performed with the $SU(2)$ Haar measure. The inner product vanishes if the graphs $\Gamma$ and $\Gamma'$ do not coincide and it is invariant under spatial diffeomorphisms, even if the individual states are not. This happens because the coincidence between two graphs is a diffeomorphism invariant notion. Therefore, there is no information about the position of the graph in (1.26).

**Area operator**

In this part we will briefly show how to construct the area operator in LQG. The volume operator is obtained with a similar construction and it will not be discussed here.

First of all we need to write the area $A(S)$ of a surface $S$ in terms of our basic variables. Classically, we have

$$A(S) = \int_U d^2u \sqrt{\det(X^*q)(u)}, \tag{1.27}$$

where $X : U \to S$ is an embedding of the coordinate chart $U$ into $S$, and $X^*q$ is the induced metric on $S$. We can partition $U$ into disjoint subsets $U = \cup_i U_i$, so that

$$A(S) = \sum_i \int_{U_i} d^2u \sqrt{\det(X^*q)(u)}. \tag{1.28}$$

In the limit of small $U_i$ one has

$$\int_{U_i} d^2u \sqrt{\det(X^*q)(u)} = \int_{X(U_i)} \sqrt{qq^{ab}ds_a ds_b} \approx \beta \sqrt{E^k(U_i)E_k(U_i)}, \tag{1.29}$$

where $E_k(U_i) = \int_{U_i} E_k^a dU_a$. Therefore

$$A(S) = \lim_{U_i \to 0} \beta \sum_i \sqrt{E^k(U_i)E_k(U_i)}. \tag{1.30}$$

We can now promote $A(S)$ to an operator in the Hilbert space by using the action of the flux operator on a state.

For simplicity, we consider a Wilson loop as our state, $\Psi = \text{Tr}(h_c^j(A))$, in the case where the curve $c$ intersect the surface $S$ only once. We obtain

$$\hat{E}^k(U_i)\hat{E}_k(U_i)|\Psi\rangle = (i)^2|\text{Tr}(h_{c_1}^j(\tau_k^{(j)}\tau^{(j)k})h_{c_2}^j) = \kappa^2 j(j+1)|\Psi\rangle. \qquad (1.31)$$

Since the operator above acts diagonally, we can use the spectral theorem to deal with the square root, hence obtaining

$$\hat{A}(S)|\Psi\rangle = \beta\kappa\sqrt{j(j+1)}|\Psi\rangle. \qquad (1.32)$$

This result can be easily generalized to more complex structures [146]. Notice that the spectrum depends on the Barbero–Immirzi parameter $\beta$.

### 1.3.2 A symmetry-reduced model

Quantum Reduced Loop Gravity (QRLG) is a framework for the quantization of symmetry-reduced sectors of GR. In particular, it was initially applied to cosmological models (an inhomogeneous extension of Bianchi I) [4, 6] and then it was realized that it corresponds to a gauge fixing in which the components of the triads are diagonal at the level of the quantum theory [7].

More specifically, QRLG implements the restriction to the diagonal spatial metric tensor and triads along some fiducial directions, along which one can define coordinates $x, y, z$. The spatial line element reads

$$dl^2 = a_1^2 dx^2 + a_2^2 dy^2 + a_3^2 dz^2, \qquad (1.33)$$

where $a_i = a_i(t, x, y, z)$.

The graph now contains only three kinds of links, each of them being the set of links $l_i$ along a fiducial direction.

Inverse densitized triads are taken to be diagonal (indeces are not summed)

$$E_a^i = p^i \delta_a^i, \quad |p^i| = \frac{a_1 a_2 a_3}{a_i}, \qquad (1.34)$$

and this implies a $SU(2)$ gauge fixing condition in the internal space. It is realized by projection of $SU(2)$ group elements, which live in the links $l_i$, onto the $U(1)$ representations obtained by stabilizing the $SU(2)$ group along the internal direction $\vec{U}_l = \vec{u}_i$, with $\vec{u}_i$ unit vectors along the three directions. Connections are generically given by

$$A_a^i = c_i u_a^i + ..., \quad c_i = \frac{\beta}{N}\dot{a}_i, \qquad (1.35)$$

dots indicate non-diagonal terms that can be disregarded in certain situations [4, 6]. With these choices, $\Gamma$ becomes a cuboidal graph.

The kinematical Hilbert space now reads

$$^R\mathcal{H}_{kin} = \underset{\Gamma}{\oplus}{}^R\mathcal{H}_\Gamma, \qquad (1.36)$$

where $^R\mathcal{H}_\Gamma$ is the reduced Hilbert space for a fixed reduced graph.

Spin network sates in LQG can be written as

$$\Psi_{\Gamma,j_l,i_n} = \langle h|\{\Gamma, j_l, i_n\} = \prod_{n \in \Gamma} i_n \cdot \prod_l D^{j_l}(h_l), \qquad (1.37)$$

where $j_l$ are labels for irreducible representations of $SU(2)$ on each link, $D^{j_l}(h_l)$ are Wigner matrices in the representation $j$ and $i_n$ are intertwiners. The dot denotes contractions of the $SU(2)$ indeces and the products extend over all the links and nodes of $\Gamma$.

The basis of states in the reduced model is obtained by projecting the Wigner matrices on the state of the maximum or minimum magnetic number $m_l = \pm j_l$, for the angular momentum component $J_l = \vec{J} \cdot \vec{u}_l$ along the link $l$:

$$^l D^{j_l}_{mlml}(h_l) = \langle m_l, \vec{u}_l | D^{j_l}(h_l) | m_l, \vec{u}_l \rangle, \quad h_l \in SU(2). \qquad (1.38)$$

Then the reduced states are called reduced spin networks and are given by

$$^R\Psi_{\Gamma,m_l,i_n}(h) = \prod_{n \in \Gamma} \langle j_l, i_n | m_l, \vec{u}_l \rangle \cdot \prod_l^l D^{j_l}_{mlml}, \quad m_l = \pm j_l, \qquad (1.39)$$

where $\langle j_l, i_n | m_l, \vec{u}_l \rangle$ are reduced intertwiners.

Finally, the reduction of canonical variables to $^R h_{l_i}$ and $^R E(s)$ is obtained by smearing along links of the reduced graph $\Gamma$ and across surfaces $S$ perpendicular to these links, respectively.

The scalar constraint operator neglecting the scalar curvature term is given by that of LQG considering only the Euclidean part and replacing LQG operators with the reduced ones.

## 1.4 Geometry and Lorentz symmetry

Metric theories of gravity are based on the *metric postulate* [153]. It essentially says that spacetime is locally Minkowskian, or, equivalently, that spacetime is a pseudo-Riemannian manifold, whose geodesics represent the possible trajectories of test particles. One could see special relativity and local LI as consequences of this fact. This is of course an assumption, and one may be tempted to relax this requirement. In particular, it is conceivable that close to the Planck scale Minkowski spacetime might not be a trustworthy description of the spacetime fabric. This consideration leads us to wonder if LI is a fundamental symmetry of nature. While in CST, this is essentially the case, in other approaches LI can be considered as a symmetry emerging below some energy scale.

From the phenomenological point of view, violations of LI are encoded into the dispersion relation[2], which is given by

$$E^2 = m^2 + p^2 + \sum_{n=1}^{\infty} a_n(\mu, M)p^n, \tag{1.40}$$

where $p = \sqrt{|\vec{p}|^2}$, $a_n$ are dimensional coefficients, $\mu$ is some particle physics mass scale and $M$ is the mass scale characterizing the physics responsible for the departure from standard LI (usually, but not necessarily, identified with the Planck mass). When $a_n = 0$, $\forall n$, then the dispersion relation is the Casimir of the Poincaré algebra and LI is recovered.

Following our line of reasoning, explicit Lorentz invariance violations (LIVs) are known to be incompatible with pseudo-Riemannian geometry (see also [88]). One way to deal with this issue is to add vector or tensor fields to the gravitational Lagrangian that spontaneously break Lorentz symmetries. An example of effective theory based on this prescription is known as Einstein-æther theory [81] and the action of the theory includes the Einstein–Hilbert term plus the most general Lagrangian for a unit, time-like vector field (representing the æther) with all of the covariant contributions having at most two derivatives. Another example is provided by the work of Kostelecky and Samuel [89]. In this thesis we will be interested in yet another possibility, that is abandoning the realm of pseudo-Riemannian geometry.

Before moving to the main points of this section, some considerations are in order. First of all, contrary to the group of rotations, which is compact, $SO(3,1)$ is a non-compact group. Among other things, this means that although we have tested LI for small values of the boost parameters we cannot extend our conclusions for arbitrarily large boosts. In particular Lorentz contraction causes the transformation of large spatial distances in a reference frame into ultra short spatial distances in another reference frame.

Of course this classical picture does not take into consideration the fact that the nature of spacetime as such scales may be completely different. Instead, according to pseudo-Riemnnian geometry, flat spacetime is a better and better approximation as we consider smaller patches[3]. Consequently,

---

[2]This is strictly speaking true in the case of rotationally invariant free field modifications. The study of generic LI violating effects require an effective field theory approach.

[3]This also implies that (classically) at those scales gravity becomes unimportant, while on the other hand QG arguments suggest that spacetime will be highly fluctuating.

this distinction between short and long scales is not compatible with the *linearity* of Lorentz transformations in Special Relativity, that does not allow for a privileged length scale discriminating between those two regimes. Whatever structure is going to replace pseudo-Riemannian geometry at the fundamental level, will have to deal with this issue.

On the other hand, deformations of the relativistic transformations are possible so to integrate a second invariant energy (or length) scale [13], leaving the number of generators untouched. Under these symmetry groups, dispersion relationns of the kind (1.40) (with some $a_n \neq 0$) can potentially be invariant. Therefore, in an attempt to provide a spacetime description of this kind of symmetries, it would be interesting to understand if these can be related to some new local structure of spacetime, possibly described by some maximally symmetric background generalizing a pseudo-Riemannian structure and Minkowski spacetime.

It has been shown in a series of papers [15, 68] that Finsler geometry [33, 144] allows to reconstruct a spacetime structure starting from modified dispersion relations (MDRs) of the kind in eq.(1.40)[4]. Finsler structures are the most studied generalizations of Riemannian geometry and are defined starting from norms on the tangent bundle instead than from inner products. When a Finsler manifold is reconstructed from a MDR (we will review the precise prescription in Chapter 4), the physical picture will be that test particles with different energies will "experience different geometries" in the sense that the metric and, in general, also the affine structure of spacetime, will become *velocity-dependent* (or, equivalently, *momentum-dependent*). That is, we can describe the motion of test particles with MDRs using an effective metric of the following kind

$$g_{\mu\nu}^F(x, p(\dot{x})) = g_{\mu\nu}(x) + h_{\mu\nu}(x, p(\dot{x})), \tag{1.41}$$

giving rise to deformed equations of motion

$$\ddot{x}^\mu + \Gamma_{\rho\sigma}^\mu(x, p(\dot{x}))\dot{x}^\rho\dot{x}^\sigma = 0, \tag{1.42}$$

where $\Gamma_{\rho\sigma}^\mu(x, p(\dot{x}))$ are the Christoffel symbols associated with the Finsler metric $g_{\mu\nu}^F(x, p(\dot{x}))$. Indeed, Finsler geometry can be seen as a consistent mathematical framework to characterize what are known as *rainbow geometries* [92, 101].

Let us stress that such models of Finslerian spacetimes do not have to be considered as definitive proposals for the description of quantum gravitational phenomena at a fundamental level. We take here the point of view for which, between the full quantum gravity regime and the classical one, there is an intermediate phase where a continuous spacetime can be described in a semi-classical fashion. In particular, if the underlying QG theory predicts that spacetime is in some way discrete, then we assume that a meaningful continuum limit can be performed and that this limit is not equivalent to a classical limit (see Section 1.1.2). The outcome of this hypothetical procedure would be a spacetime that can be described as continuum but still retaining some quantum features of the fundamental theory (causing the

---

[4]A similar situation appears in analogue models. In fact there it can be shown that departures from exact LI at low energies can be naturally described using Finsler geometries [36, 152].

deviation from a pseudo-Riemannian structure). Then the departure from the purely classical theory will be weighed by a non-classicality parameter (potentially involving the scale of Lorentz breaking/deformation) and in the limit in which this parameter goes to zero, the completely classical description of spacetime is recovered (see e.g. [30, 149] for a concrete example of such a construction).

### 1.4.1 Doubly Special Relativity

The most severe constraints have been so far obtained considering the MDR as a by-product of an effective field theory with Planck suppressed Lorentz violating operators [95]. However there is an alternative approach that tries to reconcile the relativity principle with the presence of a fundamental high-energy scale. This proposal goes under the name of Doubly or Deformed Special Relativity (DSR) [13].

The essence of this idea is to change (or deform) the transformations between inertial observers in such a way that there are two invariant quantities, the speed of light $c$ and a fundamental energy scale $E_P$ (or mass scale $m_P$). This resonates very well with was we discussed in the previous section. If the fundamental scale emerging from QG is promoted to be an observer independent quantity, it would soften the tension in the distinction between high energy and low energy regimes in a relativistic framework. Indeed, in DSR models, relativistic transformations becomes nonlinear, potentially overcoming this issue.

There are a least two ways of realizing DSR models. One way is to introduce nonlinear representations of the standard Poincaré Lie group. This is a case where the new observer independent scale of DSR characterizes representations of a still classical/undeformed Poincaré Lie group. Another way is to adopt the formalism of Hopf algebras. In essence, the difference between the two approaches is that, in the first case one substitutes the standard Poincaré generators with new generators, adapted to the nonlinear representation. In the second case, not only the commutators, but also the coproduct rules are changed and the action of symmetry transformations on products of functions is not deducible from the action on a single function using the Leibniz rule.

Hopf algebras were proposed a few decades ago to describe symmetries of noncommutative spacetimes [102]. In the QG context, a particular case of Hopf algebras has attracted some attention in the past years, the case of $\kappa$-Poincaré [99, 100, 103]. Gravity in $2+1$ dimensions can be quantized as a topological field theory and can be coupled to point particles, represented by topological defects. In [66] it was shown that, after integrating away the gravitational degrees of freedom, particles are described by representations of the $\kappa$-Poincaré group (where $\kappa$ is an energy scale). At this stage, this results cannot be extended to $3+1$ dimensions, but the $\kappa$-Poincaré group can be easily extended to higher dimensions.

In this thesis we will be interested in studying the $\kappa$-Poincaré group in the *relative locality* limit, briefly introduced in Section 1.1.2, in which one neglects both $\hbar$ and $G$ while keeping their ration fixed $E_P = \sqrt{\hbar c^5/G}$. In this case, one can effectively ignore any noncommutativity in the coordinates (driven by $\hbar$) while keeping the deformed relativistic properties. In this framework, the non-standard symmetries of spacetime, can be related

to a non-trivial curvature in momentum space. In particular, $\kappa$-Poincaré is associated with a de Sitter momentum space [70]. We will be interested in the $1 + 1$ dimensional case and we will discuss the dynamics of free particles, therefore the structure of the coproducts will not play any role. In $1+1$ dimension, the $\kappa$-Poincaré algebra is then given by the following commutators among generators

$$[P, E] = 0, \quad [N, P] = \frac{\kappa}{2}\left(1 - e^{-2E/\kappa}\right) - \frac{1}{2\kappa}P^2, \quad [N, E] = P. \qquad (1.43)$$

We give here the coproducts for the sake of completeness

$$\Delta E = E \otimes \mathbb{I} + \mathbb{I} \otimes E, \ \Delta P = P \otimes \mathbb{I} + e^{-E/\kappa} \otimes P, \qquad (1.44)$$
$$\Delta N = N \otimes \mathbb{I} + e^{-E/\kappa} \otimes N,$$

and the antipods and counits

$$S(E) = -E, \ S(P) = -e^{-E/\kappa}P, \ S(N) = -e^{-E/\kappa}N \qquad (1.45)$$
$$\epsilon(E) = \epsilon(P) = \epsilon(N) = 0.$$

Finally, the Casimir is given by

$$C_\kappa = \left(2\kappa \sinh \frac{E}{2\kappa}\right)^2 - e^{E/\kappa}P^2. \qquad (1.46)$$

All these relationships are written in the so-called bycrossproduct basis. In can be shown that a change of basis in the generators amounts to a diffeomorphism in momentum space [70]. For $\kappa \to \infty$, one recovers the Poincaré algebra.

While there is a rather clear understanding of DSR models in momentum space, the picture in spacetime is less clear and it represents a subject of debate. On the other hand, such a picture would allow these models to be more competitive in comparison to LIV scenarios. Here is where Finsler comes to the rescue as a framework that could accommodate this kind of physics, as we anticipated in the previous Section. In particular in [15], a Finsler spacetime realizing the symmetries of $\kappa$-Poincaré in $1 + 1$ dimensions was found and it was shown to reproduce the results of the usual computations in momentum space.

Among all the possible Finsler structures, a particular case is given by Berwald spaces. These are the Finsler spaces that are the closest to be Riemmanian (we will provide a more precise definition in Chapter 4). If a Finsler space is of the Berwald type then any observer in free fall looking at neighbouring test particles would observe them move uniformly over straight lines accordingly to the Weak Equivalence Principle [107]. Interestingly enough the Finsler metric correspondent to $\kappa$-Poincaré symmetries found in [15] appears to be a member of this class. However, we shall see that this come about in a somewhat trivial way as a straightforward consequence of the flatness of the metric in coordinate space. With this in mind, it would be interesting to consider examples of curved metrics associated to more general deformed algebras so to check if for these the local structure of spacetime does not reduce to the Minkowski spacetime but rather to the Finsler geometry with $\kappa$-Poincaré symmetries and furthermore for checking if also

these geometries are of the Berwald type. This will be the main subject of Chapter 4.

**Aside on the Einstein and Weak Equivalence Principles**

With a momentum-dependent metric tensor, one generically expects violations of the Equivalence Principles. Metric theories of gravity, identified by the metric postulate, can also be characterized as those theories satisfying the Einstein Equivalence Principle (EEP)[153]. The latter can be expressed as follows

**Einstein Equivalence Principle.** *The Einstein Equivalence Principle states that:*

- *The Weak Equivalence Principle is valid.*

- *The outcome of any local non-gravitational experiment is independent of the velocity of the freely-falling reference frame in which it is performed (local Lorentz invariance).*

- *The outcome of any local non-gravitational experiment is independent of where and when in the universe it is performed (local position invariance).*

The content of the WEP can be stated as follows

**Weak Equivalence Principle.** *Any observer in free fall looking at neighbouring test particles would observe them moving uniformly over straight lines, independently of their composition.*

It appears that any theory of gravity that is, in some sense, based on DSR would violate the EEP (by construction the theory would not be LI). On the other hand, the EEP could be deformed by asking that local LI is substituted with local DSR invariance. Regarding the WEP, the notion of "moving uniformly" is related to acceleration and hence to the affine structure of spacetime. Therefore, given a momentum-dependent metric tensor, the study of the geodesic equations and the *spray coefficients* will determine whether a reference frame, physically realizing the WEP, can be constructed. We will see in Chapter 4 that, in the context of Finsler geometry, this amounts to verify whether the Finsler structure is of the Berwald type. This kind of investigation, carefully considering its limitations, could potentially shed some light on the possibility of constructing a metric theory of gravity based on DSR symmetries.

# Chapter 2

# Spacetime entanglement entropy in Causal Set Theory

## 2.1 Introduction

The concept of entanglement entropy plays a crucial role in several areas of modern quantum physics, from the study of condensed matter systems to black holes. It is essentially a measure of the correlation between subparts of a quantum system. It is traditionally defined as $S = \text{Tr}\rho \log \rho^{-1}$, where $\rho$ is the reduced density matrix of the subsystem. Consider a bipartite system, whose parts are labeled by $A$ and $B$, that is described by a density matrix $\rho_{AB} \in \text{Lin}(\mathcal{H}_A \otimes \mathcal{H}_B)$. The entropy of subsystem $A$ is given by $S_A = -\text{Tr}\rho_A \log \rho_A$, where $\rho_A \equiv \text{Tr}_B \rho_{AB}$ is the reduced density matrix of system $A$ and is obtained by tracing over the degrees of freedom of system $B$. Some of the properties of $S$ are:

- $S(\rho) \geq 0$

- $S(\rho) = 0 \iff \rho$ is pure

- $S(\rho) = S(U\rho U^\dagger)$ with $U$ a unitary transformation

- concavity: $S(\sum_i \lambda_i \rho_i) \geq \sum_i \lambda_i S(\rho_i)$ with $\lambda_i > 0 : \sum_i \lambda_i = 1$

- $S_{AB} = S_A + S_B$ if $\rho_{AB} = \rho_A \otimes \rho_B$

- strong subadditivity: $S_{ABC} + S_B \leq S_{AB} + S_{BC}$

- $\dim \mathcal{H}_\mathcal{A} = d \implies S_A \leq \log(d)$ and $S_A = \log(d) \implies \rho_A = d^{-1}\mathbb{1}$

When the two systems are uncorrelated, $\rho_{AB} = \rho_A \otimes \rho_B$, knowing the parts allows one to reconstruct the entire system. On the contrary, if the systems are maximally entangled knowing the parts gives no information on the whole.

In the context of QFT, entanglement entropy is also known as *geometric entropy* [53]. The system in this case is partitioned geometrically, starting from a state $\rho_\Sigma$ defined on a fixed time hypersurface $\Sigma$ and then tracing out the degrees of freedom living "outside" a given subregion $R$. As we mentioned in the Introduction, this entropy is typically a divergent quantity due to the vacuum fluctuations with infinitely high frequencies near the boundary of $R$.

This notion is now widely believed to be of great importance in the context of QG research for several reasons. For instance: its divergences are thought to be strongly connected with the local structure of spacetime (see

Sec.1.1.1); it is a relevant concept whenever a spacetime possesses an event horizon (black holes, Rindler observers and others); gravity and its dynamics can emerge from quantum entanglement (see Jacobson's derivation [82, 83] and Van Raamsdonk's work [150]). Because it's formulated as a purely spatial notion, the traditional ways of thinking about entanglement entropy might not be suitable for QG investigations.

Motivated by these considerations, a global definition of entropy that can be applied to any globally hyperbolic region of spacetime and is particularly useful in the context of CST, was recently proposed by R. Sorkin [134]. We will refer to this quantity as spacetime entanglement entropy (SEE).

This gives on one hand a theory (CST) that provides us with a way of introducing a fundamental cutoff in a Lorentz invariant fashion and, on the other, a covariant definition of entanglement entropy. Equipped with these tools, we will investigate in this chapter the behavior of the SEE in a causal set that is well approximated by a causal diamond in two, three and four dimensions for two families of scalar Green functions. In particular, we focus on trying to motivate how the familiar *area law* in the continuum emerges from the fundamental discrete structure.[1]

The chapter is organized as follow: in Section 2.2 we briefly review the novel notion of entanglement entropy introduced in [134]; in Section 2.3, we introduce the reader to the basics of QFT in a causal set, the Sorkin–Johnston vacuum and the kind of scalar Green functions that we will use in our study; in Section 2.4, we introduce and present the main results of our work and, finally, in Section 2.5, we conclude with a discussion of our results and an outlook for further developments.

## 2.2 Spacetime entropy

In [134] a covariant definition for the entropy of a Gaussian field expressed entirely in terms of spacetime correlation functions was introduced. Consider the ground state $|0\rangle$ of a free real scalar field $\phi$ whose Wightman (W) function is given by the following expression

$$W(x, y) = \langle 0|\phi(x)\phi(y)|0\rangle, \tag{2.1}$$

which, by Wick's theorem, determines all the other $n$-point correlation functions. The imaginary part of $W$ is the Pauli-Jordan (PJ) function

$$i\Delta(x, y) = [\phi(x), \phi(y)], \tag{2.2}$$

which can be alternatively written in terms of the retarded ($G_{ret}$) and advanced ($G_{adv} = G_{ret}^T$) Green functions as

$$\Delta(x, y) = G_{ret}(x, y) - G_{adv}(x, y). \tag{2.3}$$

Given a spacetime region $R$ the SEE is defined as

$$S(R) = \sum \lambda \ln |\lambda|, \tag{2.4}$$

---

[1]An analogous investigation was carried out in [137] for two spacetime dimensions.

where $\lambda$ are the solutions of the generalized eigenvalue problem

$$\begin{cases} W_R\, v = i\lambda\, \Delta_R\, v \\ v \notin \mathrm{Ker}[\Delta_R], \end{cases} \tag{2.5}$$

and the subscript $R$ indicates the restriction of the correlation function to pairs of points $(x, y) \in R$. For any vector in the kernel of $i\Delta$, the associated $\lambda$ is not defined, hence we just exclude them (it can be shown that they would not contribute to the entropy anyway, see [134]).

It can be proven that [134] the SEE of a globally hyperbolic region of spacetime coincides with the standard entanglement entropy of any Cauchy surface $\Sigma$ of such region, i.e.

$$S(\mathcal{D}(\Sigma)) = S_{ent}(\Sigma), \tag{2.6}$$

where $\mathcal{D}(\Sigma)$ is the causal domain of development of $\Sigma$ and $S_{ent}(\Sigma)$ is the standard entanglement entropy of surface $\Sigma$.

## 2.3 Scalar fields in causal set theory and the Sorkin–Johnston vacuum

Being a covariant definition of entropy that does not require the notion of a state on a spatial hypersurface, the notion of entropy given in Section 2.2 can be successfully applied to quantum fields living on causal sets. As mentioned the Section 1.2, we will be dealing with causal sets (generated by a sprinkling process) that are well approximated by a flat continuum (Minkowski) spacetime.

It can be shown that, in general, a causal set does not admit the notion of a Cauchy hypersurface. This represents an obstacle when trying to implement traditional quantization techniques. For this reason in [1, 84, 136] (see also [135] for a recent pedagogical introduction) a different starting point was assumed to define a free scalar field theory: rather than starting from the equations of motion and the canonical commutation relations (CCR), one can start with the (retarded) Green function $G_R$ only. Given $G_{\mathrm{ret}}$ one can write the the PJ function as in (2.3) and use it to rewrite the CCR in an explicitly covariant way(see Eq.(2.2)). The PJ function gives the imaginary part of the W function

$$\Delta = 2\,i\,\Im(W) \Rightarrow W = \frac{i\,\Delta}{2} + R. \tag{2.7}$$

Is it possible unambiguously choose the vacuum if there are no equations of motion available? The answer is yes. In particular one can choose the W function to be of the positive part of $i\Delta$, i.e.

$$W_{SJ} := \frac{i\,\Delta + \sqrt{-\Delta^2}}{2} = \mathrm{Pos}(i\,\Delta). \tag{2.8}$$

Since for a Gaussian scalar field the two-point function fully determines the theory, this prescription allows us to formulate a consistent scalar field theory with the retarded Green function as the only input. In particular, eq.(2.8) specifically selects a vacuum state known as the Sorkin–Johnston

(SJ) vacuum. It can be shown that definition (2.8) is equivalent to requiring the following three conditions for $W$:

- Positivity $W \geq 0$

- Commutator $\Delta = 2\Im(W)$

- Othogonal support $W\,W^* = 0$

The first two are common to the two-point function of any state, while the third specifically selects the SJ vacuum [135]. This prescription yields distinguished ground states for a quantum scalar field in any globally hyperbolic region of spacetime or causal set, without making explicit reference to any notion of positive frequency.

Now that we have established that one can define a quantum scalar field on a causal set starting from Green functions alone, we will see what the possible choices of retarded Green functions are.

### 2.3.1 Discretizing continuum Green functions

The first possibility is to directly discretize the continuum Green functions on a causal set. This has been done in [85] and the strategy is to replace the continuum retarded Green functions with discrete analogs written in terms of objects that are well-defined on a causal set. The expressions for the retarded Green function in two, three and four spacetime dimensions are given by

$$G_{\text{ret}}^{(2)}(x,y) = \frac{1}{2}C_{xy} \tag{2.9}$$

$$G_{\text{ret}}^{(3)}(x,y) = \frac{1}{2\pi}\left(\frac{\pi\rho}{12}\right)^{1/3}\left((C+\mathbb{I})^2\right)_{xy}^{-1/3} \tag{2.10}$$

$$G_{\text{ret}}^{(4)}(x,y) = \frac{\sqrt{\rho}}{2\pi\sqrt{6}}L_{xy}, \tag{2.11}$$

for $x \prec y$ and zero otherwise. The matrix $C_{xy}$ is known as the *causal matrix* and given any two elements $a,b \in \mathcal{C}$, $C_{a,b} = 1$ if $a$ causally precedes $b$ and zero otherwise, for all $a,b \in \mathcal{C}$. $C_{a,b}$ can be used as a full specification of the causal set itself. The matrix $L_{xy}$ is the *link matrix* and given any two elements $a,b \in \mathcal{C}$, $L_{a,b} = 1$ if there are no elements $c \in \mathcal{C}$ s.t. $a \prec c \prec b$ and zero otherwise, for all $a,b \in \mathcal{C}$. Finally, $\rho = N/V$ is the density of sprinkled spacetime points.

Note that the discrete Green functions given above are defined only in terms of causal properties of the causal set.

### 2.3.2 Nonlocal wave operators on causal sets

The second possibility is to invert a wave operator properly constructed on the causal set itself. It was shown in [133] that discrete wave operators can be defined on the causal set in terms of *nearest neighbors*[2]. Such operators, once averaged over sprinklings of Minkowski spacetime, give rise to nonlocal operators which reduce to the standard d'Alembertian operator in

---

[2]The notion of nearness is given by the cardinality of the set of points between the causal past and the causal future of a couple of elements $x \preccurlyeq y$, i.e. $|z \in \mathcal{C} : x \preccurlyeq z \preccurlyeq y|$.

the continuum limit. We report here the general expression for the discrete operators in any spacetime dimension $D$ (see [69] for further details)

$$(B_\rho^{(D)}\phi)(x) = \rho^{2/D}\left(a\,\phi(x) + \sum_{n=0}^{L_{max}} b_n \sum_{y\in I_n(x)} \phi(y)\right), \qquad (2.12)$$

where $a, b_n$ are dimension dependent coefficients, $\rho = \ell^{-D}$, $\ell$ is the discreteness scale and $I_n(x)$ represents the set of past $n$-th neighbors of $x$. In the literature the first sum in eq. (2.12) is referred to as sum over *layers*, where each $I_n$ is a layer.

| | $a$ | $b_0$ | $b_1$ | $b_2$ | $b_3$ |
|---|---|---|---|---|---|
| $D=2$ | -2 | 4 | -8 | 4 | |
| $D=3$ | $-\frac{1}{\Gamma[5/3]}\left(\frac{\pi}{3\sqrt{2}}\right)^{2/3}$ | $\frac{1}{\Gamma[5/3]}\left(\frac{\pi}{3\sqrt{2}}\right)^{2/3}$ | $-\frac{27}{8\Gamma[5/3]}\left(\frac{\pi}{3\sqrt{2}}\right)^{2/3}$ | $\frac{9}{4\Gamma[5/3]}\left(\frac{\pi}{3\sqrt{2}}\right)^{2/3}$ | |
| $D=4$ | $-4/\sqrt{6}$ | $4/\sqrt{6}$ | $-36/\sqrt{6}$ | $64/\sqrt{6}$ | $-32/\sqrt{6}$ |

TABLE 2.1: Table of coefficients in Eq.(2.12) for $D = 2, 3, 4$. The number of coefficients for every dimension corresponds to the "minimal" nonlocal operators, i.e., the operators constructed with the minimum number of layers.

These operators are derived in such a way to reproduce, in the continuum limit, the standard d'Alembertian once averaged over sprinklings. However, whereas this average is well behaved in the local limit the variance is not. In order to solve this problem, a new length scale, which we call the *nonlocality* scale, can be introduced [133]. This scale serves to smear the action of the previous operators on the whole past of a given point $x$ and leads to discrete operators given by

$$(\tilde{B}_\rho^{(D)}\phi)(x) = (\epsilon\rho)^{2/D}\left(a\,\phi(x) + \sum_{m=0}^{\infty} \tilde{b}_m \sum_{y\in I_m(x)} \phi(y)\right), \qquad (2.13)$$

where $\epsilon = (\ell/\ell_k)^D$ with $\ell_k$ the nonlocality scale and

$$\tilde{b}_m = \epsilon(1-\epsilon)^m \sum_{n=0}^{L_{max}} \binom{m}{n}\frac{b_n\epsilon^n}{(1-\epsilon)^n}. \qquad (2.14)$$

Finally, by inverting the expressions in (2.13) the retarded nonlocal Green function can be obtained.

## 2.4 Spacetime entropy in Causal Set Theory

In this section we report the results of our work, i.e., the computation of the SEE, introduced in Section 2.2, for a scalar field in a causal set that is well approximated by Minkowski spacetime. First we will discuss how the system is organized, including the geometrical setup and the choice of state for the scalar field. Then we will present the results of the computations for two, three and four spacetime dimensions. Note that our analysis partially

overlaps with the one presented in [137], where a similar computation was carried out in a two dimensional causal set for the massless local Green function. Also we will not discuss here the fine details of our analysis, as we will confine ourselves to the main ideas and the most relevant outcomes. We invite the reader to look at [40] for the full investigation.

### 2.4.1 The setup

Our geometrical configuration is a fixed causal set $\mathcal{C}$ that is well approximated by a causal diamond in Minkowski spacetime. A causal diamond, or Alexandrov open set, is defined as the intersection of the future light cone of a point $p$ with the past light cone of a point $q$, i.e., $I^+(p) \cap I^-(q)$. We then consider a smaller causal diamond inside the first one, centered at the same point and with sides parallels to the ones of the large diamond. In any number of dimensions, the ratio between the volume $V$ of the outer diamond and the volume $V_d$ of the inner diamond is fixed to be $V/V_d = 4$.

   The scalar field is prepared in the SJ vacuum of the large diamond. Once we have the $W_{SJ}(x, y)$ and $\Delta(x, y)$ matrices ($(x, y)$ vary over the elements of $\mathcal{C}$) we numerically solve the generalized eigenvalue problem (2.5) restricted to the inner diamond. By applying formula (2.4), we compute the SEE of the scalar field in the inner diamond with respect to the complementary region. The resulting entropy can be interpreted, in the continuum limit, as the EE of the horizontal diagonal of the small diamond (green line in Figure 2.1) with respect to its complement given by the segments that extend the diagonal to the larger diamond (black segments in Figure 2.1). Note that the diagonal of the big diamond is a Cauchy surface. We consider this configuration in two, three and four spacetime dimensions, for the local and nonlocal massless Green functions introduced in the previous section.

   At this point we want to remind the reader that, in $D$ spacetime dimensions, the area law corresponds to a entropy that grows like that "area" of a hypersurface of codimension two. We will generically refer to this behavior as an *area law*.
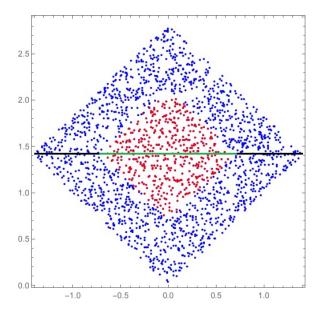


FIGURE 2.1: Inner and outer diamonds for a sprinkling in 2$D$ Minkowski, with $N = 2048$ and $V/V_d = 4$.

### 2.4.2 Premise on the spectrum of the Pauli–Jordan

In Section 2.2 we mentioned that one has to exclude the vectors in the kernel of $i\Delta$ in the computation of the SEE in order to have a well defined eigenvalue problem. As a preliminary analysis we look at the spectrum of this operator (we will sometimes refer to it as $\sigma_{i\Delta}$) in the continuum and in the causal set case. The eigevalues of $i\Delta$ in the continuum have dimensions of a length squared $L^2$, while in the causal set they have dimensions $L^{2-D}$, in $D$ dimensions. To compare the two spectra, we match their dimensions by using a factor of $\rho$.

The two dimensional continuum case was studied in [129] where the authors found that the eigenvalues of $i\Delta$ are of the form $\alpha^{cont} = \ell_d/(2k)$, where $\ell_d$ is the side of the diamond and $k = \frac{\pi n}{\ell_d}$, with $n = \pm 1, \pm 2, ...$, is the wavenumber of the eigenfunctions [129], and can be rewritten in terms of the volume of the diamond as $\alpha^{cont} = \sqrt{V}/(2k)$. The usual cutoff is then implement by retaining all the eigenvalues of $i\Delta$ up to a minimum value $\alpha_{min}^{cont}$ associated with a maximum wavenumber $k_{max}$ that, in turn, can be related to a minimum wavelength $\ell_{\min} = 2\pi\, k_{max}^{-1}$. If we want to translate this cutoff in the discrete causal set, we can identify $\ell_{\min}$ with the fundamental discreteness scale $\ell = \rho^{-1/D}$ and multiply by a factor of $\rho$, to obtain[3]

$$\alpha_{min}^{cs} = \rho\, \frac{\sqrt{V}}{2k_{max}} = \rho\, \frac{\sqrt{V}}{4\pi}\ell = \frac{V}{4\pi\sqrt{N}}, \tag{2.15}$$

where we used $\rho = N/V$.

In Figure 2.2a, we have the log-log plot of the positive part of $\sigma_{i\Delta}$ in the continuum (red dots), in the causal set (blue dots) and the cutoff $\lambda_{min}^{cs}$ (black dashed line) for the local Green function in $2D$. The spectrum in the continuum follows a power law behavior as a function of $n$, while the spectrum in the causal set matches the one in the continuum approximately up to the value of the cutoff, after which it changes drastically. On the basis of this fact, we expect a different behavior for the entropy in the two cases.
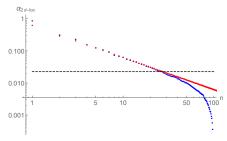
At the moment, we do not have the exact spectrum of this operator in the continuum in higher dimensions for the local and nonlocal Green functions. Nevertheless, we can look at the spectra in the causal set and we can see the it has the same shape of the two dimensional case (for instance, see Figures 2.2 for the localand nonlocal models in two dimensions).
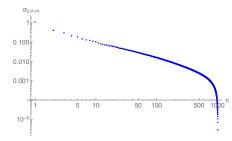
### 2.4.3 Spacetime entropy

Let us consider first the entropy associated with the large diamond (i.e., of the outer diamond in Fig. 2.1) in any number of dimensions. It is easy to show explicitly how how the SEE computation gives a zero entropy for the SJ state which is a pure state. Indeed, the fact that $W_{SJ} = \text{Pos}(i\Delta)$ implies that the eigenvalues of the problem in Eq. (2.5) are all either zero or one. Since $i\Delta$ is a skew-symmetric and Hermitian matrix, its rank is even and its non-zero eigenvalues come in positive and negative pairs. Partially following the notation in [85], we write its normalized eigenvectors and eigenvalues as follows

$$i\Delta u_a = \alpha_a u_a, \quad i\Delta v_a = -\alpha_a v_a, \quad i\Delta w_c = 0, \tag{2.16}$$

---

[3]This result agrees with the one presented in [137].

(A) Plot of $\sigma_{i\Delta}$ in two dimensions for the local Green function in the continuum (red dots), in $\mathcal{C}$ (blue dots) and the continuum cutoff (black dashed line) (N=200)

(B) Plot of $\sigma_{i\Delta}$ in two dimensions for the nonlocal Green function (N=2048)

FIGURE 2.2: Spectrum of $i\Delta$ for the local and nonlocal models in $D = 2$.

where $\alpha_a > 0$, $2s$ is the rank of $i\Delta$, $a = 1, ..., s$ and $c = 1, ..., p - 2s$ ($p$ is the number of elements in $\mathcal{C}$).[4] The eigenvectors form an orthonormal basis for $\mathbb{C}^p$ and they can be chosen such that

$$u_a = v_a^*, \ w_c = w_c^*, \ u_a^\dagger u_b = v_a^\dagger v_b = \delta_{ab}, \ u_a^\dagger v_b = w_c^\dagger u_a = w_c^\dagger v_a = 0. \quad (2.17)$$

We can therefore decompose the matrix as follows

$$i\Delta = \sum_{a=1}^{s} \alpha_a u_a u_a^\dagger - \sum_{a=1}^{s} \alpha_a v_a v_a^\dagger. \quad (2.18)$$

Since $W_{SJ} = \text{Pos}(i\Delta)$ it can be written as

$$W_{SJ} = \sum_{a=1}^{s} \alpha_a u_a u_a^\dagger. \quad (2.19)$$

Let us consider now the eigenvectors $u_a$ with positive eigenvalues. The generalized eigenvalue problem (2.5), applied to the large diamond, gives

$$W_{SJ} u_a = \alpha u_a = \lambda \alpha u_a \Rightarrow \lambda = 1. \quad (2.20)$$

Given the orthogonality relations (2.17), for the $v_a$ one gets

$$W_{SJ} v_a = 0 = \lambda \alpha v_a \Rightarrow \lambda = 0. \quad (2.21)$$

Therefore $S = \sum \lambda \ln \lambda = 0$.

We now consider the entropy of the small causal diamond obtained by tracing over the d.o.f. in its complement. To do this we numerically solve Eq. (2.5) restricted to the points inside the small diamond. We do this for different values of sprinkling density $\rho$ and, since the fundamental scale is related to the density as $\ell = \rho^{-1/D}$, we are effectively computing the SEE as a function of the fundamental discreteness scale.

Before presenting the results, a couple of comments are in order. First, for a given number of elements $N$ in the causal set, the range of scales that we investigate in different spacetime dimensions varies. For instance, to

---

[4]Note that in Section 2.4.2, the index $i$ referred to the length of each vector while here $a, b, c$ are labels.

have $\ell = 0.01$ with a unit fiducial volume $V = 1$, we need $N = 10^8, 10^6, 10^4$ for $D = 4, 3, 2$ respectively. While in two dimensions it is relatively easily to reach these densities, for higher dimensions this is not the case and this will be a source of uncertainty in the interpretation of our results. The second point is that we need to keep in mond that the nonlocal models contain a new scale $\ell_k$, the nonlocality scale introduced in Section 2.3.2, therefore it is natural to expect some departure from the local models as we probe different values of the cutoff.

For $D = 2, 3, 4$ and for local and nonlocal Green functions, we find that the entropy scales linearly with the number of points of the inner diamonds $N_d$ (see Figures 2.3a).[5] Since $N_d \propto \rho$, the SEE follows a *spacetime volume law*. Contrary to the ordinary case where the entropy is infinite unless a UV cutoff is introduced, in this case (for any finite value of $N_d$) the entropy is finite.

This result was already known to the community and it was presented in [137] for a local massless Green function in $D = 2$.

This behavior can be traced back to the part of the spectrum of eigenvalues of $i\Delta$ which does not follow a power law (see Section 2.4.2 and Figures 2.2a and 2.2b) and smoothly interpolates between the continuum behavior and zero. This fact can be verified by applying the cutoff of the continuum to the spectrum in the causal set, so that we only retain those eigenvalues that follow the continuum behavior.



| (A) Local theory in two dimensions. | (B) Nonocal theory in three dimensions. |
|---|---|
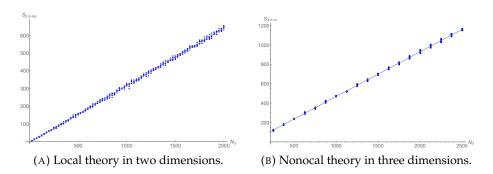
FIGURE 2.3: Spacetime volume law.

Since we do not have the exact spectrum for $i\Delta$ in dimensions higher than two and for the nonlocal Green functions, we generalize the cutoff (2.15) using general arguments. In particular we assume that in the continuum the eigenvalues are still of the form $\lambda^{cont} \propto V^{1/D}/k$ where $V^{1/D}$ is the scale that characterize the geometrical setup (the typical scale of the diamond in $D$ dimensions), and we use the prescription used to derive Eq. (2.15). We relate the maximum wavenumber with the discretization scale by $k_{max} = 2\pi/\ell$, we rewrite $\ell$ in term of the causal set density $\rho$ and finally we multiply by $\rho$ to have an expression that is dimensionally consistent. We introduce a real parameter $a \geq 0$ to take into account possible overall numerical factors coming from the exact spectrum and we write the cutoff in $D$ dimensions as

$$\alpha_{min}^{cs,D} = a\,\rho\,\ell V^{\frac{1}{D}} = a\,\rho^{1-\frac{1}{D}} V^{\frac{1}{D}} = a\,V^{\frac{2}{D}-1} N^{1-\frac{1}{D}}. \qquad (2.22)$$

---

[5]The choice of studying the entropy as a function of the number of points in the small diamonds is customary. One can also consider the total number of points $N$, the two are, on average, related as $N_d = (V_d/V)N$.

The magnitude of the eigenvalues of $i\Delta$ grows with $N$ as it can be seen from Figure 2.4. Eq. (2.22) allows the cutoff to track this growth so that it is at the same location relative to the spectrum for every $N$. Changing the value of $a$ translates the cutoff vertically in the $(n, \alpha)$ plane in Figure 2.2 (for a given value of $N$). Note that $a = 0$ corresponds to not having a cutoff. We then look at the behavior of the SEE as a function of this parameter.
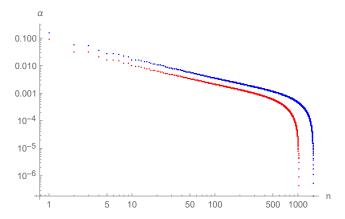


FIGURE 2.4: $\sigma_{i\Delta}$ for the local model in $D = 3$ in the outer diamond. The red dots are for N=2048 and the blue dots are for N=3072.

Our procedure is to truncate the spectrum of $i\Delta$ and $W_{SJ} = \text{Pos}(i\Delta)$ in the big diamond, by retaining only the eigenvectors compatible with the cutoff (2.22). We then restrict both matrices by evaluating them at the points of $\mathcal{C}$ that are in the inner diamond, we call the restricted matrices $\Delta_d$ and $W_d$. At this point, we apply the cutoff again (now as a function of $V_d$ and $N_d$) to the spectrum of $i\Delta_d$, we truncate $W_d$ accordingly and we solve the generalized eigenvalue problem (2.5).

**Local Green functions**

As a first check, we reproduced the results of [137] for the local Green function in two dimensions, see Figure 2.5. The SEE after imposing the cutoff follows a logarithmic law which corresponds to an area law in two spacetime dimensions (the surface of codimension two is a point). Moreover the coefficient of the logarithm is approximately $1/3$ as in [129, 137] and in the traditional computation [52], if we exclude data for small values of the density.

In Figure 2.6 the entropy is plotted for the local model in $D = 3$ for various choices of the cutoff. We find that, if we include part of the small eigenvalues of $i\Delta$ that do not follow the power law behavior, the growth of the entropy is faster than an area law, almost with $\rho(\propto N_d)$. Increasing the coefficient $a$ in front of the cutoff, the entropy starts growing at a slower rate, up to the point in which it becomes linear with $\rho^{1/3}(\propto \ell)$, essentially following an area law.

Similar considerations apply for $D = 4$. We find, for $a = 1/4$, an approximate scaling with $\rho^{1/2} = \ell^{-2}$, as it is shown in Figure 2.7. After imposing the cutoff, for the typical values of the density that we can explore in $D = 4$ (roughly in the interval $\rho \in [10^3, 10^5]$), we are left with a small number ($\sim 5$, for $\rho \approx 10^4$) of eigenvalues of $i\Delta$ in the small diamond. This is probably the

(A) SEE for the local theory with cutoff $\alpha_{min} = \sqrt{N_d}/(4\pi)$, $S_{\text{fit}} = 1.84 + 0.398 \log \alpha_{\min}$.

(B) Excluding values at low densities. $S_{\text{fit}} = 1.90 + 0.332 \log \alpha_{\min}$.
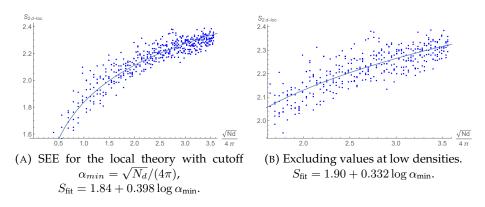
FIGURE 2.5: Area law for the local theory in $D = 2$.



(A) N=3072 and $a = 5^{-1}$.

(B) $S_{\text{fit}} = -0.385 + 0.053\rho^{1/3}$, N=$10^3$-$10^4$.

(C) N=3072 and $a = 10^{-1}$.

(D) $S_{\text{fit}} = -2.05 + 0.22\rho^{1/3} + 0.000021\rho$, N=$10^3$-$1.4 \cdot 10^4$.

(E) N=3072 and $a = 50^{-1}$.

(F) $S_{\text{fit}} = 11.5402 + 0.0045\rho$, N=$10^3$-$1.4 \cdot 10^4$.
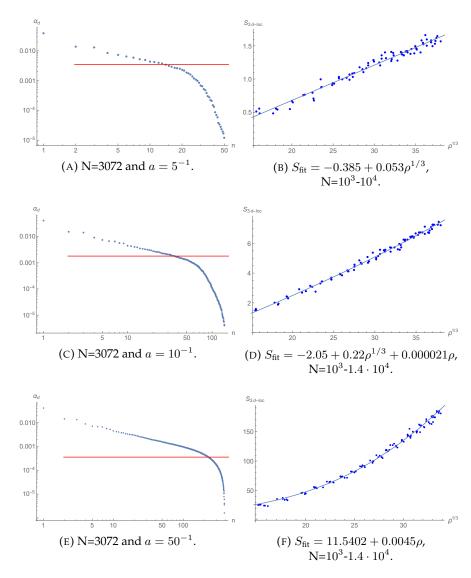
FIGURE 2.6: Local theory in $D = 3$. Plots of the cutoff on $\sigma_{i\Delta}$ and the associated SEE.

source of the fluctuations of the entropy around the scaling with the area in Figure 2.7.

(A) N=5120 and $a = 4^{-1}$.

(B) $S_{\text{fit}} = -0.1654 + 0.0028\rho^{1/2}$,
N=$10^3$-$1.4 \cdot 10^4$.
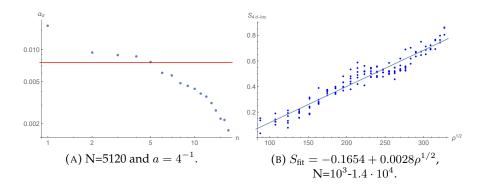
FIGURE 2.7: Local theory in $D = 4$. Plots of the cutoff on $\sigma_{i\Delta}$ and the associated SEE.

**Nonlocal Green functions**

For the nonlocal Green functions, we performed an analogous analysis to that of the local ones, at fixed values of the nonlocality scale $\ell_k$. A crucial difference with respect to the local models is that in the numerical simulations we have to take into account the constraint $\ell_k > \ell = \rho^{-1/D}$. This translates into a lower limit on the sprinkling density $\rho > \ell_k^{-D}$.

For the nonlocal model in two dimensions, we fix $\ell_k = 0.2$ and we find that the cutoff in the spectrum of $i\Delta$ that allows us to recover a logarithmic behavior for the entropy is close to the one of the local theory. In Figure 2.8 we can see that the magnitude of the entropy is also very close to the local case.



(A) N=2048 and $\alpha_{\min} = \sqrt{N_d}/(2\pi)$.

(B) $S_{\text{fit}} = 1.968 + 0.332 \log \alpha_{\min}$.
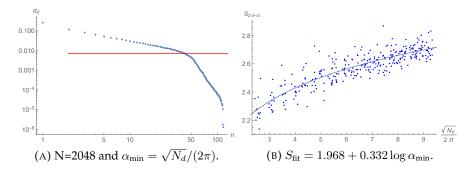
FIGURE 2.8: Nonlocal theory in $D = 2$. Plots of the cutoff on $\sigma_{i\Delta}$ and the associated SEE.

In higher dimensions we again compare the location of the cutoff with the corresponding entropy. For $D = 3$ the resulting area law is shown in Figure 2.9 ($\ell_k = 0.2$). We can see that there is some intermediate phase (around $a = 10^{-1}$) in which the entropy follows a linear scaling with the area only for large $N_d$, while for small densities the growth is slower. This effect does not seem to be present in the local models and therefore could be due to the presence of the nonlocality scale. We will return to this point at the end of this section. For $a = 1/(2\pi)$ this effect goes away and we find an approximate area law $S \propto \rho^{1/3}$. Again, by including part of the small eigenvalues, the entropy appears to grow faster than $\rho^{1/3}$.

(A) N=3072 and $a = (2\pi)^{-1}$.

(B) $S_{\text{fit}} = 3.25 + 0.50\rho^{1/3}$,
N=$2 \cdot 10^3$-$8 \cdot 10^3$.

(C) N=3072 and $a = 10^{-1}$.

(D) $S_{\text{fit}} = -29.76 + 0.23\rho^{1/3} + 17.84 \log \rho^{1/3}$,
N=$10^3$-$10^4$.

(E) N=3072 and $a = 50^{-1}$.

(F) $S_{\text{fit}} = -125.7347 + 11.7394\rho^{1/3} + 0.0042\rho$,
N=$10^3$-$10^4$.
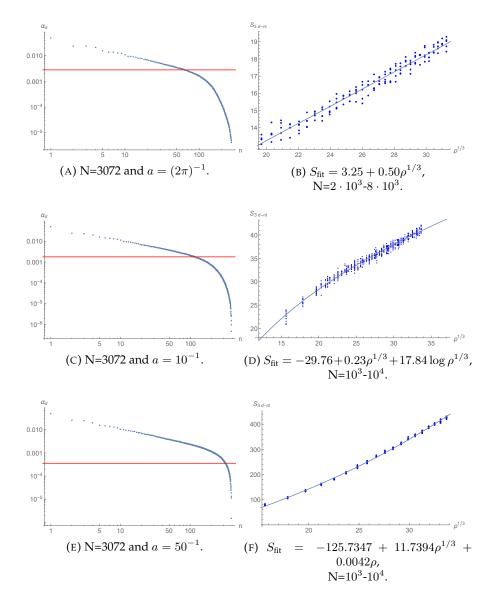
FIGURE 2.9: Nonlocal theory in $D = 3$. Plots of the cutoff on $\sigma_{i\Delta}$ and the associated SEE.

Even for the nonlocal theory in four dimensions we find a phase in which the area law is approximately valid for large densities while the entropy grows slower for small densities, see Figure 2.10. Again, due to the very small number of residual eigenvalues in the small diamond for larger values of $a$ and for the range of densities that we can explore, we do not, yet, have complete data to confirm the presence of a pure area law phase. Nevertheless, preliminary results suggest that the situation is analogous to the case in $D = 3$. In this case the nonlocality scale was fixed to be $\ell_k = 0.15$.

**Dependence on the nonlocality scale**

We dedicate this section to briefly comment on the possible dependence of our entropy results for the non local Green functions on the nonlocality scale $\ell_k$, leaving a more detailed investigation for future works.

(A) N=5120 and $a = 6^{-1}$.

(B) $S_{\text{fit}} = -87.733 - 0.092\rho^{1/2} + 32.398\log\rho^{1/2}$, N=$10^3$-$1.6\cdot10^4$.

(C) N=5120 and $a = 50^{-1}$.

(D) $S_{\text{fit}} = 111.0833 + 2.3666\rho^{1/2} + 0.0017\rho$, N=$10^3$-$10^4$.
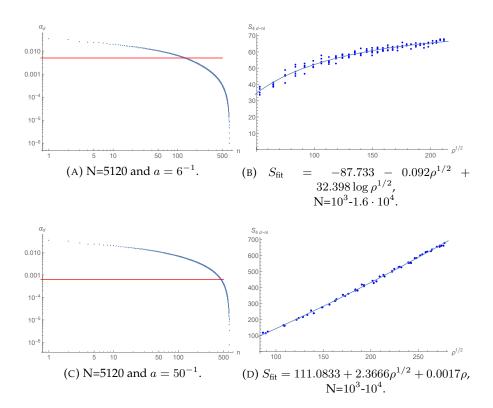
FIGURE 2.10: Nonlocal theory in $D = 4$. Plots of the cutoff on $\sigma_{i\Delta}$ and the associated SEE.

In Figure 2.12 the spectrum of $i\Delta$ for $D = 2, 3$ for various values of $\ell_k$ is plotted. One can see that the dependence on the nonlocality scale is barely noticeable in two dimensions while it is more pronounced in three dimensions. For instance, it could be logarithmic in $D = 2$ and a power law in higher dimensions. In both cases higher values of $\ell_k$ seem to suppress the spectrum. As a consequence of this dependence, the cutoff and hence the SEE, must depend on the nonlocality scale. Given that the the eigenvalues of $i\Delta$ have dimensions of $L^2$ (in the continuum, for both local and nonlocal Green functions), and the entropy is dimensionless, $\ell_k$ should enter in a dimensionless combination with another dimensionful scale.

We pointed out at the beginning of this section that the spectrum of $i\Delta$ is very similar in both the local and nonlocal cases. Although this is qualitatively true, in the nonlocal case it is typically more concave as can be seen in a direct comparison in three dimensions in Figure 2.11. This difference, most likely due to the presence of the nonlocality scale, may be the reason for the non-standard behavior of the entropy at the intermediate scales described previously. If the area law is due to the part of the spectrum in the local theory with constant slope, then it is a logical possibility that in the nonlocal case the variation of the slope would imply a more complex structure of the entropy for different cutoffs.

We postpone additional considerations on this subject to the summary of this chapter.
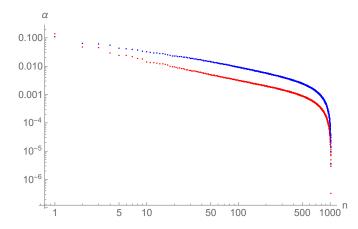
FIGURE 2.11: Comparison of the spectrum of $i\Delta$ between the local and nonlocal model in $D = 3$ ($N = 2048$).



(A) Two dimensional case.



(B) Three dimensional case.
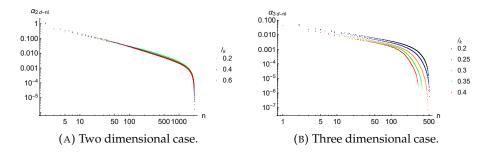
FIGURE 2.12: Dependence of the spectrum of $i\Delta$ on the nonlocality scale.

### 2.4.4 The cutoff and the kernel of the Pauli–Jordan

As we mentioned in the previous section the spectrum of $i\Delta$ on the causal set, compared to the continuum theory with the cutoff, contains a large number of non-zero eigenvalues that interpolate between the power law behavior (common to the continuum) and zero. These values are typically very small as can be seen from the plots in the previous section. Using the cutoff in the discrete framework we are effectively putting all these values inside the kernel of $i\Delta$.

It can be shown that vectors $w \in \mathrm{Ker}(i\Delta)$ define vanishing linear combinations of the field evaluated on the causal set elements, i.e., $\sum w_i \phi^i = 0$, where $i$ runs over the elements of $\mathcal{C}$. In the continuum these relations are just the equations of motion for the scalar field. In the causal set, the number of these vectors (the dimension of the kernel) is rather small compared to the number of elements in $\mathcal{C}$ where the field takes its values [135]. This amounts to saying that the equations of motion for the scalar field in the causal set are a highly underdetermined system, because we have more variables ($\phi^i$) than equations $\dim(\ker(i\Delta))$.

For instance, in two dimensions the number of variables $\phi^i$ grows like $N$, while it can be shown that $\dim(\ker(i\Delta))$ is of order $\ln N$. By applying a cutoff to the eigenvalues of $i\Delta$ we are effectively enlarging its kernel. In particular, using (2.15), $\dim(\ker(i\Delta)) = aN$, where $a \lesssim 1$, see Figure 2.13. We argue that this could be the reason why the entropy has a different scaling with the number of elements once the cutoff is implemented. In the continuum, the entanglement entropy of the small diamond is due to its

correlations with regions (1) and (2) in Figure 2.14. In fact, the lateral diamond are not in causal contact with the central one. The regions (3) and (4) do not contribute because the field there is related to the field in (1), (2) and the central diamond by the equations of motion. In the causal set, the number of relationships between the values of the fields in the regions (1),(2) and (3),(4) does not correspond to the number of links. This might be the source of the larger entropy associated with the inner region when the cutoff is not implemented.



(A) $\dim(\ker i\Delta)_{\text{fit}} = -0.964 + 1.079 \log N$     (B) $\dim(\ker i\Delta)_{\text{fit}} = -71.23 + 0.95N$
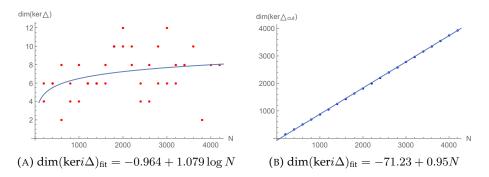
FIGURE 2.13: Dimension of the kernel in $D = 2$.
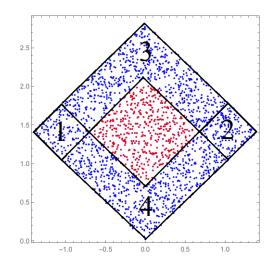


FIGURE 2.14: Regions which are causally connected and disconnected to the inner diamond in $2D$ Minkowski.

Let us now consider another situation: take a causal diamond and divide it in two equal disjoint triangles using its diagonal as in Figure 2.15, we call this configuration a *spacelike partition*. In the continuum, given some initial data on the diameter (which in this case is a Cauchy hypersurface), one can predict all the values of the field in the upper triangle, by using the equations of motion. Indeed, if the field is prepared in the $SJ$ vacuum, one can argue on general grounds that the SEE of the upper triangle with respect to the lower one is zero because they contain the same information, given the causal structure of the diamond.

Therefore the expectation would be that, at least after the cutoff on the spectrum of $i\Delta$ has been implemented, the entropy should be vanishing also in the causal set case.
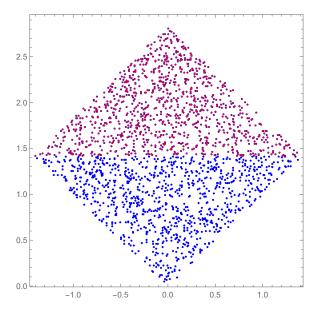
FIGURE 2.15: Upper and lower triangles for a sprinkling of a causal diamond in 2*D* Minkowski, with $N = 2048$.

As it can be seen from Figure 2.16, the behavior of the entropy is instead similar to the entanglement entropy in the case of the inner diamond vs its complement. This means that the additional conditions provided by the enlarged kernel are not enough to take into account all the possible relationships between the field in the upper triangle and in the lower one. What replaces a spatial hypersurface in a causal set is the notion of *maximal anti-chain*. An anti-chain is a set $A$ of elements in $\mathcal{C}$ such that, for all $x, y \in A$ neither $x \prec y$ nor $y \prec x$ (a set of unrelated elements). An anti-chain is then said to be *maximal* when by adding any near elements to it it ceases to be an anti-chain. Nevertheless, a maximal anti-chain $A_{\max}$ cannot play the role of a Cauchy hypersurface because there are going to be links between some points in the future and in the past of $A$ that do not go through elements of $A_{\max}$.[6] Hence, we conclude that the fundamental discretenss and nonlocality of a causal set are the source of this entropy.

Before concluding it is worth pointing out a crucial difference between the spacelike partition and the entanglement entropy. If we do not impose any cutoff in the computation of the entanglement entropy in the continuum and the SEE in the causal set the two cannot be meaningfully compared. This is because while the latter is finite, the former is divergent. On the other hand, in the case just discussed, a comparison between the continuum and the causal set is possible even without a cutoff, because the entropy is finite in both cases.

## 2.5 Summary and outlook

In this chapter we studied the behavior of the entanglement entropy of a scalar field on a causal set using the covariant approach introduced in [134].

---

[6]We remind the reader that a *link* is given by a pair of elements $x, y$, such that $\nexists z : x \prec z \prec y$.

(A) $S_{\text{fit}} = 12.91 + 0.44\rho$.

(B) $a = 10^{-1}$ and $S_{\text{fit}} = -11.9462 + 2.0077\rho^{1/3} + 4.7123 \log \rho^{1/3}$.
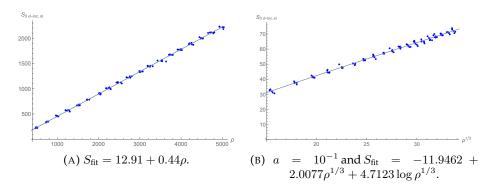
FIGURE 2.16: SEE of a spacelike partition for the nonlocal theory in $D = 3$.

We found that the entanglement entropy follows a spacetime volume law in two, three and four spacetime dimensions for both the local and nonlocal Green functions. By generalizing the two dimensional case, we defined a cutoff on the spectrum of $i\Delta$ that has the right scaling with the density of the causal set, thus allowing us to recover an area law in all cases considered. In particular, by studying the behavior of the entropy while varying the cutoff in such a way to consistently include or exclude parts of the spectrum of $i\Delta$ (this is done by changing the parameter $a$, introduced in Eq. (2.22)), we conclude that the small eigenvalues that do not follow the (expected) behavior of the spectrum in the continuum are responsible for the scaling with the spacetime volume. As a consequence, by retaining only the part of the spectrum that follows a power law with constant slope we find an area law.

We also made a connection between the equations of motion of the scalar field, defined by the vectors in the kernel of $i\Delta$, with the scaling of the entropy with $\rho$. While this interpretation seems to be a reasonable explanation of this effect, it fails when tested against the case that we call *spacelike partition* of the causal set (see Figure 2.16). This is a case in which in the continuum, using the fact that the field is in a pure state and that the diagonal of the diamond is a Cauchy hypersurface, one can show that the spacetime entropy for the upper and lower triangles should be vanishing. Without imposing any cutoff in the causal set case this entropy scales again with the spacetime volume. Therefore, the natural expectation might have been that the entropy should have been zero also in the causal set after the truncation of the spectrum of $i\Delta$. Instead the resulting entropy follows the same scaling with the area that we found in the case of the entanglement entropy of a small diamond vs its complement. This led us to conclude that although the cutoff tames the growth of the entropy as a function of the fundamental cutoff, it is not enough to compensate for the intrinsic nonlocality of the causal set.

If one were to interpret this entropy as an entanglement entropy, the fact the the entropy of the upper triangle equals the entropy of the lower one implies that the SJ vacuum is a pure state. On the other hand, since they are not vanishing, the sum of the two entropies do not equal the entropy of the full diamond, the latter being zero. This means that the two subsystems are correlated and indeed the two regions are causally connected. Given that the diameter of the diamond is not a Cauchy hypersurface in the causal set case (the best that one can do is to introduce a maximal anti-chain, which is

the analogue of a spacelike surface, see Sec. 2.4.4), some of this correlation will not be "recorded" at the boundary of the two regions (the diameter) leading to a non zero entropy even with an enlarged kernel of $i\Delta$.

We then raise the following question: is this kind of entropy also contributing to the entanglement entropy of the small diamond vs its complement? The quick answer is yes, after all it is easy to convince ourselves that these kind of causal correlations should also be present in this case. On the other hand, from the computation of the SEE in two dimensions for the local Green function with the cutoff, the resulting entropy matches almost exactly the traditional computation in the continuum, with a small departure for small densities (see Figure 2.5). Hence, one would be tempted to say that these causal correlations should affect the SEE only for small values of the density, far from the continuum limit. However, the entropy of the spacelike partition (that should be dominated by these kind of correlations) appears to be a monotonically growing function of the density and this fact seems to disfavor this interpretation. If one accepts the fact that causal correlations are an important part in the total budget of the SEE, then one can ask the further question: how is it possible that the computation in the continuum matches the one in the causal set?

We do not yet have a clear argument to explain these results. It is possible that there is a simple way to interpret the outcomes of our computations and we just missed it or, it could be a signal that something in the way QFT is constructed in CST or in the definition of SEE, have to be modified. Before concluding this part of the discussion we would like to point out one particular aspect of this investigation: the strictly exact result for the entanglement entropy in the continuum with the traditional computation based on the knowledge of the state on a spatial Cauchy hypersurface is a divergent. So one can gain very little information by comparing it with the SEE in the causal set unless a cutoff is introduced. Per contra, the spacelike partition, and possibly other configurations, allows us to directly compare results in the causal set with results in the continuum without the need of a cutoff, since both are finite, and they seem to provide important tools for understanding various aspects of CST.

A distinctive feature of the nonlocal models is that the spectrum of $i\Delta$ seems to be more concave than in the local models (for a given value of the density), and this effect appears to be more pronounced as we increase the number of spacetime dimensions. Hence, the behavior of the SEE is richer as we select which eigenvalues to include in our analysis. In particular, we found that for some values the parameter $a$ the SEE follows an area law only for large densities (see Figures 2.9d and 2.10b). This suggests that, at least for these models, the complete SEE may be composed of various phases, dictated by the shape of the spectrum of $i\Delta$. It is possible that the choice of $a$ that corresponds to the continuum result is not the one that gives a pure area law scaling. Indeed, there are some computations (see [110] and the Appendix A) showing that the entanglement entropy of a theory with modified wave operators (Lorentz violating and Lorentz invariant), characterized by the presence of a new UV scale, do follow an area law at high energies but the fundamental area is not given by the square of the cutoff but by a combination of the cutoff and the new UV scale, e.g. it could be a geometric mean of the two. This is a possibility in our theory since the Green functions that we consider in this work give rise to this kind of

modified wave operators in the continuum.

Of course, having the exact computation for the SEE and of the traditional entanglement entropy in the continuum for the Green functions that we considered would also allow one to identify precisely what the cutoff needed for a comparison with the continuum is.

# Chapter 3

# Polymer scalar fields in Loop Quantum Gravity

## 3.1 Introduction

In the Introduction to this thesis, we briefly discussed how different approaches to QG realize the paradigm of the fundamental discreteness of spacetime in different ways, focusing in particular on the difference between CST and LQG. In the first case, fundamental discreteness is a built in feature and it is imposed in a explicitly covariant fashion, i.e. by discretizing spacetime as a whole. In LQG instead, fundamental discreteness is a byproduct of the quantization, i.e., operators associated with geometrical properties of space have discrete spectra.

We dedicated Chapter 2 to the study of the effect of the covariant (and Lorentz invariant) discrete structure of CST on the entanglement entropy of scalar fields. In this chapter, we will introduce the first steps of our investigation in the direction of formulating a dynamics for a scalar field in LQG. We will see that there are two major factors causing a departure from the standard description: the discreteness of space provided by the graph $\Gamma$, defined by the node of a spin network state of the quantum geometry, where the field takes values and a non standard quantization, known as *polymer quantization*, which is suitable for a background independent quantization of matter fields (a real free scalar field in our case). The final goal is to understand how these ingredients affect the dynamics of the scalar field with particular attention to the fate of Lorentz symmetry.

The computation that we are going to present here is not complete and there is a certain number of assumptions made to simplify the problem that we will highlight along the way. Nevertheless, we will be able to draw some general conclusions on the basis of our results.

In the first part we will review polymer quantization and the relevant techniques used to regularize and quantize the matter contribution to the scalar constraint. In the second part we will define an effective Hamiltonian, based on the assumption that there is no backreaction on the geometry, and use it the derive the equations of motion for the scalar field. In the final part we will discuss our results and comment on possible future developments.

## 3.2 Polymer quantization of a scalar field

In this section, we will review the basics of polymer quantization applied to a real scalar field, loosely following [47].

The action for a minimally couple scalar field reads

$$S^{(\phi)} = \frac{1}{2\lambda} \int_{\mathcal{M}} d^D x \, \sqrt{-g} \, (g^{\mu\nu} \partial_\mu \phi \partial_\nu \phi - V(\phi)), \tag{3.1}$$

where $\lambda$ is coupling constant of dimensions $\hbar^{-1}$, and $g$ is the determinant of the spacetime metric. Note that with this convention the scalar field has dimensions $L^{1-D/2}$.

The Legendre transform gives the following Hamiltonian in the ADM formalism:

$$\begin{aligned} H^{(\phi)} = \int_\Sigma d^{D-1} x \left[ N^a \pi \partial_a \phi + N \left( \frac{\lambda}{2\sqrt{q}} \pi^2 + \frac{\sqrt{q}}{2\lambda} q^{ab} \partial_a \phi \partial_b \phi \right. \right. \\ \left. \left. + \frac{\sqrt{q}}{2\lambda} V(\phi) \right) \right] = \int_{\Sigma_t} d^{D-1} x \left( N^a \mathcal{V}_a^{(\phi)} + N H_{sc}^{(\phi)} \right), \end{aligned} \tag{3.2}$$

where $\Sigma$ is a constant time spatial slice. $N$ and $N_a$ are the lapse function and the shift vector respectively, while $\mathcal{V}_a^{(\phi)}$ and $H_{sc}^{(\phi)}$ are the contributions of the scalar field to the vector and scalar constraints. $q$ is the determinant of the spatial metric and $\pi$ is the conjugate momentum to the scalar field which in our convention has dimension of $L^{-D/2}$.

The total vector constraint is the sum of $\mathcal{V}_a^{(\phi)}$ with the gravitational part and it generates (spatial) diffeomorphisms. $H_{sc}^{(\phi)}$ is the matter field part of the smeared scalar constraint and it contains the dynamics of the field in the diffeo-invariant phase space. It can be written as:

$$H_{sc}^{(\phi)}[N] := H_{kin}^{(\phi)}[N] + H_{der}^{(\phi)}[N] + H_{pot}^{(\phi)}[N], \tag{3.3}$$

where

$$H_{kin}^{(\phi)}[N] := \int_{\Sigma_t} d^{D-1} x \, N \left( \frac{\lambda}{2\sqrt{q}} \pi^2 \right), \tag{3.4}$$

$$H_{der}^{(\phi)}[N] := \int_{\Sigma_t} d^{D-1} x \, N \left( \frac{\sqrt{q}}{2\lambda} q^{ab} \partial_a \phi \partial_b \phi \right), \tag{3.5}$$

$$H_{pot}^{(\phi)}[N] := \int_{\Sigma_t} d^{D-1} x \, N \left( \frac{\sqrt{q}}{2\lambda} V(\phi) \right). \tag{3.6}$$

We quantize the system of gravity and matter by using the techniques described in [145, 147] for LQG adapted to QRLG. The total Hilbert space is given by[1]

$$\mathcal{H}_{kin}^{(tot)} =^R \mathcal{H}_{kin}^{(gr)} \otimes \mathcal{H}_{kin}^{(\phi)}, \tag{3.7}$$

the latter being the following Hilbert space:

$$\mathcal{H}_{kin}^{(\phi)} := \overline{\{a_1 U_{\pi_1} + ... a_n U_{\pi_n} : a_i \in \mathbb{C}, \, n \in \mathbb{N}\}}. \tag{3.8}$$

To define this Hilbert space, the polymer variable $\langle \phi | U_\pi \rangle = U_\pi(\phi)$ representing the scalar field $\phi$ is assigned to every function $\pi : \Sigma \to \mathbb{R}$ of finite support $\{v_1, ..., v_n\}$ and it can be considered as an element of the Hilbert

---

[1]$R$ refers to the symmetry-reduced model, see Section 1.3.2.

space above, whose states are defined as

$$U_\pi(\phi) = e^{i\sum_{v\in\Sigma}\pi_v\phi_v} := \langle\phi|\pi\rangle, \tag{3.9}$$

where $v \in \Sigma$ labels a countable set of points $\{v_1, ..., v_n\}$ in the manifold $\Sigma$, and $\phi_v = \{\phi(v_1), ..., \phi(v_n)\}$ is the value of the field at those points. The normalization is provided given two states $U_\pi(\phi)$ and $U_{\pi'}(\phi)$ with support on the same set of points by the following scalar product

$$\langle\pi|\pi'\rangle = \delta_{\pi,\pi'}. \tag{3.10}$$

Therefore the two states are orthogonal unless they are defined on the same set of points and the have the same values for the functions $\pi$ and $\pi'$ at those points.

The basic variables act as follows

$$\hat{U}_\pi|\pi'\rangle = |\pi + \pi'\rangle, \tag{3.11}$$

$$\hat{\Pi}(V)|\pi\rangle = \hbar\sum_{v\in V}\pi_v|\pi\rangle, \tag{3.12}$$

with $\Pi(V)$ being the scalar field momentum smeared over a volume $V \in \Sigma$. It can be written as

$$\hat{\Pi}(V) = \int_V d^D x\,\hat{\pi}(x). \tag{3.13}$$

Note that $\Pi(V)$ has dimensions of $L^{D-1}$ and it is a density of weight zero, given that $\pi$ transforms as a measure.

In the case of a single point $x$, one denotes the states as

$$\langle\phi|x;\pi\rangle = e^{i\pi_x\phi_x}, \tag{3.14}$$

for which the scalar product reads

$$\langle x;\pi|y;\pi'\rangle = \delta_{x,y}\delta_{\pi,\pi'}. \tag{3.15}$$

The action of the basic operators is analogous to Eq.s (3.11). The smeared momentum operator around a point $x$ as

$$\Pi(x) := \int d^{D-1}y\,\chi_\epsilon(x,y)\pi(y), \tag{3.16}$$

where we introduced the characteristic function $\chi_\epsilon(x,y)$ of the box $B_\epsilon(x)$ centered in $x$ with coordinate volume $\epsilon^{D-1}$. Precisely,

$$\mathbf{V}(B_\epsilon(x)) := \mathbf{V}(x,\epsilon) = \epsilon^{D-1}\sqrt{q} + \mathcal{O}(\epsilon^D), \tag{3.17}$$

which allows us to smear a function at the point $x$ around an infinitesimal neighborhood, such that

$$f(x) = \int d^{D-1}\delta^{(D-1)}(x-y)\,f(y) = \lim_{\epsilon\to 0}\frac{1}{\epsilon^{D-1}}\int d^3y\,\chi_\epsilon(x,y)f(y). \tag{3.18}$$

The full Hilbert space $\mathcal{H}_{kin}^{(\phi)} := L_2(\overline{\mathbb{R}}_{Bohr}^\Sigma)$ can be obtained from the single point one $L_2(\overline{\mathbb{R}}_{Bohr})$, where $\overline{\mathbb{R}}_{Bohr}$ denotes the Bohr compactification of a

line, and the Bohr measure is defined as

$$\int_{\overline{\mathbb{R}}_{Bohr}} d\mu_{Bohr}(\phi)e^{i\pi_x\phi_x} = \delta_{0,x}. \tag{3.19}$$

This method for treating scalar fields realizes a polymer representation in the momentum polarization (also known as the point-holonomy representation) [22, 27, 59, 86, 87].

This prescription closely follows the one that leads to the spin network states. Indeed, one can think: i) to the set of points $v$ as the graph $\Gamma$, ii) to the variables $\pi_v$ as the analogous of the spin coloring $j_l$ for the links $l$ of a spin network with links $l \in \Gamma$, iii) to (3.11) as the counterpart of the holonomy-flux algebra. Indeed, in both cases, the field $\phi$ and the connection $A$ are not well defined operators on their respective Hilbert spaces, but only their holonomized versions. The latter act by multiplication creating new point holonomies in the case of the scalar field and new links in the gravitational case. The conjugate variables ($\pi$ and $E$) are well defined operators that read as eigenvalues the coloring of the holonomized field, i.e., the value of the field $\pi_v$ of the point holonomies base on the "graph" $v$ and the value of the spins of the holonomies based on the graph $\Gamma$ respectively. As in full LQG, the $\pi$ fields have support on the set of nodes of the lattice $\Gamma$ (a cuboidal graph in our case).

### 3.2.1 Regularization and quantization of the scalar Hamiltonian constraint

In this part we will briefly mention some relevant techniques used to quantize the classical Hamiltonian (3.3) and we refer the reader to [22, 27, 47] for more details. For the sake of simplicity we restrict our analysis to $3 + 1$ dimensions.

Before quantizing the scalar part of the Hamitonian constraint we need to regularize it. This procedure is carried on by rewriting (3.3) in terms of holonomies and fluxes for the gravitational part and point-holonomies and smeared momenta for the parts involving the scalar field.

The gravitational part is regularized using methods developed for the full theory, restricted to a cuboidal graph [47]. In this description, matter coupled to a dynamical spacetime is regularized by a reduction to fields coupled to a dynamical lattice.

We will now consider a free massless scalar field, so that the potential term in (3.3) is zero. We therefore need to regularize the kinetic and derivative parts, $H_{kin}^{(\phi)}$ and $H_{der}^{(\phi)}$. First of all we need to replace the spatial metric with the triads $e_a^i$. To do so we can use the following identities

$$\frac{e^2}{q} = 1, \quad \sqrt{q}q^{ab} = \frac{1}{4\sqrt{q}}\epsilon_{ijk}\epsilon^{acd}e_c^j e_d^k \epsilon_{lm}^i \epsilon^{bef} e_e^l e_f^m, \tag{3.20}$$

and we introduce the volume $\mathbf{V}(R)$ of a region $R$ using its definition

$$\mathbf{V}(R) = \int_R d^3x \sqrt{q}. \tag{3.21}$$

The resulting expression reads as

$$
\begin{aligned}
H_{sc}^{(\phi)} = \lim_{\epsilon \to 0} \Bigg[ &\frac{\lambda}{2} \int d^3x N(x)\pi(x) \int d^3y \pi(y) \int d^3t \frac{e}{(\mathbf{V}(t,\epsilon))^{3/2}} \\
&\times \int d^3u \frac{e}{(\mathbf{V}(u,\epsilon))^{3/2}} \chi_\epsilon(x,y)\chi_\epsilon(t,x)\chi_\epsilon(u,y) \\
&+ \frac{1}{8\lambda} \int d^3x N(x)\epsilon_{ijk}\epsilon^{acd}\partial_a\phi(x) \frac{e_c^j}{(\mathbf{V}(x,\epsilon))^{1/4}} \frac{e_d^k}{(\mathbf{V}(x,\epsilon))^{1/4}} \\
&\times \int d^3y \epsilon_{lm}^i \epsilon^{bef}\partial_b\phi(y) \frac{e_e^l}{(\mathbf{V}(y,\epsilon))^{1/4}} \frac{e_f^m}{(\mathbf{V}(y,\epsilon))^{1/4}} \chi_\epsilon(x,y) \Bigg].
\end{aligned}
\tag{3.22}
$$

To remove the denominators one uses the Thiemann's trick [146], given by the following expression

$$
\begin{aligned}
e_a^i(x) &= 2\frac{\delta \mathbf{V}(R)}{\delta E_i^a} = \frac{2}{n(\mathbf{V}(R))^{n-1}}\frac{\delta (\mathbf{V}(R))^n}{\delta E_i^a} \\
&= \frac{4}{n\gamma\kappa(\mathbf{V}(R))^{n-1}}\{A_a^i(x),(\mathbf{V}(R))^n\}.
\end{aligned}
\tag{3.23}
$$

Now, we need to rewrite the Hamiltonian so that it can live on a discrete quantum geometry. A method of discretization of the scalar constraint via a triangularization of the spatial manifold has been developed for pure gravity [148] and for gravity coupled to a scalar field [147]. The idea is to replace the summation $\int_\Sigma$ with the sum over all ordered tetrahedra. The sum over tetrahedra becomes the sum over all the nodes $v$ of the triangulation and over all the tetrahedra $\Delta_{l,l',l''}$ created by triple of links emanating from the nodes $v$. Given a cubolation (see Section 1.3.2 for an introduction to the QRLG framework), each node $v$ is always surrounded by three pairs of links oriented along fixed perpendicular directions. They always create eight tetrahedra around the node. Finally the integration over each tetrahedron $\int_{\Delta_{l,l',l''}}$ turns into the sum over the eight possibilities of choosing a triple of perpendicular links among each tetrahedron of the triangulation $\Delta(v)$ at each node $v$. Once this procedure has been performed, one uses the following expansion

$$
\text{Tr}(\tau^i h_{l_a}^{-1}\{\mathbf{V}^n(R),h_{l_a}\}) = -\text{Tr}(\tau^i \epsilon\{A_a,\mathbf{V}^n(R)\} + \mathcal{O}(\epsilon^2)) \approx \frac{1}{2}\epsilon\{A_a^i,\mathbf{V}^n(R)\},
\tag{3.24}
$$

to rewrite the parts with the connections in terms of $SU(2)$ holonomies. Here Tr denotes the trace over $SU(2)$ algebra and $\tau^i = -\frac{i}{2}\sigma^i$, where $\sigma^i$ are Pauli matrices.

As a last step before the quantization we need to rewrite also the spatial derivatives of the scalar field as operators acting on the matter Hilbert space, using point-holonomies $U(x) = e^{i\alpha\phi(x)}$, where $\alpha$ has dimensions of $L$. In particular, following [147], one has that $d\phi(x) = U^{-1}(x)dU(x)/\imath\alpha$ and the derivative of the scalar field at the vertex $v$ can be approximated by the following expression

$$
\partial_p\phi(v) \approx -\frac{\imath}{2\epsilon\alpha}\frac{U(v+\vec{e}_p) - U(v-\vec{e}_p)}{U(v)} = \frac{e^{\imath\alpha(\phi_{v+\vec{e}_p}-\phi_v)} - e^{\imath\alpha(\phi_{v-\vec{e}_p}-\phi_v)}}{2\imath\epsilon\alpha},
\tag{3.25}
$$

where $\phi_{v+\vec{e}_p}$ is the field at the point $v + \vec{e}_p$, which is the nearest node of $v$ along the link $e_p$ of length $\epsilon$. The two relevant limits are now given by the following expressions

$$\lim_{\epsilon \to 0} \frac{1}{2i\epsilon\alpha} \frac{U(v + \vec{e}_p) - U(v - \vec{e}_p)}{U(v)} = \partial_p \phi(x) + \mathcal{O}(\epsilon), \tag{3.26}$$

$$\lim_{\alpha \to 0} \frac{1}{2i\epsilon\alpha} \frac{U(v + \vec{e}_p) - U(v - \vec{e}_p)}{U(v)} = \frac{\phi(v + \vec{e}_p) - \phi(v - \vec{e}_p)}{2\epsilon} + \mathcal{O}(\alpha). \tag{3.27}$$

The scalar field contribution to the scalar constraint is quantized by the canonical method: the cubolation of the spatial manifold is given by the graph $\Gamma$ at which the state is based (links and nodes of the cubolation are links and nodes of $\Gamma$), while holonomies, volumes, and matter variables are changed into quantum operators acting on states belonging to the total Hilbert space:

$$\hat{H}|\Gamma; m_l, i_v; \pi\rangle_R = (\hat{H}^{(\phi)}_{kin} + \hat{H}^{(\phi)}_{der})|\Gamma; m_l, i_v; \pi\rangle_R. \tag{3.28}$$

Once the Poisson brackets have been substituted by quantum commutators and the limit $\epsilon \to 0$ has been performed (removing the dependence on the regulator), the action of the total scalar constraint operator reads as

$$\hat{H}^{(\phi)}|\Gamma; m_l, i_v; \pi\rangle_R = \sum_v N_v \left( \frac{2^{11}\lambda}{(8\pi\gamma l_p^2)^{\frac{3}{2}}} \Sigma_v^{(x)} \Sigma_v^{(y)} \Sigma_v^{(z)} \left( \Delta_v^{(x),\frac{1}{4}} \Delta_v^{(y),\frac{1}{4}} \Delta_v^{(z),\frac{1}{4}} \right)^2 \hat{\Pi}_v^2 \right.$$

$$+ \frac{2^{11}(8\pi\gamma l_p^2)^{\frac{1}{2}}}{3^4\lambda} \left( \Sigma_v^{(x)} \Sigma_v^{(y)} \Sigma_v^{(z)} \right)^{\frac{3}{4}}$$

$$\times \left[ \left( \Sigma_v^{(x)} \right)^{\frac{3}{4}} \left( \Delta_v^{(y),\frac{3}{8}} \right)^2 \left( \Delta_v^{(z),\frac{3}{8}} \right)^2 \left( \frac{e^{i\alpha\left(\hat{\phi}_{v-\vec{e}_x}-\hat{\phi}_v\right)} - e^{i\alpha\left(\hat{\phi}_{v+\vec{e}_x}-\hat{\phi}_v\right)}}{2i} \right)^2 \right.$$

$$+ \left( \Sigma_v^{(y)} \right)^{\frac{3}{4}} \left( \Delta_v^{(x),\frac{3}{8}} \right)^2 \left( \Delta_v^{(z),\frac{3}{8}} \right)^2 \left( \frac{e^{i\left(\hat{\phi}_{v-\vec{e}_y}-\hat{\phi}_v\right)} - e^{i\left(\hat{\phi}_{v+\vec{e}_y}-\hat{\phi}_v\right)}}{2i} \right)^2$$

$$+ \left. \left( \Sigma_v^{(z)} \right)^{\frac{3}{4}} \left( \Delta_v^{(x),\frac{3}{8}} \right)^2 \left( \Delta_v^{(y),\frac{3}{8}} \right)^2 \left( \frac{e^{i\left(\hat{\phi}_{v-\vec{e}_z}-\hat{\phi}_v\right)} - e^{i\left(\hat{\phi}_{v+\vec{e}_z}-\hat{\phi}_v\right)}}{2i} \right)^2 \right]$$

$$+ \left. \frac{(8\pi\gamma l_p^2)^{\frac{3}{4}}}{2\lambda} \left( \Sigma_v^{(x)} \Sigma_v^{(y)} \Sigma_v^{(z)} \right)^{\frac{1}{2}} \hat{V}(\phi_v) \right) |\Gamma; m_l, i_v; U_\pi\rangle_R$$

$$\tag{3.29}$$

## 3.3 Effective dynamics

We are interested in finding some kind of effective dynamics for the scalar field $\phi(x)$, or some expression of the field in terms of the point-holonomies $U_x(\phi)$, in this framework. As stated in the introduction to this chapter, there are a lot of issues that we need to consider and we look at this procedure as a first step in the construction of a consistent model.

First of all, we neglect the backreaction of matter on the geometry. This means that the gravitational part of the state $|\Gamma; m_l, i_v\rangle_R \otimes |\Gamma; \pi\rangle_R$ evolves

according to the following equation

$$\imath\frac{\partial}{\partial t}|\Gamma; m_l, i_v\rangle_R = \hat{H}^{(gr)}|\Gamma; m_l, i_v\rangle_R, \tag{3.30}$$

where $\hat{H}^{(gr)}$ is the gravitational contribution to the scalar constraint. Now, we consider an effective Hamiltonian for the matter sector given as $\hat{H}_{\text{eff}} =_R \langle\Gamma; m_l, i_v|\hat{H}^{(\phi)}|\Gamma; m_l, i_v\rangle_R$, effectively tracing out the gravitational degrees of freedom. Given that we are constructing a toy model, we will only consider one spatial direction and suppress the other two.

The effective Hamiltonian for the scalar field is then give by the following explicit expression

$$\begin{aligned}
\hat{H}_{\text{eff}} = \sum_v N_v &\left[ \frac{2^{11}\lambda}{(8\pi\gamma l_p^2)^{\frac{3}{2}}} \Sigma_v^{(x)}\Sigma_v^{(y)}\Sigma_v^{(z)} \left(\Delta_v^{(x),\frac{1}{4}}\Delta_v^{(y),\frac{1}{4}}\Delta_v^{(z),\frac{1}{4}}\right)^2 \hat{\Pi}_v^2 \right. \\
&+ \frac{2^{11}(8\pi\gamma l_p^2)^{\frac{1}{2}}}{3^4\lambda} \left(\Sigma_v^{(x)}\Sigma_v^{(y)}\Sigma_v^{(z)}\right)^{\frac{3}{4}} \left(\Sigma_v^{(x)}\right)^{\frac{3}{4}} \left(\Delta_v^{(y),\frac{3}{8}}\right)^2 \left(\Delta_v^{(z),\frac{3}{8}}\right)^2 \\
&\left. \times \left(\frac{e^{\imath\alpha\left(\hat{\phi}_{v-\vec{e}_x}-\hat{\phi}_v\right)} - e^{\imath\alpha\left(\hat{\phi}_{v+\vec{e}_x}-\hat{\phi}_v\right)}}{2\imath\alpha}\right)^2 \right].
\end{aligned} \tag{3.31}$$

We mimic the standard procedure by writing Hamilton's equations of motion for the point-holonomy and the smeared momentum using the effective Hamiltonian (3.31). We then compute the expectation values of the evolved operators (in the Heisenberg picture) in a gaussian state for matter. The gaussian state is defined as [2]

$$|\phi\rangle_{\mathcal{G}} = \prod_{v_i} A_i \int d\pi_i e^{-\frac{(\pi_i-\pi_i^0)^2}{2\sigma^2}+\imath\phi_i^0\pi_i}|\pi(v_i)\rangle. \tag{3.32}$$

The state is peaked around some configuration $(\phi_0, \pi_0)$, where $v_i = \{v_1, ..., v_n\}$ is the set of vertices and $A_i = (\pi)^{-1/4}\sigma_i^{-1/2}$ is the normalization of the state.

We therefore compute the following operators

$$\hat{\dot{U}}_v = \imath\left[\hat{H}_{\text{eff}}, \hat{U}_v\right], \tag{3.33}$$

$$\hat{\dot{\Pi}}_v = \imath\left[\hat{H}_{\text{eff}}, \hat{\Pi}_v\right], \tag{3.34}$$

using the commutation relations between the polymer variables given by

$$\left[\hat{\Pi}(V), \hat{U}_x(\phi)\right] = \alpha f_V(x)\hat{U}_x(\phi). \tag{3.35}$$

---

[2]Strictly speaking we should consider a summation over $\pi_i$. We choose to integrate for simplicity.

The results are

$$\dot{\hat{U}}_v = \imath \alpha N_v \frac{A_v}{2} \left( \hat{\Pi}_v \hat{U}_v + \hat{U}_v \hat{\Pi}_v \right) = \imath \alpha N_v \frac{A_v}{2} \left( 2\hat{U}_v \hat{\Pi}_v + \alpha \hat{U}_v \right), \qquad (3.36)$$

$$\dot{\hat{\Pi}}_v = \frac{1}{4\imath\alpha} N_v B_v X_v \left( \frac{U_{v+\vec{e}_x} - U_{v-\vec{e}_x}}{U_v} \right)^2 \qquad (3.37)$$

$$+ \frac{1}{4\imath\alpha} N_{v+\vec{e}_x} B_{v+\vec{e}_x} X_{v+\vec{e}_x} \frac{U_{v+2\vec{e}_x} - U_v}{U_{v+\vec{e}_x}^2} U_v$$

$$- \frac{1}{4\imath\alpha} N_{v-\vec{e}_x} B_{v-\vec{e}_x} X_{v-\vec{e}_x} \frac{U_v - U_{v-2\vec{e}_x}}{U_{v-\vec{e}_x}^2} U_v,$$

where

$$A_v = \frac{2^{12}\lambda}{(8\pi\gamma l_p^2)^{\frac{3}{2}}} \Sigma_v^{(x)} \Sigma_v^{(y)} \Sigma_v^{(z)} \left( \Delta_v^{(x),\frac{1}{4}} \Delta_v^{(y),\frac{1}{4}} \Delta_v^{(z),\frac{1}{4}} \right)^2, \qquad (3.38)$$

$$B_v = \frac{2^{12}(8\pi\gamma l_p^2)^{\frac{1}{2}}}{3^4\lambda} \left( \Sigma_v^{(x)} \Sigma_v^{(y)} \Sigma_v^{(z)} \right)^{\frac{3}{4}}, \qquad (3.39)$$

$$X_v = \left( \Sigma_v^{(x)} \right)^{\frac{3}{4}} \left( \Delta_v^{(y),\frac{3}{8}} \right)^2 \left( \Delta_v^{(z),\frac{3}{8}} \right)^2. \qquad (3.40)$$

Now, for simplicity, we can take the coefficients of the geometry $N, A, B, X$ to be the same for every $v_i$ ($N_{v+\vec{e}_x} = N_v$ for example), since our purpose is to find an effective dynamics in a homogeneous and isotropic background.

We now compute the expectation values of the Hamilton's equations (3.33) in the gaussian state (3.32). The general expression for the evolution of the expectation value in the Heisenberg picture is the following

$$\langle \dot{\hat{A}} \rangle = \frac{d}{dt} \langle \hat{A} \rangle = \imath \langle \left[ \hat{H}, \hat{A} \right] \rangle. \qquad (3.41)$$

Using (3.36), the right-hand sides read as

$$\langle \dot{\hat{U}}_v \rangle_{\mathcal{G}} = \imath N_v A_v \, \alpha \, \pi_0 \, e^{-\frac{\alpha^2}{4\sigma} - \imath\alpha\phi_v^0}, \qquad (3.42)$$

$$\langle \dot{\hat{\Pi}}_v \rangle_{\mathcal{G}} = \frac{1}{4\imath\alpha} N_v B_v X_v \left[ e^{-2\imath\alpha(\phi_{v+\vec{e}_x}^0 - \phi_v^0) - 2\frac{\alpha^2}{\sigma^2}} + e^{-2\imath\alpha(\phi_{v-\vec{e}_x}^0 - \phi_v^0) - 2\frac{\alpha^2}{\sigma^2}} \right. \qquad (3.43)$$

$$- 2e^{-\imath\alpha(\phi_{v+\vec{e}_x}^0 + \phi_{v-\vec{e}_x}^0 - 2\phi_v^0) - \frac{3}{2}\frac{\alpha^2}{\sigma^2}} - e^{-2\imath\alpha(\phi_v^0 - \phi_{v-\vec{e}_x}^0) - 2\frac{\alpha^2}{\sigma^2}}$$

$$+ e^{-\imath\alpha(\phi_{v-2\vec{e}_x}^0 + \phi_v^0 - 2\phi_{v-\vec{e}_x}^0) - \frac{3}{2}\frac{\alpha^2}{\sigma^2}} + e^{-\imath\alpha(\phi_{v+2\vec{e}_x}^0 + \phi_v^0 - 2\phi_{v+\vec{e}_x}^0) - \frac{3}{2}\frac{\alpha^2}{\sigma^2}}$$

$$\left. - e^{-2\imath\alpha(\phi_v^0 - \phi_{v+\vec{e}_x}^0) - 2\frac{\alpha^2}{\sigma^2}} \right].$$

Note that, for the sake of simplicity, the integrals in the gaussian state (3.32) over the variable $\pi_i$ are taken from $-\infty$ to $+\infty$. The second equation

can also be written as

$$
\begin{aligned}
\langle \hat{\dot{\Pi}}_v \rangle_{\mathcal{G}} =& \frac{1}{4\imath\alpha} N_v B_v X_v \left[ e^{-\frac{2\alpha^2}{\sigma^2}} \left( e^{-2\imath\alpha\Delta_1^+} + e^{2\imath\alpha\Delta_1^-} - e^{-2\imath\alpha\Delta_1^-} - e^{2\imath\alpha\Delta_1^+} \right) \right. \\
& \left. + e^{\frac{-3\alpha^2}{2\sigma^2}} \left( e^{-\imath\alpha\Delta_2^+} + e^{-\imath\alpha\Delta_2^-} - 2e^{-\imath\alpha\Delta_2} \right) \right] \\
=& N_v B_v X_v \left[ \frac{e^{\frac{-2\alpha^2}{\sigma^2}}}{2\alpha} \left( \sin(2\alpha\Delta_1^-) - \sin(2\alpha\Delta_1^+) \right) \right. \\
& \left. + \frac{e^{\frac{-3\alpha^2}{2\sigma^2}}}{4\imath\alpha} \left( e^{-\imath\alpha\Delta_2^+} + e^{-\imath\alpha\Delta_2^-} - 2e^{-\imath\alpha\Delta_2} \right) \right],
\end{aligned}
\tag{3.44}
$$

where

$$
\begin{aligned}
\Delta_1^+ &= \phi(v+e) - \phi(v), \\
\Delta_1^- &= \phi(v) - \phi(v-e), \\
\Delta_2^+ &= \phi(v+2e) + \phi(v) - 2\phi(v+e), \\
\Delta_2^- &= \phi(v-2e) + \phi(v) - 2\phi(v-e), \\
\Delta_2 &= \phi(v+e) + \phi(v-e) - 2\phi(v) = \Delta_1^+ - \Delta_1^-.
\end{aligned}
$$

are finite differences that reduce to first and second derivatives for $e \to 0$ times the appropriate power of $\epsilon = |e|$.

The expectation values of the left-hand sides of (3.33) are given by the following expressions

$$
\frac{d}{dt} \langle \hat{U}_v \rangle_{\mathcal{G}} = -\imath\alpha \dot{\phi}_v^0 e^{-\imath\alpha\phi_v^0 - \frac{\alpha^2}{\sigma^2}} = -\imath\alpha \dot{\phi}_v^0 \langle \hat{U} \rangle_{\mathcal{G}},
\tag{3.45}
$$

$$
\frac{d}{dt} \langle \hat{\Pi}_v \rangle_{\mathcal{G}} = \dot{\pi}_v^0,
\tag{3.46}
$$

where we assumed that $\sigma$ and $\alpha$ are time independent.

Finally, the expectation values of the two Hamilton equations (3.33) are

$$
\dot{\phi}_v^0 = -N_v A_v \pi_0,
\tag{3.47}
$$

$$
\begin{aligned}
\dot{\pi}_v^0 =& N_v B_v X_v \left[ \frac{e^{\frac{-2\alpha^2}{\sigma^2}}}{2\alpha} \left( \sin(2\alpha\Delta_1^-) - \sin(2\alpha\Delta_1^+) \right) \right. \\
& \left. + \frac{e^{\frac{-3\alpha^2}{2\sigma^2}}}{4\imath\alpha} \left( e^{-\imath\alpha\Delta_2^+} + e^{-\imath\alpha\Delta_2^-} - 2e^{-\imath\alpha\Delta_2} \right) \right].
\end{aligned}
\tag{3.48}
$$

There is another way to obtain the two equations (3.47) and (3.48). One can compute the expectation value of the effective Hamiltonian (3.31) on the gaussian state (3.32) and obtain a semiclassical expression $\langle \hat{H}_{\text{eff}} \rangle_{\mathcal{G}}$. Then equations (3.47) and (3.48) emerge from the classical field equations

$$
\dot{\phi}_v^0 = \frac{\delta \langle \hat{H}_{\text{eff}} \rangle_{\mathcal{G}}}{\delta \pi_v^0},
\tag{3.49}
$$

$$
\dot{\pi}_v^0 = -\frac{\delta \langle \hat{H}_{\text{eff}} \rangle_{\mathcal{G}}}{\delta \phi_v^0}.
\tag{3.50}
$$

We verified explicitly that the two procedures lead to the same set of equations.

Combining together Hamilton's equations, the second order equation of motion read as

$$\frac{\ddot{\phi}_v^0}{N_v\,A_v} = -N_v B_v X_v \left[ \frac{e^{\frac{-2\alpha^2}{\sigma^2}}}{2\alpha} \left( \sin(2\alpha\Delta_1^-) - \sin(2\alpha\Delta_1^+) \right) \right. \tag{3.51}$$
$$\left. + \frac{e^{\frac{-3\alpha^2}{2\sigma^2}}}{4\imath\alpha} \left( e^{-\imath\alpha\Delta_2^+} + e^{-\imath\alpha\Delta_2^-} - 2e^{-\imath\alpha\Delta_2} \right) \right].$$

In the limit $\alpha \to 0$ and $\epsilon \to 0$, we recover at the first nonzero order, the familiar Klein Gordon equation with the geometrical coefficients coming from the underlying quantum geometry

$$\frac{\ddot{\phi}_v^0}{N_v\,A_v} = \epsilon^2 N_v B_v X_v \partial_x^2 \phi, \tag{3.52}$$

where the residual factor of $\epsilon^2$ are expected to be eaten up by the corresponding expansion of the coefficients of the geometry. If we send $\alpha \to 0$, keeping $\epsilon$ fixed we get

$$\frac{\ddot{\phi}_v^0}{N_v\,A_v} = \frac{N_v B_v X_v}{4} \left( \phi(v+2e) + \phi(v-2e) - 2\phi(v) \right), \tag{3.53}$$

where the right-hand side is the difference corresponding to the discrete second derivative.

## 3.4 Comments

Eq. (3.51) is the main result of our computation. On the left-hand side we have a single second order time derivative, while on the right-hand side we have finite differences of the field taken at nearby vertices of the graph $\Gamma$.

Finite differences are used to approximate ordinary derivatives when dealing with numerical solutions of differential equations or, in quantum field theory, when a spatial regulator is introduced, e.g. a regular lattice. In these cases, the regulator $\epsilon$ is considered small and, typically, one is interested in the $\epsilon \to 0$ limit. In our case instead, the underlying discreteness, and hence the parameter $\epsilon$, is physical. We should imagine the limit $\epsilon \to 0$, not as a process in which the points of the spatial graph get closer and closer but rather as a procedure in which we are raising the density of points (with respect to a fiducial background metric). In this picture the finite differences approximating spatial derivatives are always local terms (being expressed in terms of nearest neighbors). When the "density of vertices" goes to infinity, then we recover ordinary spatial derivatives. Of course, to have a well defined continuum limit one should probably consider not only graph with a large number of elements but also a superposition of a large number of spin-network states.[3]

---

[3]We do not consider this possibility for the moment as it lies beyond the scopes of this chapter, see however [9]

The scale $\alpha$ is instead coming from polymer quantization. Although one is not usually allowed to expand the quantum operators in powers of $\alpha$, due to the structure of the Hilbert space, it is reasonable to consider this limit after taking expectation values over semiclassical coherent states. From Eq.(3.53), we recover a sort of discretized version of the Klein–Gordon equation. This is expected since, if we ignore the polymer structure, we quantum field behaves as if it is living on a regular lattice.

Of course the natural question that needs to be address is whether there is hope for such a model to be Lorentz invariant. It is probably premature to try to give a precise answer to this question as there are assumptions and simplifications in our computation that need to be properly understood.[4] In particular, a crucial point is the understanding of the role of the geometrical coefficients Eq. (3.51). To be consistent in performing an expansion in $\epsilon$ one should also take into account the expansion of the geometrical terms, after considering semiclassical states for the quantum geometry (as it is usually done in LQC for instance), since they depend on $\epsilon$. However we can try to discuss the various aspects of this model on general grounds.

First of all, the presence of a fundamental discreteness scale might affect the time evolution as well. Indeed, the meaning of the time derivatives on the left-hand side of Eq. (3.51) depends on the properties of the underlying geometry through the lapse function. For instance, a deparametrization of the model in terms of a physical clock field $T$ would generate a dependence of the lapse on the conjugate momentum $P_T$ which in turns will carry information about the discreteness scale $\epsilon$. This might generate an effective discrete time evolution possibly generating finite differences in the temporal part of Eq. (3.51). Similar considerations are valid for a choice of time that involves only internal geometrical variables, allowing to link the time evolution to the fact that the volume of the universe changes in discrete steps proportional to the Planck volume $\ell_{\text{Planck}}^4$.

Another important point is that there are actually three scales in this framework: the Planck length, which is a quantum scale that is related to the smallest values of the spectra of geometrical operators, the discreteness scale $\epsilon$, characterizing semiclassical states, and the polymer scale $\alpha$. Following the discussion in [146], the discreteness scale, which for a general spin-network can be considered as the average length of the edges, is bounded from below by the Planck length. This means that the continuum limit cannot be considered without taking the classical limit first. Also, in order to have well-behaved semiclassical states one needs to keep $\epsilon \gg \ell_{\text{Planck}}$. The polymer scale $\alpha$ has the dimensions of a length as well, hence to fully capture its phenomenological consequences one needs to understand its relationship with the other two. In particular, if $\alpha \propto \epsilon$, then the continuum limit gets synchronized with the non-polymer limit. In this case, polymer quantization results to be strongly linked with spatial discreteness.

In concluding this part, we can say that a careful analysis of the relationships among the scales characterizing this models is crucial for the understanding of its low-energy behavior and for potential phenomenological applications, especially in relation to Lorentz invariance (both at low-energy and in the fundamental theory). We also want to underline the fact that the model just described can be easily improved in the treatment of both the

---

[4]For a discussion on how to improve our computation see Chapter 6.

scalar field (a discussion about the proper treatment of coherent states in the framework of geometrical quantization can be found in [75, 142, 154]) and the state of the quantum geometry. The latter can also be chosen to be a semiclassical state similar to the gaussian state for the scalar field in Eq.3.32. A more complete analysis, based on the computations presented in this chapter, can be found in [9].

# Chapter 4

# Finsler geometry from Doubly Special Relativity

## 4.1 Introduction

Departure from standard LI have been nowadays considered in essentially all Quantum Gravity (QG) scenarios as it represents a major source of phenomenological investigations (see [95]). On the other hand, DSR models have mostly been studied on their own within momentum space in the Hamiltonian formalism, and only recently potential connections with other QG approaches have been established (see for instance [17, 18, 55, 65]). In particular, a spacetime picture capable of accommodating the features of DSR models would make them competitive with respect to LIV scenarios. One possibility is certainly provided by noncommutative geometry. In this scenario, quantum groups act covariantly on noncommutive spacetimes (the case of $\kappa$-Poincaré is considered in [103]). On the other hand, Finsler geometry produce a consistent mathematical framework to deal with this situation in the classical case, when spacetime coordinates are commutative but still endowed with deformed symmetries (the so-called *relative locality* limit, see Section 1.1.2).

We are interested in an example of (quantum) deformation of the ordinary Poincaré group given by the $\kappa$-Poincaré ($\kappa$P) Hopf algebra [99, 100, 103]. As we already mentioned in Section 1.4.1, $\kappa$P symmetries have been shown to characterize the kinematics of particles living on a flat spacetime and non-trivial momentum space with a de Sitter geometry [16, 70, 90, 91] and they have been shown to naturally emerge in the context of $2 + 1$ dimensional QG coupled to point particles (see e.g. [64]).

In this chapter, we will introduce the reader to the procedure presented in [68] to derive a Finsler structure starting from the MDR of a point particle. We will then review the results of [15], where the specific case of $\kappa$P was investigated. We will see that, indeed, the Finsler geometry associated with $\kappa$P represents an instance of the kind of spacetimes we are interested in (see Section 1.4), i.e., a flat maximally symmetric spacetime that is not Minkowski, respecting DSR symmetries.

Among all the possible Finsler structures, a particular case is given by Berwald spaces. Interestingly enough the Finsler metric correspondent to $\kappa$P symmetries found in [15] appears to be a member of this class. However, this come about in a somewhat trivial way as a straightforward consequence of the flatness of the metric in coordinate space. With this in mind, it would be interesting to consider examples of curved metrics associated to more general deformed algebras so to check if for these the local structure

of spacetime does not reduce to the Minkowski spacetime but rather to the Finsler geometry with $\kappa$P symmetries and furthermore for checking if also these geometries are of the Berwald type.

Missing a definitive derivation of such hypothetical curved and deformed geometries based on some quantum gravity model, one has to resort also in this case to study a case for which a deformed group of symmetry is available and a Finslerian metric can be derived. In this sense a case of particular interest is the $q$-de Sitter ($q$dS) Hopf algebra [31, 98], a quantum deformation of the algebra of isometries of the de Sitter spacetime. It represents a case in which curvature of momentum space is present together with curvature in spacetime in the context of a well defined relativistic framework.[1] As such, this represents the perfect arena for our analysis.

The purpose of this chapter is then twofold. After reviewing some basics of Fiensler geometry and presenting the analysis of [15], we will show that there exists a Finsler spacetime associated to the mass Casimir of $q$dS and explicitly compute the associate Finsler metric and Christoffel symbols. We will then discuss how, in the limit in which the curvature goes to zero, one recovers the Finsler structure of $\kappa$P thus providing an example of a curved Finsler spacetime whose local limit is not trivially given by the Minkowski spacetime. In the second part we will discuss how, in a particular limit, the Finsler structure associated with $q$dS becomes of the Berwald type. Finally, we will discuss what are the consequences of these results and speculate about possible phenomenological studies.

### 4.1.1 Basics of Finsler geometry

In this part we are going to review some elements of Finsler geometry. In Finsler geometry one starts by equipping a smooth manifold $M$ with a general length measure, instead of a metric, defined by a Finsler function $F$. The length of a curve $\gamma : \tau \to \gamma(\tau)$ is given by

$$\ell(\gamma) = \int d\tau F(\gamma, \dot{\gamma}).\tag{4.1}$$

Asking for reparametrization invariant implies that $F$ has to be homogeneous of degree one with respect to its second argument. Based on this length integral one can describe the geometry of a manifold purely by tensors derived from the Finsler function.

**Definition 4.1.1.** *Let $M$ be a $D$-dimensional manifold and $TM$ its tangent bundle. A continuous real function $F : TM \to \mathbb{R}$ is a Finsler function if it satisfies:*

- *$F$ is smooth on the tangent bundle without the zero section (the slit tangent bundle) $TM \setminus \{0\}$;*

- *$F$ is homogeneous of degree one with respect to the fibre coordinates of $TM$*

$$F(x, \lambda v) = \lambda F(x, v), \, \forall \lambda > 0;$$

---

[1]See [35] for a description of particles with modified dispersion relation in the context of Hamilton geometry.

- *The Hessian $g^F_{ab}$ of $F^2$ with respect to the tangent space coordinates has constant rank and is non-degenerate on the slit tangent bundle*

$$g^F_{ab} = \frac{1}{2}\frac{\partial^2 F^2}{\partial v^a \partial v^b}.$$

Given the definition of a Finsler function one can define a Finsler space as

**Definition 4.1.2.** *A D-dimensional manifold $M$ equipped with a Finsler function $F$ is called a Finsler space $(M, F)$.*

The homogeneity properties of the norm, and of other derived objects, will play a fundamental role through Euler's theorem. It is then useful to state its content

**Theorem 4.1.1.** *Let $f : V \to \mathbb{R}$ be a homogeneous differentiable function of degree $s$, i.e., $f(\lambda x) = \lambda^s f(x)$, from a vector space $V$ into the real numbers. The function $f$ satisfies the following partial differential equation*

$$x^a \frac{\partial f}{\partial x^a} = sf.$$

Let us see some consequences of this theorem. First of all, we introduce the Finsler metric tensor as

**Definition 4.1.3.** *The Hessian of $F^2$ with respect to the tangent space coordinates $y$ is called the Finsler tensor (or first fundamental tensor)*

$$g^F_{ab}(x, v) = \frac{1}{2}\frac{\partial^2 F^2(x, v)}{\partial v^a \partial v^b}.$$

We will often refer to this tensor as *Finsler metric*. One can then easily check that the Finsler metric is homogeneous of degree zero

$$g^F_{ab}(x, \lambda v) = g^F_{ab}(x, v). \tag{4.2}$$

Using Euler's theorem one can check the following relationship

$$g^F_{ab}(x, v)v^a v^b = \frac{1}{2}\frac{\partial^2 F^2(x, v)}{\partial v^a \partial v^b}v^a v^b = \frac{1}{2}\frac{\partial F^2(x, v)}{\partial v^a}v^a = F^2. \tag{4.3}$$

Therefore the norm can be written as

$$F(x, v) = \sqrt{g^F_{ab}(x, v)v^a v^b}. \tag{4.4}$$

Moreover, since $F^2$ is a homogeneous function of degree two in the velocities, the metric satisfies the following relations

$$v^\alpha \frac{\partial g_{\mu\nu}}{\partial v^\alpha} = v^\mu \frac{\partial g_{\mu\nu}}{\partial v^\alpha} = v^\nu \frac{\partial g_{\mu\nu}}{\partial v^\alpha} = 0. \tag{4.5}$$

Given that, by definition, $g_{\mu\nu}$ is non degenerate, the inverse exists and it satisfies $g_{\mu\nu}(x, v)g^{\nu\rho}(x, v) = \delta^\rho_\mu$.

**Definition 4.1.4.** *Let $(M, F)$ be a Finsler space. The third derivative of $F^2$ with respect to the tangent space coordinates $v$ defines the components $C_{abc}$ of the Cartan*

*tensor*

$$C_{abc}(x, v) = \frac{1}{4} \frac{\partial^3 F^2(x, v)}{\partial v^a \partial v^b \partial v^c}.$$

It is a completely symmetric tensor (if the norm is at least $\mathcal{C}^3$) homogeneous of degree one in the second argument. Consequently, it satisfies the following property:

$$C_{abc}(x, v)v^a = C_{abc}(x, v)v^b = C_{abc}(x, v)v^c = 0, \tag{4.6}$$

which can be proved using Euler's theorem. The Cartan tensor can be used to measure the deviation from Riemannian geometry. Indeed, if the norm is induced by a scalar product, the Cartan tensor is zero (see Deicke's theorem [58]).

**Definition 4.1.5.** *Let $(M, F)$ be a Finsler space. The first derivative of $F^2$ with respect to the tangent space coordinates $v$ defines the components $\omega_a$ of the Finsler one-form*

$$\omega_a = \frac{1}{2} \frac{\partial F^2}{\partial v^a}.$$

Due to Euler's theorem, $v^a \omega_a = F^2$. Later in this Chapter, we will also see how the Finsler one-form is related to the canonical momentum.

Given the above definitions, a few comments are in order. Riemannian geometry is a special case of Finsler geometry in which the norm is given by an inner product, i.e. the metric $g_{ab}^F(x, v)$ does not depend on $v \in T_x M$. The construction discussed in this section is, strictly speaking, valid in the Euclidean signature. The extension to Lorentzian signature, although not obvious, it is possible and it has been extensively studied in the literature [38, 120, 121]. For our purposes, we will assume that all the construction goes through in the indefinite case without major issues. This is a rather safe assumption for us because we will consistently treat the Finsler structure as a small deformation, therefore the signature will be essentially inherited from the underlying pseudo-Riemannian structure. Finally, the Finsler metric, being homogeneous of degree zero in its second argument, cannot be defined on the zero section of the tangent bundle. This is why Finsler geometry is usually defined on the slit tangent bundle $TM \setminus \{0\}$. This mathematical detail is not usually of much relevance as in most of the physical situations one is interested in systems with non-zero velocities. On the other hand there are ways to overcome this issue and we will dedicate some space to this point later in this chapter.

### 4.1.2 The Legendre transform

For physical applications it is useful to describe all the structure introduced so far in terms of positions and momenta rather than position and velocities. Since velocities are tangent vectors while momenta are tangent forms, we need to move our analysis to the cotangent bundle. The Legendre transform permits this passage.

The form dual to a given vector is defined as

$$\omega_\mu = g_{\mu\nu}(x, v)v^\nu. \tag{4.7}$$

It can be rewritten as

$$\omega_\mu = \frac{1}{2} \frac{\partial F^2(x, v)}{\partial v^\mu}. \tag{4.8}$$

If $g$ is non degenerate then the transformation is invertible. Therefore we can define the a norm on forms as

$$\frac{1}{2} G^2(x, \omega) = v^\nu(\omega) \omega_\nu - \frac{1}{2} F^2(x, v(\omega)), \tag{4.9}$$

or

$$G(x, \omega) = F(x, v(\omega)). \tag{4.10}$$

The tensor obtained from this new norm is given by

$$h^{\mu\nu} = \frac{1}{2} \frac{\partial^2 G^2}{\partial \omega_\mu \partial \omega_\nu}, \tag{4.11}$$

and it plays the same role of the inverse metric in pseudo-Riemannian geometry. If the vector $v$ is rescaled to $\lambda v$, the associated form $\omega$ goes to $\lambda \omega$. Therefore the norm $G$ is homogeneous of degree one in $\omega$. This construction shows that Finsler geometry can be formulated in the tangent space as well as in the cotangent space.

### 4.1.3 Geodesics, Berwald spaces and normal coordinates

*Berwald spaces are Finsler spaces that are just a bit more general than Riemannian and locally Minkowskian spaces. They provide examples that are more properly Finslerian, but only slightly so* [33].

The statement above is a good intuitive description of what Berwald spaces are. One of the (equivalent) technical characterizations of Berwald spaces is the following [33]:

- The quantities $\partial_{\dot{x}}^2(G^\mu)$, with $G^\mu := \Gamma^\mu_{\rho\sigma}(x, \dot{x}) \dot{x}^\rho \dot{x}^\sigma$, do not depend on $\dot{x}^\mu$.

The objects $\Gamma^\mu_{\rho\sigma}$ are the usual Christoffel symbols defined as

$$\Gamma^\mu_{\rho\sigma}(x, \dot{x}) = \frac{1}{2} g^{\mu\nu} \left( \partial_\rho g_{\sigma\nu} + \partial_\sigma g_{\rho\nu} - \partial_\nu g_{\rho\sigma} \right), \tag{4.12}$$

that for a general Finsler metric depend on $\dot{x}^\mu$. The coefficients $G^\mu$ are called spray coefficients and they appear in the geodesic equations, obtained by minimizing the action (4.1), as

$$\ddot{x}^\sigma + 2 G^\sigma = \frac{\dot{F}}{F} \dot{x}^\sigma, \tag{4.13}$$

where the right-hand side is vanishing for a constant speed parametrization (e.g., $F = 1$). In other words a Finsler space is of the Berwald type when the $G^\mu$ are purely quadratic in the velocities[2]. 

In pseudo-Riemannian geometry, normal coordinates can be defined in a neighbourhood of a point $p$ (Fermi coordinates along a curve $\gamma$), such that the Christoffel symbols of the connection vanish at $p$ (along $\gamma$) [105].

---

[2]For an introduction to the various kind of connections that one can define in Finsler geometry see [33].

This procedure fails in pseudo-Finsler geometry if the space is not Berwald (see [51], [33] and references therein). Therefore in Finsler geometry the existence of free falling observers looking at nearby free falling particles moving in straight lines is not guaranteed[3]. In this respect, Berwald spaces play an important role in determining whether a given Finsler structure violates the Weak Equivalence Principle (WEP).

### 4.1.4 Derivation of Finsler geometries from modified dispersion relations

In this section we review the procedure introduced in [68] for deriving the Finsler geometry associated with a particle with a modified dispersion relation.

Let us start by considering the action of a particle with a constraint imposing the on-shell relation $\mathcal{M}(p) = m^2$

$$I = \int \left[ \dot{x}^\mu p_\mu - \lambda \left( \mathcal{M}(p) - m^2 \right) \right] d\tau, \tag{4.14}$$

where $\lambda$ is a Lagrange multiplier that transforms appropriately under an arbitrary change of time parameter to ensure reparametrization invariance of the action i.e., $\lambda(\tau)d\tau = \lambda(\tau')d\tau'$. In order to find the explicit expression of the Lagrangian we use Hamilton's equations that read as

$$p_\mu = \lambda \frac{\partial \mathcal{M}}{\dot{x}^\mu}. \tag{4.15}$$

If the relation above is invertible, one is able to rewrite the action in terms of velocities and the multiplier hence obtaining[4]

$$I = \int \mathcal{L}(x, \dot{x}, \lambda) d\tau. \tag{4.16}$$

We can also eliminate the multiplier using the equation of motion obtained varying the action with respect to it so to get the expression of the Lagrangian in terms of velocities only $\mathcal{L}(x, \dot{x}, \lambda(x, \dot{x}))$.

Finally we can identify the Finsler norm through the following relation

$$\mathcal{L}(x, \dot{x}, \lambda(x, \dot{x})) = mF(x, \dot{x}), \tag{4.17}$$

and the Finsler metric is then given by the Hessian matrix of $F^2$ as in (4.1.3). Since the action (4.14) is reparametrization invariant by construction, the norm (4.17) is homogeneous of degree one in the velocities.

At this point, using (4.4), the action can be written as

$$I = m \int F d\tau = m \int \sqrt{g_{\mu\nu}(x, \dot{x})\dot{x}^\mu \dot{x}^\nu} d\tau, \tag{4.18}$$

---

[3]See however [107] and [119] for a generalization of normal coordinates which is adapted to the framework of Finsler geometry that shares most of the properties of the standard definition.

[4]The symbols $x$ and $\dot{x}$, when taken as arguments of functions, generically refer to both the time and spatial component of the coordinates and the velocities.

which correspond to the action of a free relativistic particle propagating on a spacetime described by a velocity dependent metric.

Using the definition of generalized momentum, one can now simply relate the four-momentum to the Finsler norm as

$$p_\mu = m \frac{\partial F}{\partial \dot{x}^\mu} = m \frac{g_{\mu\nu}\dot{x}^\nu}{F}. \tag{4.19}$$

Note that this relation is related to the form introduced in (4.1.5) by a factor of $F^{-1}$. This makes the momentum $p_\mu$ invariant under the rescaling $\dot{x} \to \lambda\dot{x}$ and reparametrization invariant. It is essentially the form associated with the normalized vector $F^{-1}\dot{x}^\mu$. If these variables are used to perform the Legendre transform (introduced in the Section 4.1.2) from the Lagrangian to the Hamiltonian the result is

$$H = p_\mu \dot{x}^\mu - L = m \frac{g_{\mu\nu}\dot{x}^\nu \dot{x}^\mu}{F} - m F = 0. \tag{4.20}$$

This is essentially a consequence of reparametrization invariance and homogeneity and it implies that any trajectory will automatically satisfy the mass-shell condition $\mathcal{M}(p) = m^2$, without the need of imposing the equations of motion. Indeed, using the inverse metric $g^{\mu\nu}$ one recovers the dispersion relation in a simple way as

$$m^2 = g^{\mu\nu}(\dot{x}(p))p_\mu p_\nu. \tag{4.21}$$

### 4.1.5 Results for $\kappa$-Poincaré

In this subsection we will briefly review the results obtained in [15], regarding the Finsler structure associated with the $\kappa$P group. The mass Casimir of the $\kappa$P algebra, at first order in the deformation parameter $\ell$, is given by[5]

$$C_\ell = p_0^2 - p_1^2 \left(1 + \ell p_0\right). \tag{4.22}$$

It can be derived from (1.46), upon introducing a representation of the phase space coordinates $x^\mu = \{t, x\}$ and $p_\mu = \{p_0, p_1\}$, with the ordinary symplectic structure given by

$$\begin{aligned}
\{x^\mu, x^\nu\} &= 0, \\
\{x^\mu, p_\nu\} &= -\delta^\mu_\nu, \\
\{x^\mu, x^\nu\} &= 0.
\end{aligned} \tag{4.23}$$

Following the procedure outlined in the previous subsection, the associated Finsler norm reads as

$$F_\ell = \sqrt{\dot{t}^2 - \dot{x}^2} + \frac{\ell m}{2} \frac{\dot{t}\dot{x}^2}{\dot{t}^2 - \dot{x}^2}, \tag{4.24}$$

---

[5]The $\kappa$P algebra can be derived from the $q$dS algebra in an appropriate limit (see Sec. 4.2.1). See also [70].

and, using (4.1.3), the Finsler metric is

$$
g_{\mu\nu}^{F_\ell}(x,\dot{x}) = \begin{pmatrix} 1 + \dfrac{3m\ell\dot{t}\dot{x}^4}{2(\dot{t}^2-\dot{x}^2)^{5/2}} & \dfrac{m\ell\dot{x}^3(\dot{x}^2-4\dot{t}^2)}{2(\dot{t}^2-\dot{x}^2)^{5/2}} \\ \dfrac{m\ell\dot{x}^3(\dot{x}^2-4\dot{t}^2)}{2(\dot{t}^2-\dot{x}^2)^{5/2}} & -1 + \dfrac{m\ell\dot{t}^3(2\dot{t}^2+\dot{x}^2)}{2(\dot{t}^2-\dot{x}^2)^{5/2}} \end{pmatrix}. \tag{4.25}
$$

It can be easily checked that the metric above satisfies the relations (4.5) and that it can be rewritten in momentum space as follows

$$
g_{\mu\nu}^{F_\ell}(x,p) = \begin{pmatrix} 1 + \dfrac{3}{2}\dfrac{\ell p_0 p_1^4}{m^4} & -\dfrac{\ell}{2}\dfrac{p_1^3(p_1^2-4p_0^2)}{m^4} \\ -\dfrac{\ell}{2}\dfrac{p_1^3(p_1^2-4p_0^2)}{m^4} & -1 + \dfrac{\ell}{2}\dfrac{p_0^3(2p_0^2+p_1^2)}{m^4} \end{pmatrix}. \tag{4.26}
$$

Using this expression, the dispersion relation can be simply given as

$$
g_{F_\ell}^{\mu\nu}p_\mu p_\nu = p_0^2 - p_1^2\left(1+\ell p_0\right). \tag{4.27}
$$

In [15], it was also shown that the Killing vectors associated with the metric (4.25) are compatible with the $\kappa$P symmetries.

Interestingly enought, it can be easily proven that the Finsler metric associated with $\kappa$P has vanishing Christoffel symbols and that the relation $\Gamma_{\rho\sigma}^\mu = 0$ trivially satisfies the conditions for a Berwald space. This was expected since, in [15], a deformation of a special-relativistic particle was considered and in that case the metric had no dependence on coordinates, meaning that the spacetime geometry was flat.

The subsequent question is whether that was a coincidence or not. In other words, since all locally Minkowskian spacetimes are Finsler spacetimes of the Berwald type [33], do Berwald spaces play an important role regarding the local structure of spacetime with DSR-like symmetries or it is just a trivial consequence of local flatness? To answer this question we shall then examine the Finsler geometry of a spacetime related to the $q$dS mass Casimir that reduces to the $\kappa$P Finsler geometry when the curvature goes to zero.

Before moving to the next section it is worth mentioning that, when dealing with Finsler spacetimes, geometrical objects, like the norm or the curvature, might not be well defined along certain directions. For instance, Eq.(4.24) is singular for $\dot{t}^2 = \dot{x}^2$. This seems to be a consequence of dealing with a non-homogeneous mass Casimir while working in a reparametrization invariant framework. Non-homogeneous terms in the Casimir generates additional terms in the norm but, the requirements of homogeneity in the velocities coming from the theory of Finsler spaces (see Sec.4.1.1) only allows for normalized tangent vectors to appear, causing the presence of the singular denominators. These kind of issues will also be present in our analysis in the following sections. One way to avoid this problem is to use an Hamiltonian formulation of the system, as done in [35]. In the Hamiltonian framework one typically loses full reparametrization invariance in exchange for a non-zero Hamiltonian (directly identified with the mass Casimir). This procedure is equivalent to considering the cotangent vectors $\omega_\mu$ instead of the reparametrization invariant variables $p_\mu$ (see Section 4.1.1 and Section 4.1.4). It can be shown that this analysis can be recast

in terms of a Lagrangian functional without singular denominators. Unfortunately by following this path one also loses the homogeneity properties required to correctly identify a Finsler norm. It is also possible that such singular behaviors might solved by performing a non-perturbative study. A full discussion on these themes is beyond the purposes of our investigation.

## 4.2 q-de Sitter inspired Finsler spacetime

In what follows we shall explicitly investigate the Finsler metric associated to a $q$-de Sitter Hopf algebra and consider its local limit to prove that it reproduces the $\kappa$-Poincaré Finsler geometry. We shall then also investigate if $q$-de Sitter Finsler geometry is per-se of the Berwald type.

### 4.2.1 $q$-de Sitter

Let us start by denoting the key features of the 1+1D $q$dS Hopf algebra [34]. Using the notation of [34], the commutators among the symmetry generators are

$$[P_0, P] = HP, \quad [P_0, N] = P - HN,$$
$$[P, N] = \cosh(w/2)\frac{1 - e^{\frac{-2wP_0}{H}}}{2w/H} - \frac{1}{H}\sinh(w/2)e^{\frac{-wP_0}{H}}\Theta, \tag{4.28}$$

where

$$\Theta = \left[e^{\frac{wP_0}{H}}(P - HN)^2 - H^2 e^{\frac{wP_0}{H}}N^2\right], \tag{4.29}$$

and $P_0, P, N$ refer to the generators of time translation, space translation and boost respectively, $H$ is the Hubble rate and $w$ is the deformation parameter.

For the coproducts, which are used to express the conservation of momentum when dealing with multiple particles, one has

$$\Delta(P_0) = 1 \otimes P_0 + P_0 \otimes 1, \quad \Delta(P) = e^{\frac{-wP_0}{H}} \otimes P + P \otimes 1,$$
$$\Delta(N) = e^{\frac{-wP_0}{H}} \otimes N + N \otimes 1, \tag{4.30}$$

while the antipodes are

$$S(P_0) = -P_0, \quad S(P) = e^{\frac{wP_0}{H}}P_1, \quad S(N) = e^{\frac{wP_0}{H}}N. \tag{4.31}$$

Finally the mass Casimir is

$$C_{q\mathrm{dS}} = H^2\frac{\cosh(w/2)}{w^2/4}\sinh^2\left(\frac{wP_0}{2H}\right) - \frac{\sinh(w/2)}{w/2}\Theta. \tag{4.32}$$

The parameter $w$ is usually assumed to be a dimensionless combination of a fundamental length scale $\ell$ and the dS radius $H^{-1}$. There are various possible choices (see for example [106]) and we will focus on the one that gives back the classical dS algebra for $\ell \to 0$ and the $\kappa$P algebra for $H \to 0$, i.e., $w = H\ell$.

Upon introducing a representation of the phase space coordinates $x^\mu = \{t, x\}$ and $p_\mu = \{p_0, p_1\}$, with the ordinary symplectic structure given by

$$\{x^\mu, x^\nu\} = 0,$$
$$\{x^\mu, p_\nu\} = -\delta^\mu_\nu, \tag{4.33}$$
$$\{x^\mu, x^\nu\} = 0.$$

the generators are represented, at first order in $\ell$, $H$ and $H\ell$, by

$$
\begin{aligned}
P_0 &= p_0 - Hxp, \\
P_1 &= p_1, \\
N &= p_1 t + p_0 x - H\left(p_1 t^2 \frac{p_1 x^2}{2}\right) - \ell x \left(p_0^2 + \frac{p_1^2}{2}\right) \\
&\quad + H\ell p_1 x \left(p_1 t + \frac{3}{2} p_0 x\right),
\end{aligned}
\tag{4.34}
$$

and the Casimir reads as

$$C_{q\mathrm{dS}} = p_0^2 - p_1^2 \left(1 + \ell\, p_0\right)\left(1 - 2\,H\,t\right). \tag{4.35}$$

From the expression above, as previously anticipated, taking the limit $H \to 0$ one recovers the Casimir of the $\kappa$P algebra, while in the limit $\ell \to 0$ the Casimir of the classical de Sitter algebra is obtained.

## 4.2.2 Finsler spacetime from the q-de Sitter mass Casimir

We start by considering the action of a free particle with a constraint imposing the mass shell condition in terms of the Casimir (4.35) and it is given by

$$I = \int \left[\dot{x}^\mu p_\mu - \lambda(\tau)\left(C_{q\mathrm{dS}} - m^2\right)\right] d\tau, \tag{4.36}$$

where $\lambda(\tau)$ is a lagrange multiplier enforcing the on-shell condition that we rewrite as

$$C_{q\mathrm{dS}} = m^2 \;\to\; p_0^2 = m^2 + a^{-2}(t) p_1^2 \left(1 + \ell\, p_0\right), \tag{4.37}$$

where $a(t) = e^{Ht} = 1 + Ht + \mathcal{O}(H^2)$ is the classical dS scale factor.

The associated equations of motion are given by

$$\dot{t} = \lambda\left[2p_0 - \ell\, a^{-2} p_1^2\right], \tag{4.38a}$$
$$\dot{x} = -2\lambda\, a^{-2} p_1 \left(1 + \ell p_0\right), \tag{4.38b}$$

and they can be inverted to give[6]

$$p_0 = \frac{\dot{t}}{2\lambda} + \ell\, a^2 \frac{\dot{x}^2}{8\lambda^2}, \tag{4.39a}$$
$$p_1 = -\frac{a^2\, \dot{x}}{2\lambda}\left(1 - \ell\frac{\dot{t}}{2\lambda}\right). \tag{4.39b}$$

---

[6]Assuming $\lambda \sim \mathcal{O}(1)$.

Therefore the Lagrangian in (4.36) written in terms of velocities and the Lagrange multiplier reads as

$$L = \frac{\dot{t}^2 - a^2\,\dot{x}^2}{4\lambda} + \ell\frac{a^2\,\dot{t}\dot{x}^2}{8\lambda^2} + \lambda m^2. \tag{4.40}$$

In the limit $a(t) \to 1$ we recover the Lagrangian in [15], as expected. The Lagrangian above can be minimized with respect to $\lambda$ to give

$$\lambda = \frac{1}{2}\frac{\sqrt{\dot{t}^2 - a^2\,\dot{x}^2}}{m} + \frac{\ell}{2}\frac{a^2\,\dot{t}\dot{x}^2}{\dot{t}^2 - a^2\,\dot{x}^2}. \tag{4.41}$$

The Lagrangian (4.40) can now be written in terms of velocities only and it reads as

$$L = m\left(\sqrt{\dot{t}^2 - a^2\,\dot{x}^2} + \frac{\ell m}{2}\frac{a^2\,\dot{t}\dot{x}^2}{\dot{t}^2 - a^2\,\dot{x}^2}\right). \tag{4.42}$$

The expression above is of degree one in the velocities and therefore it defines the following Finsler norm[7]

$$F = \sqrt{\dot{t}^2 - a^2\,\dot{x}^2} + \frac{\ell m}{2}\frac{a^2\,\dot{t}\dot{x}^2}{\dot{t}^2 - a^2\,\dot{x}^2}. \tag{4.43}$$

According to the relation (4.1.3), a Finsler metric can be derived from (4.43) and it reads as

$$g_{\mu\nu}^F(x,\dot{x}) = \begin{pmatrix} 1 + \frac{3a^4 m\ell\dot{t}\dot{x}^4}{2\left(\dot{t}^2 - a^2\dot{x}^2\right)^{5/2}} & \frac{m\ell a^4\dot{x}^3\left(a^2\dot{x}^2 - 4\dot{t}^2\right)}{2\left(\dot{t}^2 - a^2\dot{x}^2\right)^{5/2}} \\ \frac{m\ell a^4\dot{x}^3\left(a^2\dot{x}^2 - 4\dot{t}^2\right)}{2\left(\dot{t}^2 - a^2\dot{x}^2\right)^{5/2}} & -a^2 + \frac{m\ell a^2\dot{t}^3\left(2\dot{t}^2 + a^2\dot{x}^2\right)}{2\left(\dot{t}^2 - a^2\dot{x}^2\right)^{5/2}} \end{pmatrix}. \tag{4.44}$$

When $\ell \to 0$ the metric above reduces to the one of a classical de Sitter space in coordinate time and for $a(t) \to 1$ the Finsler metric associated with $\kappa P$ is recovered. The norm (4.43) and the metric (4.44) satisfy all the identities of a proper Finsler spacetime introduced in Sec.4.1.1.

Using (4.41) one can rewrite (4.38) to get

$$p_0 = \frac{m\dot{t}}{\sqrt{\dot{t}^2 - a^2\dot{x}^2}} - \frac{\ell m^2 a^2\dot{x}^2\left(a^2\dot{x}^2 + \dot{t}^2\right)}{2\left(\dot{t}^2 - a^2\dot{x}^2\right)^2}, \tag{4.45a}$$

$$p_1 = -\frac{m\,a^2\dot{x}}{\sqrt{\dot{t}^2 - a^2\dot{x}^2}} + \frac{\ell m^2 a^2\dot{t}^3\dot{x}}{\left(\dot{t}^2 - a^2\dot{x}^2\right)^2}, \tag{4.45b}$$

and the following relations can be found as well

$$\frac{m\dot{t}}{\sqrt{\dot{t}^2 - a^2\dot{x}^2}} = p_0 + \frac{\ell a^{-2} p_1^2}{2m^2}\left(a^{-2}p_1^2 + p_0^2\right), \tag{4.46a}$$

$$\frac{m\,a\dot{x}}{\sqrt{\dot{t}^2 - a^2\dot{x}^2}} = -a^{-1}p_1\left(1 + \frac{\ell}{m^2}p_0^3\right). \tag{4.46b}$$

---

[7]It is worth noticing that, while finishing this work, the paper [96] appeared. The authors arrive to a similar result working in conformal time instead of comoving time.

Using the relations above one recovers the mass shell condition as

$$m^2 = \left(\frac{m\,\dot{t}}{\sqrt{\dot{t}^2 - a^2\dot{x}^2}}\right)^2 - \left(\frac{m\,a\,\dot{x}}{\sqrt{\dot{t}^2 - a^2\dot{x}^2}}\right)^2 = p_0^2 - a^{-2}\,p_1^2(1 + \ell p_0). \quad (4.47)$$

and the Finsler metric (4.44) can be rewritten in terms of momenta as

$$g_{\mu\nu}^F(x,p) = \begin{pmatrix} 1 + \frac{3}{2}\frac{\ell p_0 p_1^4}{m^4} & -\frac{a}{2}\frac{\ell p_1^3\left(p_1^2 - 4p_0^2\right)}{m^4} \\ -\frac{a}{2}\frac{\ell p_1^3\left(p_1^2 - 4p_0^2\right)}{m^4} & -a^2 + \frac{a^2}{2}\frac{\ell p_0^3\left(2p_0^2 + p_1^2\right)}{m^4} \end{pmatrix}. \quad (4.48)$$

By comparing (4.43) with the Finsler norm associated with the $\kappa$P symmetries in [15], it can be noted that the two are conformally related as in the classical case.

Using (4.45) and (4.46) it can be shown that the inverse metric satisfies the following relations

$$g_F^{\mu\nu}(x,\dot{x})p_\mu(\dot{x})p_\nu(\dot{x}) = m^2, \quad (4.49a)$$

$$g_F^{\mu\nu}(x,p)p_\mu p_\mu = p_0^2 - a^{-2}p_1^2(1 + \ell p_0). \quad (4.49b)$$

We have shown so far that a particle with the $q$dS mass Casimir can be described in terms of a Finsler geometry through the norm (4.43) and the metric (4.44, 4.48) and we noticed that this structure is conformally related to the one of $\kappa$P introduced in [15].[8]

In the tangent space, the corrections to the ordinary Minkowski norm (or metric) are given by terms which are of the form $\ell m\, f(\dot{x})$ or $\ell m\, g(p/m)$ in momentum space, with $f$ and $g$ some functions of velocities and momenta respectively. These kinds of corrections are typical of *rainbow gravity* scenarios [101] (see also [97]). Similar results where also found in [30, 149] where the propagation of particle in a quantum geometry was analyzed and the deviations from the classical results were given in terms of a dimensionless *non-classicality* parameter $\beta$, involving expectation values of the geometrical operators over a state of the quantum geometry, and functions of $p/m$, without an explicit dependence on any fundamental scale. In the framework presented here, the analogous parameter would be represented by the dimensionless combination $\ell m$, which makes manifest the presence of a fundamental scale.

In the following subsection, we will explicitly derive the worldline of a particle propagating on this Finsler geometry associated to the dispersion relation $C_{q\mathrm{dS}} = m^2$ and we will study the associated Christoffel symbols.

### 4.2.3 Christoffel symbols and geodesic equations

Worldlines in Finsler geometry can be derived using Euler–Lagrange equations which is equivalent to computing the geodesic equations given by

$$\ddot{x}^\mu + \Gamma^\mu_{\rho\sigma}(x,\dot{x})\dot{x}^\rho\dot{x}^\sigma = 0, \quad (4.50)$$

---

[8]The analsysis of the Killing equation, needed to prove the full equivalence between the symmetries of the Finsler geometry compatible with the $q$dS mass Casimir and the the $q$dS Hopf algebra, is not among the objectives of this work. See however [96].

once the parameter $\tau$ has be chosen to be affine. The Christoffel symbols are defined as in Riemannian geometry

$$\Gamma^\mu_{\rho\sigma}(x,\dot{x}) = \frac{1}{2} g^{F\mu\nu}(x,\dot{x}) \left(\partial_\rho g^F_{\sigma\nu} + \partial_\sigma g^F_{\rho\nu} - \partial_\nu g^F_{\rho\sigma}\right), \qquad (4.51)$$

but now they depend on the velocities through the metric tensor.

From (4.44), they are explicitly given by

$$\Gamma^0_{00} = \frac{3Hm\ell\dot{t}a^4\dot{x}^4 \left(4\dot{t}^2 + a^2\dot{x}^2\right)}{4 \left(\dot{t}^2 - a^2\dot{x}^2\right)^{7/2}}, \qquad (4.52a)$$

$$\Gamma^0_{01} = \frac{Hm\ell a^4\dot{x}^3 \left(4\dot{t}^2 - a^2\dot{x}^2\right)}{2 \left(\dot{t}^2 - a^2\dot{x}^2\right)^{5/2}}, \qquad (4.52b)$$

$$\Gamma^1_{00} = -\frac{Hm\ell a^2\dot{x}^3 \left(16\dot{t}^4 - 2a^2\dot{t}^2\dot{x}^2 + a^4\dot{x}^4\right)}{2 \left(\dot{t}^2 - a^2\dot{x}^2\right)^{7/2}}, \qquad (4.52c)$$

$$\Gamma^0_{11} = Ha^2 - \frac{1}{4} \frac{Hm\ell a^2\dot{t} \left(4\dot{t}^6 + 10\dot{t}^4 a^2\dot{x}^2 + 7\dot{t}^2 a^4\dot{x}^4 - 6a^6\dot{x}^6\right)}{\left(\dot{t}^2 - a^2\dot{x}^2\right)^{7/2}}, \qquad (4.52d)$$

$$\Gamma^1_{01} = H - \frac{3Hm\ell a^2\dot{t}^3\dot{x}^2 \left(4\dot{t}^2 + a^2\dot{x}^2\right)}{4 \left(\dot{t}^2 - a^2\dot{x}^2\right)^{7/2}}, \qquad (4.52e)$$

$$\Gamma^1_{11} = -\frac{Hm\ell a^4\dot{x}^3 \left(a^2\dot{x}^2 - 4\dot{t}^2\right)}{2 \left(\dot{t}^2 - a^2\dot{x}^2\right)^{5/2}}. \qquad (4.52f)$$

In the limit $\ell \to 0$ they reduce to the Christoffel symbols of a classical de Sitter space while for $H \to 0$ they vanish in agreement with the fact that in this limit the Finsler metric of $\kappa$P is recovered. We also notice that the correction terms to the *classical* results are proportional to the combination $H\ell$.

With the parametrization $F = 1$ applied to the norm (4.43), the geodesic equations are specifically given by

$$\ddot{t} + H a^2\dot{x}^2 \left(1 - 2\ell m\dot{t}\right) = 0, \qquad (4.53a)$$

$$\ddot{x} + H\dot{x} \left(2\dot{t} + \ell m a^2\dot{x}^2\right) = 0, \qquad (4.53b)$$

and their dependence on the mass $m$ signals a violation of the WEP.

In order to explore the consequences of these corrections one can expand (4.52) up to second order in $H$ obtaining

$$\Gamma^0_{00} \simeq 3H\ell m \dot{t} \left( \frac{4\dot{t}^2\dot{x}^4 + \dot{x}^6}{4\left(\dot{t}^2 - \dot{x}^2\right)^{7/2}} + \frac{Ht\left(16\dot{t}^4\dot{x}^4 + 18\dot{t}^2\dot{x}^6 + \dot{x}^8\right)}{4\left(\dot{t}^2 - \dot{x}^2\right)^{9/2}} \right), \quad (4.54\text{a})$$

$$\Gamma^0_{11} \simeq H + 2H^2 t - H\ell m \dot{t} \left( \frac{4\dot{t}^6 + 10\dot{t}^4\dot{x}^2 + 7\dot{t}^2\dot{x}^4 - 6\dot{x}^6}{4\left(\dot{t}^2 - \dot{x}^2\right)^{7/2}} + \quad (4.54\text{b}) \right.$$

$$\left. + \frac{Ht\left(8\dot{t}^8 + 60\dot{t}^6\dot{x}^2 + 72\dot{t}^4\dot{x}^4 - 41\dot{t}^2\dot{x}^6 + 6\dot{x}^8\right)}{4\left(\dot{t}^2 - \dot{x}^2\right)^{9/2}} \right),$$

$$\Gamma^1_{01} \simeq H - 3H\ell m \dot{t}^3 \dot{x}^2 \left( \frac{4\dot{t}^2 + \dot{x}^2}{4\left(\dot{t}^2 - \dot{x}^2\right)^{7/2}} + \frac{Ht\left(8\dot{t}^4 + 24\dot{t}^2\dot{x}^2 + 3\dot{x}^4\right)}{4\left(\dot{t}^2 - \dot{x}^2\right)^{9/2}} \right),$$

$$(4.54\text{c})$$

and similarly for the other components. One finds terms that are purely of order $H\ell$ and others that are of order $H\ell Ht$. If $t$ is at most $\mathcal{O}(H^{-1})$, the second kind of corrections is never bigger than the first one and this is true also for the higher order corrections since they are all multiplier by coefficients of the type $H\ell(Ht)^{n-1}$.

Therefore, if one neglects correction terms which are proportional to $H\ell$, the Christoffel symbols become independent of $\dot{x}^\mu$ and this condition is preserved as long as $t$ is not larger than $H^{-1}$. In this limit the Finsler structure associated to $q$dS is approximately of the Berwald type and the Christoffel symbols are the same of a classical dS spacetime.

What happens at the metric tensor in this limit? Expanding (4.44) up to first order in $H$ one gets

$$g^F_{00} = 1 + \frac{3\ell m \dot{t}\dot{x}^4}{2\left(\dot{t}^2 - \dot{x}^2\right)^{5/2}} + \frac{3Ht\ell m \dot{t}\dot{x}^4\left(4\dot{t}^2 + \dot{x}^2\right)}{2\left(\dot{t}^2 - \dot{x}^2\right)^{7/2}}, \quad (4.55\text{a})$$

$$g^F_{11} = -1 + 2Ht + \frac{\ell m \dot{t}^3}{2} \left( \frac{\left(2\dot{t}^2 + \dot{x}^2\right)}{\left(\dot{t}^2 - \dot{x}^2\right)^{5/2}} + \frac{Ht\left(4\dot{t}^4 + 10\dot{x}^2\dot{t}^2 + \dot{x}^4\right)}{\left(\dot{t}^2 - \dot{x}^2\right)^{7/2}} \right),$$

$$(4.55\text{b})$$

$$g^F_{01} = g^F_{10} = -\frac{\ell m \dot{x}^3 \left(4(4Ht + 1)\dot{t}^4 - (2Ht + 5)\dot{x}^2\dot{t}^2 + (Ht + 1)\dot{x}^4\right)}{2\left(\dot{t}^2 - \dot{x}^2\right)^{7/2}}. \quad (4.55\text{c})$$

In the metric above the constant $H$ always comes together with the coordinate time $t$ and this is also true for higher order terms that would come with coefficients of the type $(Ht)^n$. Therefore, while at the level of the Christoffel symbols these terms can be neglected as long as $t \lesssim H^{-1}$, this is not true for the metric tensor as one would get terms which are of the same order as the terms of $\mathcal{O}(\ell)$ i.e., $\ell(Ht)^n \sim \ell$ for $t \sim H^{-1}$. The metric is, therefore, still of Finslerian type form.

Having said that, at first order in $H$ and $\ell$ and ignoring terms proportional to $H\ell$ not enhanced by a factor of $t$, the geodesic equations (4.50) are now the same that one would obtain from a classical dS spacetime[9]. They

---

[9]Note that analogous conclusions can be obtained in the framework presented in [35] under similar hypothesis.

are given by

$$\ddot{t} + H\dot{x}^2 = 0, \tag{4.56a}$$

$$\ddot{x} + 2H\dot{t}\dot{x} = 0, \tag{4.56b}$$

where any dependence on the mass has disappeared. Comparing (4.56) with (4.53), it is clear that in the former case the additional mass dependent term behaves like a force carrying the particle away from the classical geodesic motion.

On the other hand, the chronometric structure will still be velocity dependent and it will contain information on both the fundamental scale $\ell$ and the curvature scale $H$. For example, in the equations above, the derivatives are performed with respect to an affine parameter. In this respect, with the usual definition of proper time, from the metric (4.48) one obtains

$$\Delta\tau = \int_{t_1}^{t_2} \sqrt{g_{00}^F}\, dt = \int_{t_1}^{t_2} \left(1 + \frac{3}{2}\frac{\ell p_0\, p_1^4}{m^4}\right) dt = \Delta t \left(1 + \frac{3}{2}\frac{\ell p_0\, p_1^4}{m^4}\right) \tag{4.57}$$

where we chose $dx = 0$, so that no other components of the metric need to be considered and $p_0 = const$ (in this frame there are no effects associated with $H$). Therefore the proper time turns out to be momentum (or velocity) dependent and particles with different energy will experience different elapsed proper time intervals $\Delta\tau$, given the same coordinate time interval $\Delta t$.

Let us now compute the trajectory of a particle as a function of coordinate time to show that indeed the non trivial structure of momentum space is not lost. Since the Lagrangian (4.42) does not depend on the spatial coordinate $x$, Euler–Lagrange equations tell us that the generalized momentum (4.45b) is conserved, i.e., $\dot{p}_1 = 0$. Therefore eq. (4.45b) can be integrated, in the gauge $\tau(t) = t$ with the condition $x(0) = 0$, and the result is given by

$$x(t) = \frac{p_1 t}{\sqrt{p_1^2 + m^2}} \left[1 - \frac{Ht}{2}\left(1 + \frac{m^2}{p_1^2 + m^2}\right)\right] - \ell p_1 t\,(1 - Ht), \tag{4.58}$$

for an incoming particle. The derivative of (4.58) gives the speed of propagation that reads as[10]

$$v(t) = \frac{p_1}{\sqrt{p_1^2 + m^2}} \left[1 - Ht\left(1 + \frac{m^2}{p_1^2 + m^2}\right)\right] - \ell p_1(1 - 2Ht)$$
$$\xrightarrow{m^2 \to 0} \quad v(t) = 1 - Ht - \ell p_1(1 - 2Ht). \tag{4.59}$$

Before going to the conclusion, let us briefly recap the results of this section. Eq.s (4.54) show that, in general, the $q$dS Finsler geometry is not of the Berwald type, since the spray coefficients (defined in Sec. 4.1.3) are not quadratic in the velocities. However, it turns out that, in the specific regime $t \lesssim H^{-1}$, the Christoffel symbols become velocity-independent, and identical to the ones of a classical dS spacetime, and the Finsler geometry is approximately of the Berwald type.[11] Yet, the chronometric structure of the

---

[10]This result is in agreement with what has been found in [34, 96].

[11]Taking this limit is equivalent to ignore correction terms proportional to $(H\ell)^n$ which are not enhanced by a factor of $t^n$.

model does not become classical and the non trivial structure of the Finsler metric is maintained.

## 4.3 Conclusions and outlook

In this chapter, we extended the relationship between theories with deformed relativistic symmetries and Finsler geometry by including the presence of spacetime curvature. In the first part, we have shown that the propagation of particles with deformed de Sitter symmetries, given by the $q$dS Hopf algebra, can be described in terms of a velocity and coordinate dependent Finsler norm and we noted that the latter is conformally related to the $k$P Finsler norm introduced in [15]. Then, we studied the affine structure of the model by computing the generalized Christoffel symbols and pointing out that in general they remain velocity dependent. This allowed us to conclude that the $q$dS Finsler spacetime is not in general of the Berwald type and therefore the WEP is violated.

Nevertheless, we have shown that when the correction terms proportional to $H\ell$ (the product of the inverse of the curvature scale and the fundamental length scale) can be disregarded, the affine structure become classical, at least for a time scale which is at most comparable with the Hubble time $H^{-1}$. In this limit the Finsler structure becomes of the Berwald type and the WEP is recovered. On the other hand, in the same regime, the chronometric structure does not become completely classical. Indeed, the typical DSR effects, such as momentum dependent speeds of propagation for massive and massless particles, are still present and they come with both Planck scale and curvature corrections.

Deformations of the standard Poincaré algebra have been largely considered in the literature in the last twenty years but they are mostly used to described kinematical properties of particles with modified dispersion relations in a well defined relativistic framework. Whether these symmetry groups can be used to construct families of *momentum dependent* (metric) theories of gravity, which would modify GR incorporating some QG features, is currently an open question. In the absence of concrete and realistic proposals for such kinds of theories, the study of deformed symmetry groups of non-flat spacetimes is a first step in understanding if such theories can be constructed.

As we anticipated in the introduction, two fundamental ingredients of any metric theory of gravity are LI and the WEP. The former can somehow be extended to include deformed symmetry groups and we have shown that indeed the $q$dS Finsler spacetime locally reduces to the flat $\kappa$P Finsler spacetime introduced in [15]. Therefore one may think of building a theory of gravity whose solutions locally look like a flat spacetime with $\kappa$P symmetries e.g., the $\kappa$P Finsler spacetime. However, the WEP is broken in $q$dS. Indeed, we found that the corrections to the ordinary geodesic equations come with a mass dependence. This additional component is negligible in the limit of small curvature and for typical time scales smaller than the Hubble time. In this limit the Finsler structure associated with $q$dS becomes of the Berwald type, which represents a subclass of Finsler spaces for which free falling (Fermi) normal coordinates can be defined and any free falling observer looking at neighboring free falling particles observes them

moving uniformly over straight lines (formally implementing the idea of the *Einstein's elevator*, see also [107] and [119]). Therefore, comparing the geodesic equations in this limit to the ones obtained without any approximation, we realized that the correction terms can be interpreted as force-like contributions.

The most stringent bounds on violations of the WEP come from high precision Eötvös-type experiments, but they are mostly performed in the gravitational field produced by the Earth and for macroscopic, composite bodies (see [153] and references therein). The relevant parameter used to constrain violations of the WEP is the so called *Eötvös ratio η* that measures the fractional difference in acceleration between two bodies and it is currently bounded to be less or equal than about $10^{-13}$. Obviously, this bound cannot be directly applied to the present framework and tests of the WEP on cosmological scales would be more appropriate.

On the other hand, assuming that today's total energy density can be completely associated with the cosmological constant and that the universe is described by the $q$dS Finsler geometry, one can try to estimate how good is the Berwald approximation. Today's value of the Hubble parameter is approximately given by $H_0 \simeq 68 \,(\text{km/s})/\text{Mpc}$ which corresponds, in seconds, to $H_0 \simeq 2.2 \times 10^{-18} \, \text{s}^{-1}$. Assuming that $\ell$ is of the order of the Planck length $\ell_P \simeq 1.6 \times 10^{-35} \, \text{m}$, the dimensionless combination $\ell H$, in natural units, is given by $\ell H \simeq 3.7 \times 10^{-62} \ll 1$. Since this is the combination driving the correction terms in the geodesic equations, we expect the violation of the WEP to be very much suppressed in this context.

At this point, one may wonder whether the effective gravitational dynamics for this theory can be described in terms of a sort of metric-affine theory of gravity[12] (at least for a time scale $t \lesssim t_H$), where the connections are the ones associated with a classical dS spacetime while the chronometric properties are given by the velocity dependent Finsler metric of $q$dS. In this case the Ricci tensor would be constructed solely on the basis of the classical connections and the Ricci scalar would be the contraction of the Finsler metric with the Ricci tensor. Still, it would be interesting to have a definite model providing such a dynamics.

Finally, one can also speculate that similar effects would be present in some kind of $\kappa$P-like deformation of the spherically symmetric gravitational field generated by a mass $M$. This would actually provide a framework to realistically test DSR models through tests of the WEP, as a bound on $\eta$ could imply a bound on the fundamental scale $\ell$. [13] We hope to further develop these themes in future works.

---

[12]See e.g. [151] for background material.

[13]In the limit in which the Finsler structure is of the Berwald type, we do not consider energy dependent velocities as sources of WEP violations because particles with the same masses and same initial velocities will (approximately) experience the same acceleration.

# Chapter 5

# Effective geometries from quantum gravity

## 5.1 Introduction

As we briefly discussed in the Introduction, in phenomenological investigations of QG theories, there are tipically two limits playing a major role, the continuum and the classical limit. Noticeably these two limits do not need to coincide and their order does matter in extracting phenomenological consequences. A very illustrative and general example in this sense was presented in a recent paper [30], where a mechanism for emergence of cosmological spacetime geometry from a quantum gravity setting was discussed. Such a mechanism was based on very general assumption about the existence of quantum gravitational degrees of freedom to be described in terms of a state $\Psi_0$ in a Hilbert space $\mathcal{H}_G$, which can be considered "heavy" compared to the matter degrees of freedom (in the Born-Oppenheimer sense). Assuming negligible back reaction of the matter degrees of freedom on the gravitational ones, one can suitably trace away the latter so to obtain an effective continuous spacetime characterised by a dimensionless parameter measuring its degree of classicality and in principle energy dependent (from here the name of rainbow geometry [92, 101]). In [30] a low momentum approximation was used to derive a modified dispersion relation showing a different limit speed of propagation for elementary particles plus higher order terms in momentum.

In this chapter we shall revise the analysis of [30] and discuss its phenomenological implications. In particular, we avoid any low momentum approximation and perform an exact computation. By doing this we shall show that while a rainbow (energy dependent) geometry indeed emerges from the framework devised in [30], the related modified dispersion relation is momentum independent and does not rely on the explicit form of the scale factor which determines the geometry. So we show that the result obtained in the low momentum limit by [30] is an exact result, i.e. no momentum dependent departures from Lorentz invariance appear. Finally, we shall discuss in detail what kind of phenomenological constraints can be derived for such modified dispersion relation and which perspectives for improvements are offered by this general treatment.

## 5.2 Cosmological spacetimes from quantum gravity

Following [30] we shall start by considering a massive scalar field $\phi$ minimally coupled to gravity in cosmological setting. When performing a separation of the homogeneous and the inhomogeneous degrees of freedom, as in the analysis presented in [23], one can describe the classical dynamics for a mode $\vec{k}$ of the field (up to second order) via an Hamiltonian of the form

$$H_{\vec{k}} = H_0 - \frac{1}{2} H_0^{-1} \Big[ \pi_{\vec{k}}^2 + (\vec{k}^2 a^4 + m^2 a^6) \phi_{\vec{k}}^2 \Big], \tag{5.1}$$

with $H_0$ the Hamiltonian of the homogeneous gravitational degrees of freedom $(a, \pi_a)$ and where $(\phi_{\vec{k}}, \pi_{\vec{k}})$ are the variables in the phase space of the $\vec{k}$-mode of the scalar field [23]. After formal quantization of matter and gravity, (5.1) can be used to define a Schrödinger-like equation [30]. The formal procedure followed in [23, 30] for quantizing of the Hamiltonian (5.1) is to consider the product space $\mathcal{H} = \mathcal{H}_G \otimes \mathcal{H}_m$, with $\mathcal{H}_G$ the Hilbert space for the gravitational degrees of freedom and $\mathcal{H}_m$ the Hilbert space for matter, represented here by a scalar field. Assuming negligible back reaction by matter one can write a generic state $\Psi \in \mathcal{H}$ as $\Psi = \psi_0 \otimes \varphi$, where $\varphi \in \mathcal{H}_m$ is the state associated to matter, and $\psi_0 \in \mathcal{H}_G$ is a generic gravitational state for the homogenous degrees of freedom (which will be evolved only thought $H_0$). We can then trace away the gravitational degrees of freedom described by $\psi_0$, and so formally obtain an effective Hamiltonian for the matter sector

$$\hat{H}_{\vec{k}}^{\text{traced}} = \frac{1}{2} \Big[ \langle\psi_0|\hat{H}_0^{-1}|\psi_0\rangle \, \hat{\pi}_{\vec{k}}^2 + \langle\psi_0|\hat{\Omega}(\vec{k}, m)|\psi_0\rangle \, \hat{\phi}_{\vec{k}}^2 \Big], \tag{5.2}$$

with

$$\hat{\Omega}(\vec{k}, m) = \vec{k}^2 \widehat{H_0^{-1} a^4} + m^2 \widehat{H_0^{-1} a^6}. \tag{5.3}$$

It is worth stressing that this result does not rely on the specific form of $\mathcal{H}_G$.

The Hamiltonian (5.2) is similar to the one of a quantum scalar field in a *classical* FRLW spacetime given by the following line element

$$\bar{g}_{\mu\nu} dx^\mu dx^\nu = -\bar{N}^2 dt^2 + \bar{a}^2 \left( dx^2 + dy^2 + dz^2 \right). \tag{5.4}$$

The quantum Hamiltonian of a $\vec{k}$-mode is then given by [109]

$$\hat{H}_{\vec{k}, m}^{\text{eff}} = \frac{1}{2} \frac{\bar{N}}{\bar{a}^3} \Big[ \hat{\pi}_{\vec{k}}^2 + (\vec{k}^2 \bar{a}^4 + m^2 \bar{a}^6) \hat{\phi}_{\vec{k}}^2 \Big]. \tag{5.5}$$

Following [30] one can then use the formal analogy between the traced, QG-derived, Hamiltonian (5.2) and the quantum Hamiltonian (5.5). The matching of the two operators requires that the relations [30]

$$\bar{a}^6 + \frac{\vec{k}^2}{m^2} \bar{a}^4 - \delta = 0, \quad \text{and} \quad \frac{\bar{N}}{\bar{a}^3} = \langle\psi_0|\hat{H}_0^{-1}|\psi_0\rangle, \tag{5.6}$$

are simultaneously satisfied, where parameter $\delta$ is defined by

$$\delta := \frac{\langle\hat{\Omega}(\vec{k}, m)\rangle}{m^2 \langle\hat{H}_0^{-1}\rangle}. \tag{5.7}$$

As pointed out in [30], in contrast with the standard FLRW metric, in this case the metric (5.4) allows for a non-trivial dependence of $\bar{N}$ and $\bar{a}$ on $\vec{k}$, due to the conditions (5.6). Thus, modes with different momenta will in general see different spacetimes properties, hence the name of rainbow geometry.

## 5.3   Exact derivation of the quantum geometry

Let us first of all introduce, for the sake of convenience, the parameters $\eta$ and $\xi$ by

$$\delta = \frac{\vec{k}^2}{m^2} \frac{\langle \widehat{H_0^{-1} a^4} \rangle}{\langle \widehat{H_0^{-1}} \rangle} + \frac{\langle \widehat{H_0^{-1} a^6} \rangle}{\langle \widehat{H_0^{-1}} \rangle} := \frac{\vec{k}^2}{m^2} \xi + \eta. \tag{5.8}$$

The three solutions of the first equation in (5.6) can be written in the following form

$$\bar{a}_n^2 = -\frac{1}{3} \left[ \frac{\vec{k}^2}{m^2} + u_n \left( \frac{\vec{k}^6}{m^6} - \frac{27}{2} \left( \frac{\vec{k}^2}{m^2} \xi + \eta \right) + \frac{1}{2} \sqrt{-27\Delta} \right)^{1/3} + \right.$$
$$\left. + \frac{\vec{k}^4/m^4}{u_n \left( \frac{\vec{k}^6}{m^6} - \frac{27}{2} \left( \frac{\vec{k}^2}{m^2} \xi + \eta \right) + \frac{1}{2} \sqrt{-27\Delta} \right)^{1/3}} \right], \tag{5.9}$$

with $n = \{1, 2, 3\}$ and $u_n = \{1, (1/2)(-1 + \imath\sqrt{3}), (1/2)(-1 - \imath\sqrt{3})\}$.
It is possible to distinguish all the cases studying the discriminant given by

$$\Delta = \left( \frac{\vec{k}^2}{m^2} \xi + \eta \right) \left[ 4 \frac{\vec{k}^6}{m^6} - 27 \left( \frac{\vec{k}^2}{m^2} \xi + \eta \right) \right]. \tag{5.10}$$

It is easy to see that the study of the sign of (5.10) boils down to the study of the following equation

$$\frac{4}{27} \frac{\vec{k}^6}{m^6} - \left( \frac{\vec{k}^2}{m^2} \xi + \eta \right) = 0. \tag{5.11}$$

This equation is exactly the equation $\dfrac{4}{27} \dfrac{\vec{k}^6}{m^6} = \delta$ that differentiates the two branches in [30].

It can be shown that for $\Delta = 0$ (one multiple root and all the roots are real) the solutions $\bar{a}_2^2$ and $\bar{a}_3^2$ collapse to a double root that is real but negative. For $\Delta > 0$ (three real distinct roots) all the solutions are real but only $\bar{a}_1^2$ is positive. On the other hand, for $\Delta < 0$ (one real root and two complex conjugate roots), $\bar{a}_1^2$ is real and positive while $\bar{a}_2^2$ and $\bar{a}_3^2$ are two complex conjugate solutions. Hence it turns out that only the first solution $\bar{a}_1^2$ is positive over the possible values of $k, \xi$ and $\eta$. From now on, the real, positive solution $\bar{a}_1^2$ will be denoted by $\bar{a}^2$.

**Classical limit**

It is natural to require for *classical spacetimes*, that is, spacetimes where quantum effects are disregarded, to be independent of the momentum label $\vec{k}$. This condition can be implemented at the level of equation (5.6) that can be rewritten, using (5.8), as

$$(\bar{a}^6 - \eta) + \frac{\vec{k}^2}{m^2}(\bar{a}^4 - \xi) = 0. \tag{5.12}$$

It can be checked that the solution of the above equation that is independent of $\vec{k}$ is $\bar{a}^6 = \eta$ together with the condition $\eta^2 = \xi^3$. The latter requirement is exactly the classicality condition given in [30]. This solution can also be found by solving the equation $\partial \bar{a}^2 / \partial |\vec{k}|^2 = 0$ using the explicit form of the scale factor given in (5.9).

**Parameter of non-classicality**

While it is clear that there are two independent parameters associated to the non-classicality of the fundamental Hamiltonian, $\eta$ and $\xi$, we can also define, following [30], a parameter $\beta$ which is more convenient for measuring the departure of our geometry from its classical limit. This is defined by the expression

$$\beta \equiv \frac{\langle \widehat{H_0^{-1} a^4} \rangle}{\langle \widehat{H_0^{-1} a^6} \rangle^{2/3} \langle \widehat{H_0^{-1}} \rangle^{1/3}} - 1 = \frac{\xi}{\eta^{2/3}} - 1. \tag{5.13}$$

It is trivial to see that $\beta = 0$ when the above derived classicality condition $\xi = \eta^{2/3}$ is met. Furthermore the expansion of $\bar{a}^2$ around $\vec{k} = \vec{0}$ (equal to the non-relativistic expansion given in [30]) is

$$\bar{a}^2(\vec{k}^2/m^2) \approx \eta^{1/3} \left[ 1 + \frac{\beta}{3} \left( \frac{\vec{k}/\eta^{1/6}}{m} \right)^2 \right]. \tag{5.14}$$

Thus we see in the low momentum limit $\vec{k}/m \ll 1$, the parameter $\beta$ again measures the deviation from classicality.

## 5.4 Dispersion relation on a quantum, cosmological spacetime

The dispersion relation for a $\vec{k}$-mode of a scalar field with mass $m$ in a FRLW spacetime is determined by the equations of motion of the Hamiltonian (5.5) in the classical limit,

$$\dot{\phi}_{\vec{k}} = \frac{\bar{N}}{\bar{a}^3} \pi_{\vec{k}}, \quad \dot{\pi}_{\vec{k}} = -\phi_{\vec{k}} \frac{\bar{N}}{\bar{a}^3}(\vec{k}^2 \bar{a}^4 + m^2 \bar{a}^6). \tag{5.15}$$

Therefore one has

$$\ddot{\phi}_{\vec{k}} = \left( -3H + \frac{\dot{\bar{N}}}{\bar{N}} \right) \dot{\phi}_{\vec{k}} - \bar{N}^2 \phi_{\vec{k}} \left( \frac{\vec{k}^2}{\bar{a}^2} + m^2 \right), \tag{5.16}$$

where we use the definition of the Hubble rate $H = \dot{\bar{a}}/\bar{a}$.

In the eikonal approximation the mode of the field can be written as

$$\phi_{\vec{k}}(t) = A_{\vec{k}}(t)e^{i\theta_{\vec{k}}(t)}, \tag{5.17}$$

where the following conditions hold

$$\dot{\theta}^2 \gg \frac{\ddot{A}}{A}, \quad \ddot{\theta} \ll \dot{\theta}^2. \tag{5.18}$$

Using (5.17) and (5.18) in (5.16) (together with the assumption that also geometrical variables are slowly varying $\dot{N}, \dot{a} \ll \dot{\theta}$), the dispersion relation of a $\vec{k}$-mode reads as

$$\frac{k_0^2}{\bar{N}^2} = \frac{\vec{k}^2}{\bar{a}^2} + m^2, \tag{5.19}$$

where in the eikonal approximation $k_0 \equiv \dot{\theta}$.

We now introduce a comoving cosmological observer with four-velocity $u^\mu = (1/\bar{N}_{obs}, 0, 0, 0)$. [1]. This observer will experience a metric defined as

$$\bar{g}_{\mu\nu}^{obs} dx^\mu dx^\nu = -\bar{N}_{obs}^2 dt^2 + \bar{a}_{obs}^2 \left(dx^2 + dy^2 + dz^2\right). \tag{5.20}$$

In this framework it is natural not to assume that the $\vec{k}$-mode of the field and the observer experience the same spacetime (i.e. metric tensor). As a matter of fact $\bar{g}_{\mu\nu}^{obs}$ is still the homogeneous and isotropic rainbow metric satisfying the constraints (5.6) but it is evaluated at $|\vec{k}| = 0$. Therefore the metric experienced by a cosmological observer coincides with the metric of macroscopic objects with $m \gg |\vec{k}|$, as it should be expected.

Then the energy and the momentum of the particle measured by the observer are the following

$$E = u^\mu k_\mu = \frac{k_0}{\bar{N}_{obs}}, \quad \vec{p}^2 = \left(\bar{g}_{obs}^{\mu\nu} + u^\mu u^\nu\right) k_\mu k_\nu = \frac{\vec{k}^2}{\bar{a}_{obs}^2}, \tag{5.21}$$

The on-shell relation written in terms of the $(E, \vec{p})$ variables reads as

$$-m^2 = -f^2 E^2 + g^2 \vec{p}^2, \tag{5.22}$$

where the rainbow functions are defined as $f := \frac{\bar{N}_{obs}}{\bar{N}}$ and $g := \frac{\bar{a}_{obs}}{\bar{a}}$ [30]. The previous relation can be rewritten as

$$E^2 = \frac{1}{f^2}m^2 + \frac{g^2}{f^2}\vec{p}^2. \tag{5.23}$$

Using the second constraint in (5.6) and recalling that the expectation value $\langle\psi_0|\hat{H}_0^{-1}|\psi_0\rangle$ depends only on the gravitational degrees of freedom therefore it is the same for the observer and for the $\vec{k}$-mode of the field, one can write

$$E^2 = \frac{\bar{a}^4}{\bar{a}_{obs}^4}\vec{p}^2 + \frac{\bar{a}^6}{\bar{a}_{obs}^6}m^2. \tag{5.24}$$

---

[1] Indeed also observers on Earth can be considered as almost comoving given that the peculiar velocity of Earth is only about 360 Km/s ($\beta = v/c \approx 10^{-3}$) with respect to the CMB/cosmological frame

By means of the equation in (5.6) and the definition of $\delta$ in terms of $\eta$ and $\xi$, it follows the relation

$$m^2\,\frac{\bar{a}^6}{\bar{a}_{obs}^6} \;=\; m^2\Big(-\frac{\vec{k}^2}{m^2}\,\frac{\bar{a}^4}{\bar{a}_{obs}^6} + \frac{\vec{k}^2}{m^2}\,\frac{\xi}{\bar{a}_{obs}^6} + \frac{\eta}{\bar{a}_{obs}^6}\Big). \tag{5.25}$$

The relation (5.24) can then be written as

$$E^2 \;=\; \frac{\big[\bar{a}_{obs}^2\,c^2\,\vec{p}^2(1+\beta) + c^4\,m^2\eta^{1/3}\big]\,\eta^{2/3}}{\bar{a}_{obs}^6}. \tag{5.26}$$

At this point we use the fact that the comoving observer has zero or negligible peculiar velocity and accordingly, making use of (5.14), one can use the relation $\bar{a}_{obs}^6 = \eta$. This allows us to rewrite the dispersion relation (5.24) as

$$E^2 \;=\; m^2\,c^4 + (1+\beta)\,\vec{p}^2\,c^2, \tag{5.27}$$

where we have explicitly introduced $c$ for the present (classical) value of the speed of light in vacuum.

Remarkably, in our quantum gravity derived geometry the dispersion relation (5.27) is indeed exact, since no further assumptions than the ones defining the model as realized in [30] have been used in deriving this relation. Thus, (5.27) is valid not only in the low energy limit $|\vec{k}|/m \ll 1$ as suggested in [30] but also in the high energy limit $m/|\vec{k}| \to 0$ and it does not show corrections proportional to higher power of the momentum[2].

## 5.5 Phenomenology of the rainbow dispersion relation

Having now derived an exact form of the dispersion relation induced by the deviation from classicality of the effective spacetime geometry, it is possible to address the kind of phenomenological constraints which can be derived in this context. In this sense we have to take into account two facts. First, the above derivation was done for a scalar field in a cosmological (homogeneous and isotropic) setting. We do not know how this treatment generalises to different background geometries and different fields. For the first point we shall hence avoid statements based on ground based experiments or particle phenomenology in strong gravity environments where the isotropy and homogeneity requirements for the metric will fail. Second, the treatment as proposed in [1] clearly differentiates between quantum gravitational and quantum matter degrees of freedom (the former being traced out). If the quantum nature of the fields is a necessary requirement for seeing quantum features of spacetime then when dealing with low-energy classical gravitational waves one can assume that they would propagate at the standard speed of light $c$.

Given these facts one can envisage three possible scenarios:

---

[2]We take the point of view that since the peculiar velocity of the observer is negligible, we use (5.14) to justify the choice of $\bar{a}_{obs}^2$. One might wonder whether the choice of a non-comoving frame would bring additional corrections to (5.27). This is probably the case. However, these corrections would be proportional to the velocity of the frame and not to the particle momentum and as such would not be intrinsic to the particle physics.

- **Scenario 1: field dependent** $\beta$. Let us assume for the moment that the parameter of deviation from classicality $\beta$ depends on the type of field considered. Even sticking to cosmological constraints this would severely constraint the parameter. Just to make an example if light and electrons have different limit speeds the constraints on the relative difference would be $(|\Delta c^2|/c^2)_{\gamma,e} = O(10^{-16})$ just using the absence of gamma decay in electron-positron pair for the 80 TeV photons reaching us from the Crab nebula and the deduced at least comparable energy for the electrons responsible of such photons via inverse Compton scattering [95] (the constraint can be reduced to $O(10^{-15})$ if one prefers to use 20 TeV gamma rays reaching us from cosmological distances, e.g. from an active galactic nuclei as Markarian 501 [56]).

- **Scenario 2: Universal** $\beta$. The expression (5.13) shows that the parameter $\beta$ only depends on the quantum gravity state $\psi \in \mathcal{H}_G$. This provides an argument in favour of the universality of the expression (5.27). However, universality of $\beta$ has strong consequences for the phenomenology of (5.27). In this case the only observable effects would be associated to the interaction of matter with gravity[3] which, as said before, could be unaffected by the gravitational quantum correction and hence characterized by the geometric limit speed $c$ as set by the classical limit of the metric. Therefore if $\beta > 0$, one would naturally expect that particles will be able to rapidly loose energy via vacuum Čerenkov radiation of gravitons. Constraints from the observation of ultra high energy cosmic rays where derived in [108]. The rate of energy loss was calculated to be

$$\frac{dE}{dt} = \frac{Gp^4}{3}(c_p - c)^2 \tag{5.28}$$

where $c_p = c\sqrt{1 + \beta}$ is the speed of the particle and $G$ is Newton's constant. The corresponding constraint from the observation of high energy cosmic rays is $\beta \lesssim O(10^{-15})$. This bound assumes that the cosmic rays are protons, uses the highest record energy $3 \cdot 10^{20}$ eV, and assumes that the protons have traveled over at least 10 kpc. Assuming (as normally given) that these cosmic ray reach us from extra-galactic distances improves the limit up to $\beta \lesssim O(10^{-19})$ [108].

If $\beta$ is taken to be negative, although bounded from below ($\beta \geq -1$) assuming $\eta$ and $\xi$ positive, then the speed of gravity is higher than the limit speed of massive particles. In this case one can still put a bound on the value of the parameter considering emission of photons from gravitational waves through ordinary Čerenkov effect, but it is much less stringent being based on precision tests of General Relativity. In this context the prediction of the orbital decay of binary pulsars agrees with $c_g = c$ at $1\%$ [54, 79].

For the sake of completeness, we report here the bound that can be extracted from the direct detection of gravitational waves GW150914 [113]. The deviation of the speed of gravitational waves from the

---

[3]Within the matter sector a universal $\beta$ could be reabsorbed by a simple redefinition of the speed of light and of the particle masses.

speed of light is parametrized in [143] with a mass term in the gravitational dispersion relation, i.e. $E^2 = p^2\,c^2 + m_g^2\,c^4$. The observation gave an upper limit of $m_g \leq 1.2 \cdot 10^{-22}\,\mathrm{Ev/c^2}$, or a Compton wavelength $\lambda_g \geq 10^{13}\,\mathrm{km}$ [143]. Using the lowest observed frequency of 35Hz, one obtains the upper limit $1 - c_g/c \lesssim 7 \cdot 10^{-19}$. A model independent analysis was carried out in [57], where the time delay between gravitational wave signals detected at widely separated detectors was used. The resulting bound constrains the speed of gravity within $20\%$ of the speed of light. The authors point out that, with just few detections from the LIGO-Virgo-Kagra network, one would be able to constrain the speed of gravity to within $1\%$ of the speed of light. It is also worth pointing out that, a combined detection of a gravitational wave signals with electromagnetic counterparts would provide a bound several order of magnitude stronger [62, 63, 94, 112].

- **Scenario 3: Time dependent** $\beta$. Within a cosmological context it is still conceivable that the classicalization of the universe has progressed in time starting from a relatively large value of $\beta$ which has been driven towards zero with cosmological expansion. This hypothesis would require some plausible argument for the initial value of $\beta$ and his evolution in time. Determining such evolution is beyond the scope of this work but one can easily foresee that a varying $\beta$ could be easily be responsible for interesting phenomenology. For example if a universal (except for gravity) $\beta(t)$ had a dramatic transition from approximately one (quantum phase) to zero (classical phase) in the early universe this would reproduce the basic setting for bi-metric varying speed of light scenario (see e.g. [37]) which can lead to a spectrum of primordial perturbations and a resolution of the horizon problem. From the point of view of phenomenological constraints this scenario could be tested via future observation of primordial gravitational waves imprint in the B modes of the cosmic microwave background (as the scalar to tensor ratio would be modified if the speed of light/inflaton and gravity do not coincide). In the most general case that different matter field are endowed with different $\beta$ with non-negligible differences in the early universe, constraints on $\Delta\beta$ could be provided by Big Bang nucleosynthesis and CMB observations (e.g. via possible modifications of the physic at recombination).

## 5.6 Conclusions

In conclusion one can say that the framework developed in [23, 30] and in the present work offers a very general prediction for a regime, stemming from a quantum treatment of the gravitational sector, where a continuous spacetime has emerged but might retain a quantum nature which can be probed by quantum fields. In this chapter we have shown that an exact treatment of the emergent rainbow ($\vec{k}$-depedent) geometry lead, surprisingly, to a dispersion relation which is of relativistic form albeit characterized by a shift in the limit speed of propagation. In particular, differently from [30], in deriving our main result (5.27) we did not need to use the general explicit solution (5.9) that we derived in Section 5.3 or any expansion

of it for low momenta but we only used the equation that has to be satisfied by the rainbow scale-factor (5.12). So if (as it seems to be hinted by the present derivation) the non-classicality parameter $\beta$ is universal for any non-gravitational field, then no Lorentz violation will be detectable in the matter sector of the Standard Model and only gravity-matter phenomenology might be able to show any deviation from standard physics (see [130] for an example of a universal, but frequency-dependent, correction to the dispersion relation in the context of deformed special relativity and its phenomenological implications).

Of course, the simplicity of the present model does not allow to have sharp predictions for what regards the phenomenology associated to this approach. Still we have seen that present constraints on the value of $\beta$ are already very stringent both in the first two of the above discussed scenarios (if $\beta > 0$). This seems to hint that if this framework is indeed realised in nature then, after the continuous limit, a "classicalization" ($\beta \to 0$) of spacetime should be achieved before it could leave a strong imprint on cosmological observations well explained by the standard model of cosmology. It would be hence important to further develop this framework by investigation a possible time evolution of the $\beta$ factor in the early universe. This in turn could allow to discuss interesting phenomenology (e.g. varying speed of light scenarios) and cast constraints.

It would be also interesting to investigate what are the consequences of abandoning the non-backreaction hypothesis which was at the root of this model so far. We can speculate about two possible effects. The first one is that, since the gravitational state $\psi$ (including also non-homogeneous degrees of freedom) will now depend on the state of matter, then the parameters $\xi$ and $\eta$ will generically depend on the momentum $k^\mu$ of each matter mode (and hence $\beta$ will do so as well). Secondly, if one relaxes the test-field approximation, the backreaction will allow the Newton constant $G_N$ to appear in the computations as an additional scale beside the dimensionless parameter $\beta$. These two facts could potentially lead to higher order corrections to the dispersion relation which are not emerging in the present analysis.

Finally, this framework has been so far developed only for cosmological solutions. It would be interesting to extend it to more general backgrounds such as very high precision ground based experiments with quantum objects (e.g. Bose–Einstein condensates [14]) could be more appropriate to test this kind of tiny deviations from classical spacetime.

# Chapter 6

# Conclusions

The quest for a theory of QG is as old as GR itself and it has been engaging researchers in the field for almost a century now. For all this time the lack of experimental guidance has been the main reason for the development of an enormous variety of theoretical approaches to this problem, each proposal being based on one or more concepts or techniques that are considered more essential than others. For instance, one could start by assuming fundamental discreteness and Lorentz invariance as in CST, or making background independence and non-perturbative techniques the central building blocks of the theory as in LQG, while in Hořava—Lifshitz gravity the guiding principle is renormalizability.

However, in the last twenty years the idea that the QG regime is actually experimentally accessible has started to gain support by the community, perhaps as a consequence of decades of theoretical speculation. From the phenomenological point of view, the plethora of QG approaches stimulates the need to be able to distinguish among the various predictions of different models in a refined way. As an example, modified dispersion relations are typically a common feature of Lorentz violating and DSR theories but their phenomenology is actually different, to which degree depending on the specific models. Similarly, it is important to point out what are the unique features associated with models that realize spacetime discreteness in a particular way.

Specifically, Chapter 2 of this thesis is dedicated to investigating the distinct way discretization is incorporated in CST. A causal set is in fact at the same time discrete and Lorentz invariant and the outcome of this union is an instrinsic nonlocality. We study the consequences of this structure from the point of view of entanglement entropy. As we already pointed out in the introductory chapter, the latter has become a standard tool of investigation in QG research due to its potential connections with the fundamental structure of spacetime. One could indeed argue that the typical divergences of the entanglement entropy in QFT are essentially due to the fact that the background is a continuous manifold. Therefore in ordinary QFT on a classical spacetimes, one has to introduce a cutoff to make the entanglement entropy finite and this choice is often implicitly justified by the expectation that QG would somehow provide a physical motivation for the existence of a minimal length. More specifically, we analyze the entanglement entropy of a scalar field living on a causal set using a covariant approach introduced in [134].

Our computation shows that while the entropy is indeed regularized by the presence of a fundamental scale, in CST the area law is replaced by a spacetime volume law. We show that this result is common to local and

nonlocal Green functions for two, three and four spacetime dimensions. We also study how, truncating the spectrum of the Pauli–Jordan matrix in the appropriate way, it is possible to recover the area law in all the cases we consider, hence making contact with the results in the continuum. The second point of our analysis is that in the nonlocal models the presence of a new scale induces a more complex structure of the entanglement entropy with possible subleading terms for small values of the density. In the last part of Chapter 2 we extensively discuss how all these effects are direct consequences of the specific kind of Lorentz invariant discretization implemented in CST.

Another framework that provides a fundamental discreteness scale is LQG. In this case the classical variables are functionals defined on a continuum spatial hypersurface and geometrical operators acquire discrete spectra after quantization. In Chapter 3, we start posing the basis for the study of modified wave equations for scalar fields coupled to the quantum geometry described by LQG.

There are here two ingredients that cause a departure from the standard picture: the background discrete quantum geometry and the non standard quantization procedure known as polymer quantization, a technique imported from the gravitational sector that allows one to perform a background independent quantization of matter fields in the spirit of the LQG programme. Given that, at least at the kinematical level, the discretization predicted by LQG is purely spatial, our analysis reveals that only the spatial part of the wave equation acquires non-standard features while the temporal part is untouched. Although, this might seem to suggest that the dynamics cannot be Lorentz invariant there are other elements that have to be taken into consideration. For instance, the time parameter used for the evolution could be taken to be a clock field. The coupling of this field with the quantum geometry might induce a discrete time evolution that could in principle modify the temporal part of the wave equation so to give, loosely speaking, an overall Lorentz invariant dynamics. It is also possible that the modified wave equation is invariant under a deformed symmetry group preserving the discretization scale and maintaining the relativity principle.

It is rather clear at this point that the presence of a fundamental scale is strictly related to the fate of Lorentz symmetry. Departures from Lorentz invariance are usually parametrized by modifications to the special relativistic dispersion relation weighted by a dimensionful parameter representing the scale at which the modifications become important.[1] Lorentz transformations, being linear, cannot preserve this new scale and therefore these MDR are Lorentz violating. On the other hand, as we already mentioned earlier, DSR relativistic theories admit an additional non trivial invariant energy scale beside the speed of light. In this framework, the relativity principle is preserved even with a non homogeneous dispersion relation. In Chapter 4 we show that by adopting the framework of Finsler geometry a velocity-dependent (or equivalently, momentum-dependent) spacetime metric can be extracted from a modified dispersion relation compatible with the symmetries of $q$-de Sitter, a deformation of the standard de Sitter group,

---

[1]It can be shown that in CST, the discrete d'Alembertian operator, once averaged over several sprinklings of Minkowski spacetime, has a continuum representation in terms of a nonlocal continuum wave operator with an associated undeformed dispersion relation, hence preserving Lorentz symmetry.

offering a consistent geometrical scheme for treating what are known as rainbow geometries. We analyze the properties of this spacetime and we recover the dynamics of point-like particles usually obtained with the Hamiltonian formalism, in a fully reparametrization invariant way. Moreover we find that the Finsler spacetime associated with $q$-de Sitter is not of the Berwald type, the subclass of Finsler spaces for which the weak equivalence principle holds. However, we evaluate with an order of magnitude estimation that the deviation from the free falling trajectory is extremely suppressed.

In Chapter 5, we study a model in which a mechanism for the emergence of a cosmological spacetime geometry from a quantum gravity setting is proposed. The hypothesis on the underlying quantum geometry are rather general and, after integrating out the quantum gravitational degrees of freedom in a Born–Oppenheimer approximation, we show with an exact computation that the effective geometry turns out to be a cosmological rainbow geometry. We also compute the dispersion relation of point-like particles measured by a comoving observer and show that it does not contain momentum dependent modifications of the dispersion relation. The parameter determining the departure from the ordinary classical spacetime is a combination of expectation values of products of geometrical operator over the gravitational quantum state. In the limit in which the products can be factorized, the background becomes completely classical. This model represents an example of a non trivial spacetime which is the result of a continuum but non classical limit.

**Outlook**

Having reviewed the main results presented in this thesis, we now discuss some open questions and possible future developments of our work.

- For what concerns the computation of the entanglement entropy in causal set theory, one key result that we hope to obtain in the near future is the precise computation of the amount of information, encoded in causal relations, that is not explained by the equations of motion and that gives rise to a non vanishing entropy in the case of the spacelike partition. It can be argued that this kind of entropy has to contribute to the total balance also in the case of the entanglement entropy, posing a problem with respect to the confrontation with the continuum limit in which causally related spacetime points should not contribute to the entanglement entropy. Another possibility in this direction is the study of the SEE for different topologies and spacetimes with curvature.

  We presented a generalization to higher dimensions and non local models of the two dimensional cutoff on the PJ matrix needed to match the continuum results, based on dimensional arguments and numerical simulations. However, a direct computation of the SEE in the continuum would allow us to check our results, in particular for the nonlocal models for which the behavior of the entropy is richer than in the local models.

- The procedure that we followed in Chapter 3 produced a modified KG equation with non linear combinations of finite difference replacing second order spatial derivatives.

  In obtaining our result, we ignore possible dependence of the spread $\sigma$ on the phase space variables while generically it is implied by the dynamical evolution and the requirement that the state remains sharply peaked around a classical configuration. This is a point that we will address in the near future. Moreover, if our objective is to find corrections to the ordinary dynamics in Minkowski spacetime or in a cosmological background, we should also consider coherent states of gravity beside the matter ones.

  A part from representing a framework suitable for investigating LI, this model can be easily used to extend results obtained in the context of LQC, where, until now, polymer quantized gravitational variables had been coupled to field quantized with the standard prescription while it would be natural to use polymer quantization for both.

- The study of the Finsler geometry associated with the $q$-de Sitter group revealed that these kind of models are expected to violate the WEP. This Finsler spacetime is essentially a spacetime that reduces to the classical de Sitter spacetime when the typical length of the deformation goes to zero, while reproduces the Finsler spacetime associated with $\kappa$-Poincaré in the limit in which the curvature goes to zero. In this sense it represent an example of curved spacetime with local $\kappa$-Poincaré symmetries. It would then be interesting if one could introduce an analogous model in the spherically symmetric case. This would provide a natural framework to test DSR models through violations of the WEP.

  It would be interesting to explicitly explore the symmetries of the Finsler geometry associated with the $q$-de Sitter using the (generalized) Killing equations to check if the results for $\kappa$-Poincaré are also valid in this case.

  Another development could be the study of the connections associated with a Finsler structure to see if all the properties of the momentum space of $q$-de Sitter or $\kappa$-Poincaré can be reconstructed.

- The system investigated in Chapter 5 is probably too simplified to provide a really viable model for phenomenology. It should be possible however to make a direct comparison between the results obtained for the scalar field with similar computations for vector fields, spinors and perturbations of the metric tensor itself, that in the low-energy limit should be approximately described by perturbations of the effective rainbow metric.

In conclusion, the work presented in this thesis covers some aspects of the investigation of the quantum properties of spacetime, from theories with fundamental discreteness to effective low-energy descriptions in terms of rainbow geometries. We think that formulating convincing procedures to extract the effective dynamics of matter fields couple to quantum spacetimes is of capital importance in the direction of building a consistent

phenomenological framework to test QG theories that differ in the way fundamental discretization is implemented. On the other side of the spectrum, Finsler geometry provides a solid geometrical structure for the description of rainbow geometries that can emerge for models with deformed or broken relativistic symmetries seen as departures from the classical description of spacetime at intermediate scales.

We think that all these themes will prove themselves quite relevant for the advancement of QG phenomenology in the next coming years.

# Bibliography

[1]  Niayesh Afshordi, Siavash Aslanbeigi, and Rafael D. Sorkin. "A Distinguished Vacuum State for a Quantum Field in a Curved Spacetime: Formalism, Features, and Cosmology". In: *JHEP* 08 (2012), p. 137. arXiv: `1205.1296 [hep-th]`.

[2]  Ivan Agullo and Alejandro Corichi. "Loop Quantum Cosmology". In: *Springer Handbook of Spacetime*. Ed. by Abhay Ashtekar and Vesselin Petkov. 2014, pp. 809–839. arXiv: `1302.3833 [gr-qc]`.

[3]  Ivan Agullo and Parampreet Singh. "Loop Quantum Cosmology: A brief review". In: (2016). arXiv: `1612.01236 [gr-qc]`.

[4]  Emanuele Alesci and Francesco Cianfrani. "A new perspective on cosmology in Loop Quantum Gravity". In: *Europhys. Lett.* 104 (2013), p. 10001. arXiv: `1210.4504 [gr-qc]`.

[5]  Emanuele Alesci and Francesco Cianfrani. "Quantum Reduced Loop Gravity". In: *PoS* FFP14 (2016), p. 153. arXiv: `1506.07484 [gr-qc]`.

[6]  Emanuele Alesci and Francesco Cianfrani. "Quantum-Reduced Loop Gravity: Cosmology". In: *Phys. Rev.* D87.8 (2013), p. 083521. arXiv: `1301.2245 [gr-qc]`.

[7]  Emanuele Alesci, Francesco Cianfrani, and Carlo Rovelli. "Quantum-Reduced Loop-Gravity: Relation with the Full Theory". In: *Phys. Rev.* D88 (2013), p. 104001. arXiv: `1309.6304 [gr-qc]`.

[8]  Emanuele Alesci et al. "Cosmological singularity resolution from quantum gravity: the emergent-bouncing universe". In: (2016). arXiv: `1612.07116 [gr-qc]`.

[9]  Emanuele Alesci et al. "Polymer scalar fields in LQG". In: (). In preparation.

[10]  D. Amati, M. Ciafaloni, and G. Veneziano. "Can Space-Time Be Probed Below the String Size?" In: *Phys. Lett.* B216 (1989), pp. 41–47.

[11]  J. Ambjorn, J. Jurkiewicz, and R. Loll. "Emergence of a 4-D world from causal quantum gravity". In: *Phys. Rev. Lett.* 93 (2004), p. 131301. arXiv: `hep-th/0404156 [hep-th]`.

[12]  Giovanni Amelino-Camelia. "Quantum-Spacetime Phenomenology". In: *Living Reviews in Relativity* 16.1 (2013), p. 5. ISSN: 1433-8351.

[13]  Giovanni Amelino-Camelia. "Relativity in space-times with short distance structure governed by an observer independent (Planckian) length scale". In: *Int. J. Mod. Phys.* D11 (2002), pp. 35–60. arXiv: `gr-qc/0012051 [gr-qc]`.

[14]  Giovanni Amelino-Camelia et al. "Constraining the Energy-Momentum Dispersion Relation with Planck-Scale Sensitivity Using Cold Atoms". In: *Phys. Rev. Lett.* 103 (17 2009), p. 171302.

[15] Giovanni Amelino-Camelia et al. "Realization of doubly special relativistic symmetries in Finsler geometries". In: *Phys. Rev.* D90.12 (2014), p. 125030. arXiv: 1407.8143 [gr-qc].

[16] Giovanni Amelino-Camelia et al. "Relative-locality distant observers and the phenomenology of momentum-space geometry". In: *Class. Quant. Grav.* 29 (2012), p. 075007. arXiv: 1107.1724 [hep-th].

[17] Giovanni Amelino-Camelia et al. "Relativistic Planck-scale polymer". In: (2017). arXiv: 1707.05017 [gr-qc].

[18] Giovanni Amelino-Camelia et al. "Spacetime-noncommutativity regime of Loop Quantum Gravity". In: *Phys. Rev.* D95.2 (2017), p. 024028. arXiv: 1605.00497 [gr-qc].

[19] A. Ashtekar, John C. Baez, and Kirill Krasnov. "Quantum geometry of isolated horizons and black hole entropy". In: *Adv. Theor. Math. Phys.* 4 (2000), pp. 1–94. arXiv: gr-qc/0005126 [gr-qc].

[20] A. Ashtekar et al. "Quantum geometry and black hole entropy". In: *Phys. Rev. Lett.* 80 (1998), pp. 904–907. arXiv: gr-qc/9710007 [gr-qc].

[21] Abhay Ashtekar and Aurelien Barrau. "Loop quantum cosmology: From pre-inflationary dynamics to observations". In: *Class. Quant. Grav.* 32.23 (2015), p. 234001. arXiv: 1504.07559 [gr-qc].

[22] Abhay Ashtekar, Stephen Fairhurst, and Joshua L. Willis. "Quantum gravity, shadow states, and quantum mechanics". In: *Class. Quant. Grav.* 20 (2003), pp. 1031–1062. arXiv: gr-qc/0207106 [gr-qc].

[23] Abhay Ashtekar, Wojciech Kaminski, and Jerzy Lewandowski. "Quantum field theory on a cosmological, quantum space-time". In: *Phys. Rev.* D79 (2009), p. 064030. arXiv: 0901.0933 [gr-qc].

[24] Abhay Ashtekar and Jerzy Lewandowski. "Background independent quantum gravity: A Status report". In: *Class. Quant. Grav.* 21 (2004), R53. arXiv: gr-qc/0404018 [gr-qc].

[25] Abhay Ashtekar and Jerzy Lewandowski. "Quantum theory of geometry. 1: Area operators". In: *Class. Quant. Grav.* 14 (1997), A55–A82. arXiv: gr-qc/9602046 [gr-qc].

[26] Abhay Ashtekar and Jerzy Lewandowski. "Quantum theory of geometry. 2. Volume operators". In: *Adv. Theor. Math. Phys.* 1 (1998), pp. 388–429. arXiv: gr-qc/9711031 [gr-qc].

[27] Abhay Ashtekar, Jerzy Lewandowski, and Hanno Sahlmann. "Polymer and Fock representations for a scalar field". In: *Class. Quant. Grav.* 20 (2003), pp. L11–1. arXiv: gr-qc/0211012 [gr-qc].

[28] Abhay Ashtekar and Parampreet Singh. "Loop Quantum Cosmology: A Status Report". In: *Class. Quant. Grav.* 28 (2011), p. 213001. arXiv: 1108.0893 [gr-qc].

[29] Siavash Aslanbeigi, Mehdi Saravani, and Rafael D. Sorkin. "Generalized causal set d'Alembertians". In: *JHEP* 06 (2014), p. 024. arXiv: 1403.1622 [hep-th].

[30] Mehdi Assanioussi, Andrea Dapor, and Jerzy Lewandowski. "Rainbow metric from quantum gravity". In: *Phys. Lett.* B751 (2015), pp. 302–305. arXiv: 1412.6000 [gr-qc].

[31] A Ballesteros et al. "Quantum structure of the motion groups of the two-dimensional Cayley-Klein geometries". In: *Journal of Physics A: Mathematical and General* 26.21 (1993), p. 5801.

[32] Kinjal Banerjee, Gianluca Calcagni, and Mercedes Martin-Benito. "Introduction to loop quantum cosmology". In: *SIGMA* 8 (2012), p. 016. arXiv: 1109.6801 [gr-qc].

[33] D Bao, SS Chern, and Z Shen. "An Introduction to Riemannian Finsler Geom". In: *Graduate Texts in Math* 200 (2000).

[34] Leonardo Barcaroli and Giulia Gubitosi. "Kinematics of particles with quantum-de Sitter-inspired symmetries". In: *Phys. Rev.* D93.12 (2016), p. 124063. arXiv: 1512.03462 [gr-qc].

[35] Leonardo Barcaroli et al. "Hamilton geometry: Phase space geometry from modified dispersion relations". In: *Phys. Rev. D* 92 (8 2015), p. 084053.

[36] Carlos Barcelo, Stefano Liberati, and Matt Visser. "Refringence, field theory, and normal modes". In: *Class. Quant. Grav.* 19 (2002), pp. 2961–2982. arXiv: gr-qc/0111059 [gr-qc].

[37] Bruce A. Bassett et al. "Geometrodynamics of variable-speed-of-light cosmologies". In: *Phys. Rev. D* 62 (10 2000), p. 103518.

[38] John K. Beem. "Indefinite Finsler spaces and timelike spaces". In: *Canad. J. Math.* 22 (1970), pp. 1035–1039.

[39] Alessio Belenchia, Dionigi M. T. Benincasa, and Stefano Liberati. "Nonlocal Scalar Quantum Field Theory from Causal Sets". In: *JHEP* 03 (2015), p. 036. arXiv: 1411.6513 [gr-qc].

[40] Alessio Belenchia et al. "Spacetime entropy in causal set theory". In: (). In preparation.

[41] Alessio Belenchia et al. "Spectral Dimension from Nonlocal Dynamics on Causal Sets". In: *Phys. Rev.* D93.4 (2016), p. 044017. arXiv: 1507.00330 [gr-qc].

[42] Alessio Belenchia et al. "Tests of quantum-gravity-induced nonlocality via optomechanical experiments". In: *Phys. Rev.* D95.2 (2017), p. 026012. arXiv: 1611.07959 [gr-qc].

[43] Dionigi M. T. Benincasa and Fay Dowker. "The Scalar Curvature of a Causal Set". In: *Phys. Rev. Lett.* 104 (2010), p. 181301. arXiv: 1001.2725 [gr-qc].

[44] Dionigi M. T. Benincasa, Fay Dowker, and Bernhard Schmitzer. "The Random Discrete Action for 2-Dimensional Spacetime". In: *Class. Quant. Grav.* 28 (2011), p. 105018. arXiv: 1011.5191 [gr-qc].

[45] V.B. Berestetskii, E.M. Lifshitz, and L.P. Pitaevski. *Quantum Electrodynamics*. Course of theoretical physics. Butterworth-Heinemann, 1982. ISBN: 9780750633710.

[46] Micheal S. Berger, V. Alan Kostelecký, and Zhi Liu. "Lorentz and CPT Violation in Top-Quark Production and Decay". In: *Phys. Rev.* D93.3 (2016), p. 036005. arXiv: 1509.08929 [hep-ph].

[47] Jakub Bilski, Emanuele Alesci, and Francesco Cianfrani. "Quantum reduced loop gravity: Extension to scalar fields". In: *Phys. Rev. D* 92 (12 2015), p. 124029.

[48] Luca Bombelli, Joe Henson, and Rafael D. Sorkin. "Discreteness without symmetry breaking: A Theorem". In: *Mod. Phys. Lett.* A24 (2009), pp. 2579–2587. arXiv: gr-qc/0605006 [gr-qc].

[49] Luca Bombelli et al. "Space-time as a causal set". In: *Phys. Rev. Lett.* 59 (5 1987), pp. 521–524.

[50] Michel Buck et al. "Boundary Terms for Causal Sets". In: *Class. Quant. Grav.* 32.20 (2015), p. 205004. arXiv: 1502.05388 [gr-qc].

[51] H. Busemann. "On Normal Coordinates in Finsler Spaces." In: *Mathematische Annalen* 129 (1955), pp. 417–423.

[52] Pasquale Calabrese and John L. Cardy. "Entanglement entropy and quantum field theory". In: *J. Stat. Mech.* 0406 (2004), P06002. arXiv: hep-th/0405152 [hep-th].

[53] Curtis G. Callan Jr. and Frank Wilczek. "On geometric entropy". In: *Phys. Lett.* B333 (1994), pp. 55–61. arXiv: hep-th/9401072 [hep-th].

[54] S. Carlip. "Aberration and the speed of gravity". In: *Physics Letters A* 267.2 (2000), pp. 81 –87. ISSN: 0375-9601.

[55] Francesco Cianfrani et al. "Symmetries of quantum spacetime in three dimensions". In: *Phys. Rev.* D94.8 (2016), p. 084044. arXiv: 1606.03085 [hep-th].

[56] Sidney Coleman and Sheldon L. Glashow. "High-energy tests of Lorentz invariance". In: *Phys. Rev. D* 59 (11 1999), p. 116008.

[57] Neil Cornish, Diego Blas, and Germano Nardini. "Bounding the speed of gravity with gravitational wave observations". In: (2017). arXiv: 1707.06101 [gr-qc].

[58] Arno Deicke. "Über die Finsler-Räume mit Ai= 0". In: *Archiv der Mathematik* 4.1 (1953), pp. 45–51.

[59] Marcin Domagala, Michal Dziendzikowski, and Jerzy Lewandowski. "The polymer quantization in LQG: massless scalar field". In: *Proceedings, 3rd Quantum Geometry and Quantum Gravity School: Zakopane, Poland, February 28-March 13, 2011.* 2012. arXiv: 1210.0849 [gr-qc].

[60] Fay Dowker and Lisa Glaser. "Causal set d'Alembertians for various dimensions". In: *Class. Quant. Grav.* 30 (2013), p. 195016. arXiv: 1305.2588 [gr-qc].

[61] Fay Dowker, Steven Johnston, and Rafael D. Sorkin. "Hilbert Spaces from Path Integrals". In: *J. Phys.* A43 (2010), p. 275302. arXiv: 1002.0589 [quant-ph].

[62] John Ellis, Nick E. Mavromatos, and Dimitri V. Nanopoulos. "Comments on Graviton Propagation in Light of GW150914". In: *Mod. Phys. Lett.* A31.26 (2016), p. 1675001. arXiv: 1602.04764 [gr-qc].

[63] Xi-Long Fan et al. "Speed of Gravitational Waves from Strongly Lensed Gravitational Waves and Electromagnetic Signals". In: *Phys. Rev. Lett.* 118.9 (2017), p. 091102. arXiv: 1612.04095 [gr-qc].

[64] Laurent Freidel, Jerzy Kowalski-Glikman, and Lee Smolin. "2+1 gravity and doubly special relativity". In: *Phys. Rev.* D69 (2004), p. 044001. arXiv: hep-th/0307085 [hep-th].

[65]    Laurent Freidel, Robert G. Leigh, and Djordje Minic. "Quantum Gravity, Dynamical Phase Space and String Theory". In: *Int. J. Mod. Phys.* D23.12 (2014), p. 1442006. arXiv: 1405.3949 [hep-th].

[66]    Laurent Freidel and Etera R. Livine. "Effective 3-D quantum gravity and non-commutative quantum field theory". In: *Phys. Rev. Lett.* 96 (2006), p. 221301. arXiv: hep-th/0512113 [hep-th].

[67]    Luis J. Garay. "Quantum gravity and minimum length". In: *Int. J. Mod. Phys.* A10 (1995), pp. 145–166. arXiv: gr-qc/9403008 [gr-qc].

[68]    Florian Girelli, Stefano Liberati, and Lorenzo Sindoni. "Planck-scale modified dispersion relations and Finsler geometry". In: *Phys. Rev.* D75 (2007), p. 064015. arXiv: gr-qc/0611024 [gr-qc].

[69]    Lisa Glaser. "A closed form expression for the causal set d'Alembertian". In: *Class. Quant. Grav.* 31 (2014), p. 095007. arXiv: 1311.1701 [math-ph].

[70]    Giulia Gubitosi and Flavio Mercati. "Relative Locality in $\kappa$-Poincaré". In: *Class. Quant. Grav.* 30 (2013), p. 145002. arXiv: 1106.5710 [gr-qc].

[71]    Stephen Hawking. "The occurrence of singularities in cosmology. III. Causality and singularities". In: *Proc. Roy. Soc. Lond.* A300 (1967), pp. 187–201.

[72]    Stephen W Hawking, A Ro King, and PJ McCarthy. "A new topology for curved space–time which incorporates the causal, differential, and conformal structures". In: *Journal of mathematical physics* 17.2 (1976), pp. 174–181.

[73]    S.W. Hawking and G.F.R. Ellis. *The Large Scale Structure of Space-Time*. Cambridge Monographs on Mathematical Physics. Cambridge University Press, 1973. ISBN: 9780521099066.

[74]    Joe Henson. "Discovering the Discrete Universe". In: *Proceedings, Foundations of Space and Time: Reflections on Quantum Gravity: Cape Town, South Africa*. 2010. arXiv: 1003.5890 [gr-qc].

[75]    Hoshang Heydari. "Geometric formulation of quantum mechanics". In: (2015). arXiv: 1503.00238 [quant-ph].

[76]    Petr Horava. "Quantum Gravity at a Lifshitz Point". In: *Phys. Rev.* D79 (2009), p. 084008. arXiv: 0901.3775 [hep-th].

[77]    Sabine Hossenfelder. "Experimental Search for Quantum Gravity". In: *Workshop on Experimental Search for Quantum Gravity NORDITA, Stockholm, Sweden, July 12-16, 2010*. 2010. arXiv: 1010.3420 [gr-qc].

[78]    Sabine Hossenfelder. "Minimal Length Scale Scenarios for Quantum Gravity". In: *Living Rev. Rel.* 16 (2013), p. 2. arXiv: 1203.6191 [gr-qc].

[79]    J.P. Hsu and D. Fine. *100 Years of Gravity and Accelerated Frames: The Deepest Insights of Einstein and Yang-Mills*. Advanced series on theoretical physical science. World Scientific, 2005. ISBN: 9789812703408.

[80]    T. Jacobson, Stefano Liberati, and D. Mattingly. "A Strong astrophysical constraint on the violation of special relativity by quantum gravity". In: *Nature* 424 (2003), pp. 1019–1021. arXiv: astro-ph/0212190 [astro-ph].

[81]   Ted Jacobson. "Einstein-aether gravity: A Status report". In: *PoS* QG-PH (2007), p. 020. arXiv: `0801.1547 [gr-qc]`.

[82]   Ted Jacobson. "Entanglement Equilibrium and the Einstein Equation". In: *Phys. Rev. Lett.* 116.20 (2016), p. 201101. arXiv: `1505.04753 [gr-qc]`.

[83]   Ted Jacobson. "Thermodynamics of space-time: The Einstein equation of state". In: *Phys. Rev. Lett.* 75 (1995), pp. 1260–1263. arXiv: `gr-qc/9504004 [gr-qc]`.

[84]   Steven Johnston. "Feynman Propagator for a Free Scalar Field on a Causal Set". In: *Phys. Rev. Lett.* 103 (2009), p. 180401. arXiv: `0909.0944 [hep-th]`.

[85]   Steven Paul Johnston. "Quantum Fields on Causal Sets". PhD thesis. Imperial Coll., London, 2010. arXiv: `1010.5514 [hep-th]`.

[86]   Wojciech Kaminski, Jerzy Lewandowski, and Marcin Bobienski. "Background independent quantizations: The Scalar field. I." In: *Class. Quant. Grav.* 23 (2006), pp. 2761–2770. arXiv: `gr-qc/0508091 [gr-qc]`.

[87]   Wojciech Kaminski, Jerzy Lewandowski, and Andrzej Okolow. "Background independent quantizations: The Scalar field II". In: *Class. Quant. Grav.* 23 (2006), pp. 5547–5586. arXiv: `gr-qc/0604112 [gr-qc]`.

[88]   V. Alan Kostelecký. "Gravity, Lorentz violation, and the standard model". In: *Phys. Rev. D* 69 (10 2004), p. 105009.

[89]   V. Alan Kostelecký and Stuart Samuel. "Spontaneous breaking of Lorentz symmetry in string theory". In: *Phys. Rev. D* 39 (2 1989), pp. 683–685.

[90]   Jerzy Kowalski-Glikman. "De sitter space as an arena for doubly special relativity". In: *Phys. Lett.* B547 (2002), pp. 291–296. arXiv: `hep-th/0207279 [hep-th]`.

[91]   Jerzy Kowalski-Glikman and Sebastian Nowak. "Doubly special relativity and de Sitter space". In: *Class. Quant. Grav.* 20 (2003), pp. 4799–4816. arXiv: `hep-th/0304101 [hep-th]`.

[92]   Rene Lafrance and Robert C. Myers. "Gravity's rainbow". In: *Phys. Rev.* D51 (1995), pp. 2584–2590. arXiv: `hep-th/9411018 [hep-th]`.

[93]   Jerzy Lewandowski et al. "Uniqueness of Diffeomorphism Invariant States on Holonomy–Flux Algebras". In: *Communications in Mathematical Physics* 267.3 (2006), pp. 703–733. ISSN: 1432-0916.

[94]   Xiang Li et al. "GRB/GW association: Long-short GRB candidates, time-lag, measuring gravitational wave velocity and testing Einstein's equivalence principle". In: *Astrophys. J.* 827.1 (2016), p. 75. arXiv: `1601.00180 [astro-ph.HE]`.

[95]   Stefano Liberati. "Tests of Lorentz invariance: a 2013 update". In: *Class. Quant. Grav.* 30 (2013), p. 133001. arXiv: `1304.5795 [gr-qc]`.

[96]   Iarley P. Lobo, Niccoló Loret, and Francisco Nettel. "Investigation on Finsler geometry as a generalization to curved spacetime of Planck-scale-deformed relativity in the de Sitter case". In: (2016). arXiv: `1611.04995 [gr-qc]`.

[97]  Iarley P. Lobo, Niccoló Loret, and Francisco Nettel. "Rainbows without unicorns: Metric structures in theories with Modified Dispersion Relations". In: (2016). arXiv: 1610.04277 [gr-qc].

[98]  Jerzy Lukierski, Anatol Nowicki, and Henri Ruegg. "Real forms of complex quantum anti-De Sitter algebra U-q(Sp(4:C)) and their contraction schemes". In: *Phys. Lett.* B271 (1991), pp. 321–328. arXiv: hep-th/9108018 [hep-th].

[99]  Jerzy Lukierski and Henri Ruegg. "Quantum kappa Poincare in any dimension". In: *Phys. Lett.* B329 (1994), pp. 189–194. arXiv: hep-th/9310117 [hep-th].

[100] Jerzy Lukierski et al. "q-deformation of Poincaré algebra". In: *Physics Letters B* 264.3 (1991), pp. 331 –338. ISSN: 0370-2693.

[101] Joao Magueijo and Lee Smolin. "Gravity's rainbow". In: *Class. Quant. Grav.* 21 (2004), pp. 1725–1736. arXiv: gr-qc/0305055 [gr-qc].

[102] S. Majid. *Foundations of Quantum Group Theory*. Cambridge University Press, 2000. ISBN: 9780521648684.

[103] S. Majid and H. Ruegg. "Bicrossproduct structure of kappa Poincare group and noncommutative geometry". In: *Phys. Lett.* B334 (1994), pp. 348–354. arXiv: hep-th/9405107 [hep-th].

[104] David B Malament. "The class of continuous timelike curves determines the topology of spacetime". In: *Journal of mathematical physics* 18.7 (1977), pp. 1399–1404.

[105] F. K. Manasse and C. W. Misner. "Fermi Normal Coordinates and Some Basic Concepts in Differential Geometry". In: *Journal of Mathematical Physics* 4.6 (1963), p. 735. ISSN: 00222488.

[106] Antonino Marciano et al. "Interplay between curvature and Planck-scale effects in astrophysics and cosmology". In: *JCAP* 1006 (2010), p. 030. arXiv: 1004.1110 [gr-qc].

[107] E. Minguzzi. "Special coordinate systems in pseudo-Finsler geometry and the equivalence principle". In: (2016). arXiv: 1601.07952 [gr-qc].

[108] Guy D. Moore and Ann E. Nelson. "Lower bound on the propagation speed of gravity from gravitational Cherenkov radiation". In: *JHEP* 09 (2001), p. 023. arXiv: hep-ph/0106220 [hep-ph].

[109] Viatcheslav Mukhanov and Sergei Winitzki. *Introduction to quantum effects in gravity*. Cambridge University Press, 2007. ISBN: 9780521868341, 9781139785945.

[110] Dmitry Nesterov and Sergey N. Solodukhin. "Gravitational effective action and entanglement entropy in UV modified theories with and without Lorentz symmetry". In: *Nucl. Phys.* B842 (2011), pp. 141–171. arXiv: 1007.1246 [hep-th].

[111] Dmitry Nesterov and Sergey N. Solodukhin. "Short-distance regularity of Green's function and UV divergences in entanglement entropy". In: *JHEP* 09 (2010), p. 041. arXiv: 1008.0777 [hep-th].

[112] Atsushi Nishizawa and Takashi Nakamura. "Measuring Speed of Gravitational Waves by Observations of Photons and Neutrinos from Compact Binary Mergers and Supernovae". In: *Phys. Rev.* D90.4 (2014), p. 044048. arXiv: 1406.5544 [gr-qc].

[113] "Observation of Gravitational Waves from a Binary Black Hole Merger". In: *Phys. Rev. Lett.* 116 (6 2016), p. 061102.

[114] Daniele Oriti. "Group Field Theory and Loop Quantum Gravity". In: 2014. arXiv: 1408.7112 [gr-qc].

[115] Daniele Oriti. "The Group field theory approach to quantum gravity: Some recent results". In: *AIP Conf. Proc.* 1196 (2009), pp. 209–218. arXiv: 0912.2441 [hep-th].

[116] Onkar Parrikar and Sumati Surya. "Causal Topology in Future and Past Distinguishing Spacetimes". In: *Class. Quant. Grav.* 28 (2011), p. 155020. arXiv: 1102.0936 [gr-qc].

[117] Roberto Percacci. "Asymptotic Safety". In: (2007). arXiv: 0709.3851 [hep-th].

[118] Alejandro Perez. "The Spin Foam Approach to Quantum Gravity". In: *Living Rev. Rel.* 16 (2013), p. 3. arXiv: 1205.2019 [gr-qc].

[119] Christian Pfeifer. "The tangent bundle exponential map and locally autoparallel coordinates for general connections on the tangent bundle with application to Finsler geometry". In: *Int. J. Geom. Meth. Mod. Phys.* 13.03 (2016), p. 1650023. arXiv: 1406.5413 [math-ph].

[120] Christian Pfeifer and Mattias N. R. Wohlfarth. "Causal structure and electrodynamics on Finsler spacetimes". In: *Phys. Rev.* D84 (2011), p. 044039. arXiv: 1104.1079 [gr-qc].

[121] Christian Pfeifer and Mattias N. R. Wohlfarth. "Finsler geometric extension of Einstein gravity". In: *Phys. Rev.* D85 (2012), p. 064009. arXiv: 1112.5641 [gr-qc].

[122] J. Polchinski. *String Theory: Volume 2, Superstring Theory and Beyond*. Cambridge Monographs on Mathematical Physics. Cambridge University Press, 1998. ISBN: 9781139457415.

[123] D. P. Rideout and R. D. Sorkin. "Classical sequential growth dynamics for causal sets". In: *Phys. Rev. D* 61 (2 1999), p. 024002.

[124] Carlo Rovelli. "Black hole entropy from loop quantum gravity". In: *Phys. Rev. Lett.* 77 (1996), pp. 3288–3291. arXiv: gr-qc/9603063 [gr-qc].

[125] Carlo Rovelli. "Loop Quantum Gravity". In: *Living Reviews in Relativity* 11.1 (2008), p. 5. ISSN: 1433-8351.

[126] Carlo Rovelli. "Notes for a brief history of quantum gravity". In: *Recent developments in theoretical and experimental general relativity, gravitation and relativistic field theories. Proceedings, 9th Marcel Grossmann Meeting, MG'9, Rome, Italy, July 2-8, 2000. Pts. A-C*. 2000, pp. 742–768. arXiv: gr-qc/0006061 [gr-qc].

[127] Carlo Rovelli and Lee Smolin. "Discreteness of area and volume in quantum gravity". In: *Nucl. Phys.* B442 (1995). [Erratum: Nucl. Phys.B456,753(1995)], pp. 593–622. arXiv: gr-qc/9411005 [gr-qc].

[128]   Mehdi Saravani and Siavash Aslanbeigi. "Dark Matter From Space-time Nonlocality". In: *Phys. Rev.* D92.10 (2015), p. 103504. arXiv: `1502.01655 [hep-th]`.

[129]   Mehdi Saravani, Rafael D. Sorkin, and Yasaman K. Yazdi. "Space-time entanglement entropy in 1 + 1 dimensions". In: *Class. Quant. Grav.* 31.21 (2014), p. 214006. arXiv: `1311.7146 [hep-th]`.

[130]   Lee Smolin. "Falsifiable predictions from semiclassical quantum gravity". In: *Nuclear Physics B* 742.1 (2006), pp. 142 –157. ISSN: 0550-3213.

[131]   Lee Smolin. "Recent developments in nonperturbative quantum gravity". In: (1992). arXiv: `hep-th/9202022 [hep-th]`.

[132]   Rafael D. Sorkin. "Causal sets: Discrete gravity". In: *Lectures on quantum gravity. Proceedings, School of Quantum Gravity, Valdivia, Chile, January 4-14, 2002.* 2003, pp. 305–327. arXiv: `gr-qc/0309009 [gr-qc]`.

[133]   Rafael D. Sorkin. "Does locality fail at intermediate length-scales". In: (2007). arXiv: `gr-qc/0703099 [GR-QC]`.

[134]   Rafael D. Sorkin. "Expressing entropy globally in terms of (4D) field-correlations". In: *J. Phys. Conf. Ser.* 484 (2014), p. 012004. arXiv: `1205.2953 [hep-th]`.

[135]   Rafael D. Sorkin. "From Green Function to Quantum Field". In: *Int. J. Geom. Meth. Mod. Phys.* 14.08 (2017), p. 1740007. arXiv: `1703.00610 [gr-qc]`.

[136]   Rafael D. Sorkin. "Scalar Field Theory on a Causal Set in Histories Form". In: *J. Phys. Conf. Ser.* 306 (2011), p. 012017. arXiv: `1107.0698 [gr-qc]`.

[137]   Rafael D. Sorkin and Yasaman K. Yazdi. "Entanglement Entropy in Causal Set Theory". In: (2016). arXiv: `1611.10281 [hep-th]`.

[138]   Thomas P. Sotiriou and Valerio Faraoni. "f(R) Theories Of Gravity". In: *Rev. Mod. Phys.* 82 (2010), pp. 451–497. arXiv: `0805.1726 [gr-qc]`.

[139]   Floyd W. Stecker et al. "Searching for Traces of Planck-Scale Physics with High Energy Neutrinos". In: *Phys. Rev.* D91.4 (2015), p. 045009. arXiv: `1411.5889 [hep-ph]`.

[140]   K. S. Stelle. "Classical Gravity with Higher Derivatives". In: *Gen. Rel. Grav.* 9 (1978), pp. 353–371.

[141]   Sumati Surya. "Directions in Causal Set Quantum Gravity". In: (2011). arXiv: `1103.6272 [gr-qc]`.

[142]   V.M. Taveras. *Loop Gravity: An Application and an Extension*. 2009.

[143]   "Tests of General Relativity with GW150914". In: *Phys. Rev. Lett.* 116 (22 2016), p. 221101.

[144]   *The differential geometry of Finsler spaces*. 1959.

[145]   T. Thiemann. "Kinematical Hilbert spaces for Fermionic and Higgs quantum field theories". In: *Class. Quant. Grav.* 15 (1998), pp. 1487–1512. arXiv: `gr-qc/9705021 [gr-qc]`.

[146]   T. Thiemann. *Modern Canonical Quantum General Relativity*. Cambridge Monographs on Mathematical Physics. Cambridge University Press, 2007. ISBN: 9781139467599.

[147] T. Thiemann. "QSD 5: Quantum gravity as the natural regulator of matter quantum field theories". In: *Class. Quant. Grav.* 15 (1998), pp. 1281–1314. arXiv: `gr-qc/9705019 [gr-qc]`.

[148] T Thiemann. "Quantum spin dynamics (QSD)". In: *Classical and Quantum Gravity* 15.4 (1998), p. 839.

[149] Ricardo Gallego Torromé, Marco Letizia, and Stefano Liberati. "Phenomenology of effective geometries from quantum gravity". In: *Phys. Rev.* D92.12 (2015), p. 124021. arXiv: `1507.03205 [gr-qc]`.

[150] Mark Van Raamsdonk. "Building up spacetime with quantum entanglement". In: *Gen. Rel. Grav.* 42 (2010). [Int. J. Mod. Phys.D19,2429(2010)], pp. 2323–2329. arXiv: `1005.3035 [hep-th]`.

[151] Vincenzo Vitagliano, Thomas P. Sotiriou, and Stefano Liberati. "The dynamics of metric-affine gravity". In: *Annals Phys.* 326 (2011). [Erratum: Annals Phys.329,186(2013)], pp. 1259–1273. arXiv: `1008.0171 [gr-qc]`.

[152] Silke Weinfurtner, Stefano Liberati, and Matt Visser. "Analogue spacetime based on 2-component Bose-Einstein condensates". In: *Lect. Notes Phys.* 718 (2007), pp. 115–163. arXiv: `gr-qc/0605121 [gr-qc]`.

[153] Clifford M. Will. "The Confrontation between General Relativity and Experiment". In: *Living Reviews in Relativity* 9.3 (2006).

[154] J. L. Willis. "On the low-energy ramifications and a mathematical extension of loop quantu m gravity". PhD thesis. The Pennsylvania State University, Pennsylvania, USA, 2004.

# Appendix A

# Entanglement entropy of nonlocal scalar fields via the replica trick

In this appendix, we briefly review the computation of the entanglement entropy of a quantum field using the *replica trick* [53, 110] and use it in the case of the nonlocal scalar field theory emerging from CST in the continuum limit in two, three and four spacetime dimensions.

## A.1  The replica trick

Let us consider a quantum field $\phi(x)$ on a $d$-dimensional spacetime with coordinates $x^\mu = (\tau, x, z^i, i = 1, ..., d - 2)$, where $\tau$ is the Euclidean time, and a hypersurface $\Sigma$ defined by the condition $x = 0$. The coordinates $z^i$ are therefore the coordinates on $\Sigma$.

Entanglement entropy is computed by preparing the field in the vacuum state and then tracing out the degrees of freedom which are inside (outside) the surface $\Sigma$. The computation goes as follows.

First, we define the vacuum state of scalar field by a path integral over half of the Euclidean space defined by $\tau \leq 0$ in such a way that the field assumes the boundary condition $\phi(\tau = 0, x, z) = \phi_0(x, z)$,

$$\Phi[\phi_0(x, z)] = \int_{\phi(x^\mu)|_{\tau=0}=\phi_0(x,z)} \mathcal{D}\phi \, e^{-W[\phi]}, \tag{A.1}$$

where $W[\phi]$ is the action of the field. The surface $\Sigma$, given by $(\tau = 0, x = 0)$, separates the boundary data in two parts $\phi_-(x, z)$ for $x < 0$ and $\phi_+(x, z)$ for $x > 0$. Now tracing over $\phi_-(x, z)$ one obtains a reduced density matrix

$$\rho(\phi_+^1, \phi_+^2) = \int \mathcal{D}\phi_- \, \Phi(\phi_+^1, \phi_-)\Phi(\phi_+^2, \phi_-), \tag{A.2}$$

where the path integral goes over fields defined on the whole Euclidean space-time except a cut $(\tau = 0, x > 0)$. In the path integral the field $\phi(x^\mu)$ takes a boundary value $\phi_+^2$ above the cut and $\phi_+^1$ below the cut.

The trace of $n$-th power of the density matrix (A.2) is given by the Euclidean path integral over fields defined on an $n$-sheeted covering of the cut space-time. Essentially one considers $n$ copies of this space-time attaching one copy to the next through the cut gluing analytically the fields. Passing from Cartesian coordinates $(\tau, x)$ to polar ones $(r, \alpha)$, the cut corresponds

to the values $\alpha = 2\pi k$ with $k = 1, 2, ..., n$. This $n$-fold space is geometrically a flat cone $C_n$ with a deficit angle $2\pi(n-1)$. Therefore one has

$$\mathrm{Tr}\rho^n = Z[C_n], \tag{A.3}$$

where $Z[C_n]$ is the Euclidean path integral over the n-fold cover of the Euclidean space, i.e. over the cone $C_n$.

It can be shown that it is possible in (A.3) to analytically continue to non-integer values of $n \to \beta$. With that said, one observes that $-\mathrm{Tr}\hat{\rho}\ln\hat{\rho} = -(\beta\partial_\beta - 1)\ln\rho^\beta|_{\beta=1}$, where $\hat{\rho} = \frac{\rho}{\mathrm{Tr}\rho}$. In polar coordinates $(r, \alpha)$, the conical space $C_\beta$ is defined by making the coordinate $\alpha$ periodic with the period $2\pi\beta$, where $(1 - \beta)$ is very small. Then introducing $W(\beta) = \ln Z[C_\beta]$, one has

$$S = (\beta\partial_\beta - 1)W(\beta)|_{\beta=1}. \tag{A.4}$$

At this point in order to calculate $W(\beta)$ one can use the heat kernel method in the context of manifolds with conical singularities (see [110] and references therein).

Once the effective action $W(\beta)$ is calculated, the entanglement entropy is simply given by the following formula

$$S = \frac{A(\Sigma)}{12(4\pi)^{(d-2)/2}} \int_{\epsilon^2}^{\infty} \frac{ds}{s} \, P_{d-2}(s), \tag{A.5}$$

where $\epsilon$ is a UV cut-off that makes the integral finite ($s$ has dimensions of a length squared) and

$$P_{d-2}(s) = \frac{2}{\Gamma(\frac{d-2}{2})} \int_0^{\infty} dp \, p^{d-3} \, e^{-sF(p^2)}. \tag{A.6}$$

$F(p^2)$ is the Fourier transform of kinetic operator of a non-interacting Lorentz invariant scalar field theory.

## A.2    The case of the nonlocal scalar field theories from CST

We will now apply the procedure described above to the case of nonlocal scalar field theories from CST. In particular we will consider the continuum d'Alembertians obtained by averaging the operators (2.13) over all sprinklings of Minkowski spacetime. The result of the averaging process is given by the following expression

$$\Box_{\rho_k}^{(d)}\phi(x) = \rho^{2/d}\left(a\phi(x) + \rho\sum_{n=0}^{L_{max}} \frac{b_n}{n!} \int_{J^-(x)} e^{-\rho V(x,y)} [\rho V(x,y)]^n \, \phi(y) \, dy\right), \tag{A.7}$$

where $\rho_k = l_k^{-d}$, $l_k$ being the nonlocality scale, $J^-(x)$ is the causal past of $x$ and $V(x, y)$ is the spacetime volume between the past light cone of $x$ and the future light cone of $y$.

Following the discussion in [29], the momentum space representation of (A.7) can be considered for $p^2 \ll \rho_k^{-2/d}$ (IR limit) and $p^2 \gg \rho_k^{-2/d}$ (UV

limit). The former is universal and given by

$$F_{\rho_k}(p^2) \to -p^2, \quad \text{for} \quad p^2 \ll \rho_k^{-2/d}, \tag{A.8}$$

while the latter depends on the spacetime dimensions and can be given as

$$F_{\rho_k}(p^2) \to a\,\rho_k^{2/d} + b\,\rho_k^{2/d+1} k^{-d} + ..., \quad \text{for} \quad p^2 \gg \rho_k^{-2/d}. \tag{A.9}$$

From Eq.(A.9), one can see that the nonlocal d'Alembertian goes to a constant in the UV. This term correspons to a delta function for the Green functions in real space in the coincident limit and it is essentially a remnant of the fundamental discreteness of the causal set (see the discussion in [29]). This term can be subtracted and one can define a regularized d'Alembertian operator as

$$F_{\text{reg}}(p^2) = \frac{a\,\rho_k^{2/d} F_{\rho_k}(p^2)}{a\,\rho_k^{2/d} - F_{\rho_k}(p^2)}. \tag{A.10}$$

The operator (A.10) maintains the correct IR limit given by Eq.(A.8) and possesses the new UV behavior displayed by the following expression

$$F_{\text{reg}} \to -\frac{a^2}{b}\rho_k^{2/d-1}\, p^d + ..., \quad \text{for} \quad p^2 \gg \rho_k^{-2/d}. \tag{A.11}$$

In order to compute the entanglement entropy via the replica trick we need to Wick rotate the operator $F_{\text{reg}}$ or, equivalently, its retarded propagator. However this cannot be done on the retarded propagator because the contour, $\Gamma_R$, would cross singularities. To avoid this problem one must use the Feynman propagator whose contour can be Wick rotated without crossing any singularities (see [39, 41, 128] for further details).

**IR and UV behavior of the entanglement entropy**

The behavior of (A.10) for $p^2 \ll \rho_k^{2/d}$, for negligible nonlocal effects, is given by eq.(A.8). Hence the entanglement entropy computed solely on the basis of this contribution scales with the area of the surface $\Sigma$. In particular, in $d = 2, 3, 4$, the entropy is given by

$$\begin{aligned} S_{loc}^{(2)} &= \frac{1}{6}A(\Sigma)\ln\left(L/\epsilon\right) \\ S_{loc}^{(3)} &= \frac{A(\Sigma)}{12\sqrt{\pi}}\frac{1}{\epsilon} \\ S_{loc}^{(4)} &= \frac{A(\Sigma)}{48\pi}\frac{1}{\epsilon^2}, \end{aligned} \tag{A.12}$$

where $L$ is a IR cutoff and $\epsilon$ is a UV cutoff needed to make the entanglement entropy finite.

In the UV the entropy is dominated by the UV behavior of the momentum space d'Alembertian. For $d = 2, 3, 4$ the expansion of (A.10) in the limit

$p^2 \gg \rho_k^{2/d}$ is given by the following expressions

$$F^{(2)}(p^2) \to -\frac{p^2}{2},$$

$$F^{(3)}(p^2) \to -\frac{p^3}{\rho_k^{1/3}}, \qquad \text{(A.13)}$$

$$F^{(4)}(p^2) \to -\frac{p^4}{\rho_k^{1/2}}.$$

By using (A.13) in (A.5) and (A.6), one can estimate the leading contribution to the entanglement entropy in the limit $p^2 \gg \rho_k^{2/d}$ for the nonlocal models in the continuum. The results are

$$S_{UV}^{(2)} \propto A(\Sigma) \ln (L/\epsilon),$$

$$S_{UV}^{(3)} \propto \frac{A(\Sigma)}{\epsilon^{2/3} l_k^{1/3}}, \qquad \text{(A.14)}$$

$$S_{UV}^{(4)} \propto \frac{A(\Sigma)}{\epsilon \, l_k}.$$

where $l_k = \rho_k^{1/d}$. In $d = 3, 4$, the scaling of the entropy with respect to the cutoff $\epsilon$ is weaker with respect to the local case due to the presence of the nonlocality scale. In $d = 2$, the nonlocality scale does not enter the UV expansion of the wave operator, hence the leading contribution to the entanglement entropy in the UV is untouched with respect to the local theory.

# Appendix B

# Propagation of massless particles

Let us apply the procedure reviewed in Sec.5.2 to a massless field $\theta$. The constraints (5.6) read as

$$\frac{\bar{N}_\theta}{\bar{a}_\theta^3} = \langle \hat{H}^{-1} \rangle, \quad \frac{\bar{N}_\theta}{\bar{a}_\theta^3} \vec{k}^2 \bar{a}_\theta^4 = \langle \hat{\Omega}(\vec{k}, m = 0) \rangle. \tag{B.1}$$

In this case it is possible to solve for $\bar{a}_\theta^2$ straightforwardly from (B.1),

$$\bar{a}_\theta^2 = \frac{1}{|\vec{k}|} \left( \frac{\langle \hat{\Omega}(\vec{k}, m) \rangle}{\langle \hat{H}_0^{-1} \rangle} \right)^{1/2}. \tag{B.2}$$

For $m = 0$ one has that (see (5.3))

$$\hat{\Omega}(\vec{k}, m = 0) = \vec{k}^2 \widehat{H_0^{-1} a^4}. \tag{B.3}$$

It follows that

$$\langle \hat{\Omega}(\vec{k}, m = 0) \rangle = \vec{k}^2 \langle \widehat{H_0^{-1} a^4} \rangle = \vec{k}^2 \langle \hat{H}_0^{-1} \rangle \xi. \tag{B.4}$$

Hence in the massless case the scale-factor $\bar{a}_\theta^2$ and the lapse time function $\bar{N}_\theta$ are independent of $\vec{k}$,

$$\bar{a}_\theta^2 = \left( \frac{\langle \widehat{H_0^{-1} a^4} \rangle}{\langle \hat{H}_0^{-1} \rangle} \right)^{1/2} = \sqrt{\xi}, \quad \bar{N}_\theta = \left( \langle \widehat{H_0^{-1} a^4} \rangle \right)^{3/4} \langle \hat{H}_0^{-1} \rangle^{1/4} = \xi^{3/4} \langle \hat{H}_0^{-1} \rangle. \tag{B.5}$$

Therefore, massless particles with different $\vec{k}$ experience the same scale-factor and hence the same metric. Moreover, it can be seen from (B.5) that the scale factor carries information only about the parameter $\xi$ and does not depend on $\eta$. It is not possible to reconstruct $\beta$ probing the quantum geometry using only massless test particles. Hence, even if spacetime has quantum features ($\beta \neq 0$), still massless particles would see it as classical.

Note that in the classical limit $\beta \to 0$, one can write

$$\xi = \frac{\langle \widehat{H_0^{-1} a^4} \rangle}{\langle \hat{H}_0^{-1} \rangle} \to a_{cl}^4, \tag{B.6}$$

$$\eta = \frac{\langle \widehat{H_0^{-1} a^6} \rangle}{\langle \hat{H}_0^{-1} \rangle} \to a_{cl}^6, \tag{B.7}$$

and the metric defined by (B.5) becomes an ordinary FRW flat metric given by the following line element

$$ds^2 = g^{(cl)}_{\mu\nu} dx^\mu dx^\nu = -N_{cl}^2 dt^2 + a_{cl}^2 (dx^2 + dy^2 + dz^2). \qquad \text{(B.8)}$$

If we assume that the weak equivalence principle holds and no backreaction, then Eq. (B.8) has to provide the same metric given by the classical limit of the one experienced by a massive field. This is indeed the case given that in the limit $\beta \to 0$ the general rainbow scale factor $\bar{a}^2$, introduced in (5.9) for a massive scalar field, reduces to $\bar{a}^2(\vec{k}, m, \xi, \eta) \to \bar{a}_0^2 = \sqrt{\xi} = \eta^{1/3}$ giving then the classical scale factor by means of Eqs. (B.6) and (B.7).